THE APPLICATION OF GREEN CHEMISTRY AND ENGINEERING TO NOVEL SUSTAINABLE SOLVENTS AND PROCESSES

A Thesis
Presented to
The Academic Faculty

by

Gregory Alan Marus

In Partial Fulfillment
of the Requirements for the Degree
Doctor of Philosophy in the
School of Chemical and Biomolecular Engineering

Georgia Institute of Technology
May 2012

THE APPLICATION OF GREEN CHEMISTRY AND ENGINEERING TO NOVEL SUSTAINABLE SOLVENTS AND PROCESSES

Approved by:

Dr. Charles A. Eckert, Advisor
School of Chemical and Biomolecular Engineering
Georgia Institute of Technology

Dr. Charles L. Liotta, Co-Advisor
School of Chemistry & Biochemistry
Georgia Institute of Technology

Dr. Facundo Fernandez
School of Chemistry & Biochemistry
Georgia Institute of Technology

Dr. Carson Meredith
School of Chemical and Biomolecular Engineering
Georgia Institute of Technology

Dr. Amyn Teja
School of Chemical and Biomolecular Engineering
Georgia Institute of Technology

Date Approved: December 9th, 2011

For my Family –
and all their love, vision and support

ACKNOWLEDGEMENTS

I would first like to thank my advisors, Dr. Eckert and Dr. Liotta, as both have been integral in guiding my development through graduate school. I especially would like to thank Dr. Eckert for his encouragement to pursue innovative ideas and collaborate with researchers to find unique solutions. I thank Dr. Liotta for his enthusiasm and passion for research.

I thank my committee members, Dr. Fernandez, Dr. Meredith, and Dr. Teja for their advice, support, and helpful comments throughout this research.

I thank Deborah Babykin for helping with the administrative tasks and purchase orders, which have made my time here easier.

I would also like to thank all members of the Eckert-Liotta group, both former and current, as their friendships have enriched my life and suggestions have helped me view research in a different light. I especially thank the post-docs in the group, including Pamela Pollet for her guidance and suggestions in research and life in general, Eduardo Vyhmeister for his knowledge inside and out of the laboratory, and Rani Jha for her insightful discussions. I also want to acknowledge the undergraduates who have helped me work on many of the research projects, including Jacob, Sean, Michael, Martin, and Renee.

I thank my family and friends for their loving support and truly enriching experiences. Lauren has always been a source of inspiration and pride and someone who I have enjoyed sharing my life with, Leslie for her support and being the amazing person she is, and my parents for their love and vision.

TABLE OF CONTENTS

LIST OF TABLES

LIST OF FIGURES

LIST OF SYMBOLS AND ABBREVIATIONS

$Al(OiPr)_3$	Aluminum tri-isopropoxide
$Al(OtBu)_3$	Aluminum tri-tertbutoxide
CO_2	Carbon dioxide
DMF	Dimethylformamide
DMSO	Dimethylsulfoxide
FID	Flame ionization detector
GC	Gas chromatograph
HMF	Hydroxymethylfurfural
5-HMF	Hydroxymethylfurfural
HPLC	High Performance Liquid Chromatography
IL	Ionic Liquid
*i*PrOH	isopropanol
MIBK	Methylisobutylketone
MPV	Meerwein-Ponndorf-Verley
MS	Mass Spectrometer
NCW	Near Critical Water
NMR	Nuclear Magnetic Resonance
P	Pressure
PS	Piperylene Sulfone
PTC	Phase Transfer Catalysis
PTFE	Polytetrafluoroethane
$scCO_2$	Supercritical carbon dioxide

SO_2	Sulfur dioxide
(S)-CMK	*N*-(*tert*-butyloxycarbonyl)-(3*S*)-3-amino-1-chloro-4-phenyl-2-butanone
T	Temperature
t	Time
TGA	Thermo gravimetric analysis
UV-vis	Ultra violet - visible

SUMMARY

The implementation of sustainable solvents and processes is critical to new developments in reducing environmental impact, improving net efficiency, and securing economic profitability in the chemical and pharmaceutical industries.

In order to address the challenge of sustainability, researchers have used switchable solvents for both reaction and separation by utilizing a built-in switch to undergo a step change in chemical and physical properties. This allows us to facilitate reactions in the solvent then activate the switch to enable separation and facile product recovery. Subsequently, we can recover the solvent for reuse and avoid energy- or waste-intensive separation processes; thus we are developing and using these switchable solvents as sustainable and environmentally benign alternatives to traditional processes.

In this research, we enable the sustainable scale-up of a switchable solvent – piperylene sulfone – a "volatile" and recyclable DMSO replacement. In the development of this process, we improved the reaction performances and developed a green purification method.

Furthermore, we enable and demonstrate the implementation of a Meerwein-Ponndorf-Verley (MPV) reduction, a pharmaceutically relevant reaction, into a continuous flow platform. The innovation of continuous flow processes can replace traditional batch reaction technology, and is indeed a key research area that has been acknowledged by the pharmaceutical industry.

Additionally, we utilize the switchable sulfone solvents, piperylene and butadiene sulfone, for reaction and separation of HMF produced from monosaccharides as an alternative to a process which has been limited by an inefficient separation step.

CHAPTER I

INTRODUCTION

Economic viability is cornerstone to the development of all products and processes. The US government has implemented policies to regulate the generation of waste, which is impacting the companys' profit margins [1]. This regulation and legislative pressure has in turn caused companies to adjust by adopting more environmentally friendly methods in their research and development and manufacturing processes. Additionally, mounting concern about environmental impact and regulation resulting from use of petroleum-based resources, and the interest of many countries to become independent from importing foreign sources of oil, has caused momentous research and development growth in production of chemicals, materials, and energy that are derived from renewable resources.

Solvents take a key role in almost all of these products and processes. Solvents are used to accomplish mass transfer through creating monophasic or multi-phase conditions for chemical reactions, heat transfer through controlling temperatures, as well as decontaminating reaction vessels and equipment, isolating and purifying compounds, etc. [2]. In many wet solution chemistry cases, solvents remain the largest amount (by mass or volume) of chemical needed in a reaction process [3]. In fact, some processes contain 85 mass% solvent [4]. Thus, the realization of even small improvements in a solvent can have profound implications in reducing the energy for separations and costs associated with the regulation of waste.

Furthermore, the separation of solvents from mixed aqueous waste streams is complex and expensive and therefore often results in copious waste [1]. This is problematic from an environmental perspective because the typical method of disposal for mixed aqueous/organic wastes is incineration. As an example, in three life cycle assessment case studies involving the implementation of green solvent recovery processes to pharmaceutical firms, it was determined that the manufacture and incineration of solvents make a significant contribution to the life cycle emissions [3]. Additionally, the replacement for polar aprotic solvents was cited as a vital area of research [1].

Researchers have strived to develop sustainable alternatives to the commonly used waste intensive solvents. In the following chapters, we focus our research on the application of green chemistry in the development and innovation of smart solvents for reaction and separation, and we focus on the implementation of green engineering to the pharmaceutical industry by means of continuous flow processing.

In Chapter II, we discuss how we have utilized advanced laboratory techniques, such as in-situ high pressure ^{1}H NMR, to make a commercially unavailable novel smart solvent an industrial reality. Our aim is to permit the development of an economically viable piperylene sulfone (PS) production process. In order to enable the industrial scale production of PS, we must overcome the limitations of low yields and a waste intensive purification that have prevented large scale synthesis of this sulfone.

Thus, our first research objective was to achieve a more fundamental understanding of the piperylene sulfone synthesis where we (1) improve the reaction performances and (2) develop a more sustainable purification strategy. Although this

retro-cheletropic reaction for piperylene sulfone is known, it has not been well studied. We have analyzed the kinetic parameters of the piperylene sulfone reaction and determined the rate constant, reaction order, and the activation energy. Additionally, with the implementation of a novel inhibitor, we have demonstrated high synthetic yields, and developed an effective separation method that uses a green solvent to significantly reduce the waste in product purification.

In Chapter III, we enable the implementation of a pharmaceutically relevant Meerwein-Ponndorf-Verley (MPV) reduction into a continuous flow reactor. The American Chemical Society (ACS) Green Chemistry Institute and several major pharmaceutical firms established the Pharmaceutical Roundtable in 2005 with the objective of implementing green chemistry and engineering into pharmaceutical research. At the top of their list of key green engineering research areas is continuous flow processing. To meet increasing cost pressures and market demands, continuous processing is acknowledged as a vital part of a process intensification scheme [5].

The MPV reduction is a reaction important in both industry and academia as a means to reduce carbonyls to their respective alcohols; we selected the MPV reduction to implement in our Advanced Flow Reactor from Corning. We demonstrate the transition from batch to continuous flow for the successful MPV reductions of an aldehyde and a ketone (benzaldehyde and acetophenone, respectively) at two temperatures with the use of a highly active, efficient and cost-effective catalyst, $Al(O\mathit{t}Bu)_3$. With the use of this catalyst, we have lowered the catalyst loadings, from 50 mol% to 20 mol% and even 5 mol%, without significantly impacting reaction time and efficiency.

In Chapter IV, we report on the application of our switchable solvent, piperylene sulfone, in the reaction and separation of 5-hydroxymethylfurfural (5-HMF). HMF is a versatile chemical intermediate that could replace heavily consumed petroleum-based compounds that are currently being used in the production of plastics and fine chemicals. It is the efficient production of pure 5-HMF which continues to be a challenge to researchers; the current production methods are limited by the efficient separation of product from solvent.

We demonstrated the use of thermally switchable solvents, using both piperylene sulfone and butadiene sulfone to replace DMSO in the reaction and problematic separation of this high-value intermediate. Initially, we have shown the effective separation of piperylene sulfone and butadiene sulfone from HMF at moderate temperatures. Next, we have used these sulfones as reaction media in the production of HMF. The dehydration reaction uses fructose as the starting material to produce 5-HMF as the product and is acid catalyzed. We explore two routes to provide the acid for this catalysis: first by leveraging the equilibrium switch of our sulfone molecules to generate SO_2, and with the addition of water, we generate sulfurous acid in-situ; second, we add a heterogeneous ion exchange resin acid catalyst which has been used in DMSO to achieve quantitative yield.

Lastly, in Chapter V, we consider the conclusions and recommendations for this research. This research has could lead to many opportunities for additional applications.

1.1 References

[1] Constable, David J.C.; Dunn, Peter J.; Hayler, John D.; et al, *Key green chemistry research areas–a perspective from pharmaceutical manufacturers*. Green Chem., 2007. **9**: p. 411.

[2] Horváth, I. T., *Solvents from nature*. Green Chem., 2008. **10**: p. 1024.

[3] Raymond, Michael J.; Slater, C. Stewart; Savelski, Mariano J., *LCA approach to the analysis of solvent waste issues in the pharmaceutical industry*. Green Chem., 2010. **12**: p. 1826.

[4] Sheldon, R.A., *Green Solvents for sustainable organic synthesis: state of the art*. Green Chem., 2005. **7**: p. 267.

[5] Jimenez-Gonzales, Concepcion; Poechlauer, Peter; Broxterman, Quirinus B.; et al, *Key Green Engineering Research Areas for Sustainable Manufacturing: A perspective from Pharmaceutical and Fine Chemicals Manufacturers*, Organic Process R&D, 2011. **15**: p. 900.

CHAPTER II

NOVEL SWITCHABLE SOLVENTS

2.1 Introduction:

The awareness of increasing sustainability of manufacturing processes has driven a greater effort to environmentally conscious designs, as it is becoming less profitable to dispose of significant quantities of waste and solvents [1]. With this mounting interest in designing products and processes that have less of an environmental impact, more consideration is being given to implementing green chemistry and engineering [2]. Solvents in particular have a great potential to contribute to the net efficiency and success of a process, in terms of increasing product quality and decreasing price and environmental impact.

In order to take advantage of these opportunities and address these challenges, researchers have developed and used a number of innovative solvents and solvent systems for reaction and separation. These tunable and smart solvents include supercritical fluids [3], gas-expanded organics [4], near critical water [5], smart organic solvents [6], ionic liquids [7], and others. A tunable solvent is a solvent where we can gradually adjust the properties to induce the desired effect. Examples of these solvents include supercritical fluids, gas expanded liquids, and near critical water where subtle changes in pressure translate to variations in physical properties (e.g. density). Another innovative type of solvent is the smart solvent, where the chemical and physical properties undergo a step change upon the induction of a stimulus, such as heat, light, or pH. Importantly, these properties can allow for a more efficient (1) separation of solvent

from the product and (2) subsequent recycle and reuse of the solvent, making the process sustainable by design.

The selection of solvent and solvent system is important when simultaneously considering reaction and separation. For example, the ability to create monophasic conditions between inorganic salts and organic components can be difficult and is typically overcome with the use of a strong polar, aprotic solvent (DMSO, DMF, NMP) or phase-transfer catalysts. Although these strategies have been successful in promoting reaction, they suffer from several drawbacks. The former have high boiling points (189 ^{O}C in the case of DMSO) resulting in expensive separations, and the latter are also difficult to separate, as they require several washing cycles.

The separation of polar aprotic solvents is primarily conducted via one of two methods. The first is an energy-intensive distillation to remove the high boiling solvents. The second is via the addition of large amounts of water to precipitate the product; unquestionably this last strategy is product-dependent and requires that the product is hydrophobic. In addition it generates large amount of organic contaminated aqueous waste. On top of that, the preferred method of disposal for mixed aqueous/organic wastes is incineration. Separation of solvent from mixed systems in a batch type context is expensive energetically and monetarily, favoring incineration. This requires fuel for combustion and generates additional NO_x and CO_x gases [8]. Another study demonstrated that the manufacture and incineration of solvents makes a significant contribution to the life cycle emissions of an Active Pharmaceutical Ingredient (API) [9].

The use of a switchable smart solvent may not only result in lower energy requirements but also in a decreased E-factor, as it is common to incorporate the E-factor

as a green chemistry metric to measure efficiency in chemical processes. The E-factor is a measure of the total mass of waste divided by mass of product produced [10]. Additionally, the replacement of DMSO was cited as key research need by a pharmaceutical industry evaluation [11]. Researchers have targeted tunable and smart solvents at addressing these traditionally challenging areas by employing the unique properties of the solvent for reaction and separation.

Piperylene sulfone (PS) is a smart solvent that can solve such problems; it is a polar aprotic molecule with solvent properties similar to those of DMSO; and it can be easily separated and recycled under modest reaction conditions. PS is not volatile in and of itself, but is converted to volatile species via shifting an equilibrium reaction upon heating, as shown in Figure 2-1. These decomposition species can be collected and reformed into the piperylene sulfone molecule at room temperature.

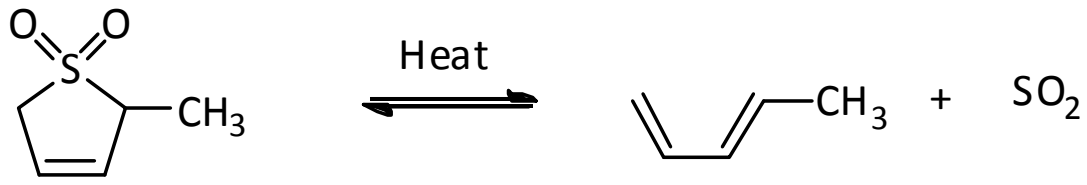

Figure 2-1. Decomposition of piperylene sulfone to form *trans*-1,3-pentadiene and SO_2.

The thermal "switch" that enables the easy removal of PS can be activated at temperatures over 100^{o}C, where PS breaks into two gases, *trans*-piperylene and sulfur dioxide, enabling separation. A free radical inhibitor is required to suppress polymerization of the diene. Subsequently, the *trans*-piperylene and sulfur dioxide can

be cooled and recombined to re-form PS, enabling recyclability. This cycle is illustrated in Figure 2-2, where one can envision a stream of reactants being fed to a reactor containing liquid piperylene sulfone. Reaction can then be carried out. After reaction completion, the piperylene sulfone is separated using the thermal switch at just over 100 ^{o}C effectively allowing for separation of solvent from the products. The volatile *trans*-piperylene and sulfur dioxide are separately condensed and re-form piperylene sulfone at room temperature. The process can then be repeated.

We have demonstrated such a process using the reactants benzyl chloride and potassium thiocyanate where 96% reaction yields were obtained and 87% of the solvent was recovered. As these reactions were run on a small laboratory scale, we attribute high solvent losses (13%) to un-optimized reaction conditions and small-scale transfer losses, and quantitative recovery is expected on larger scale.

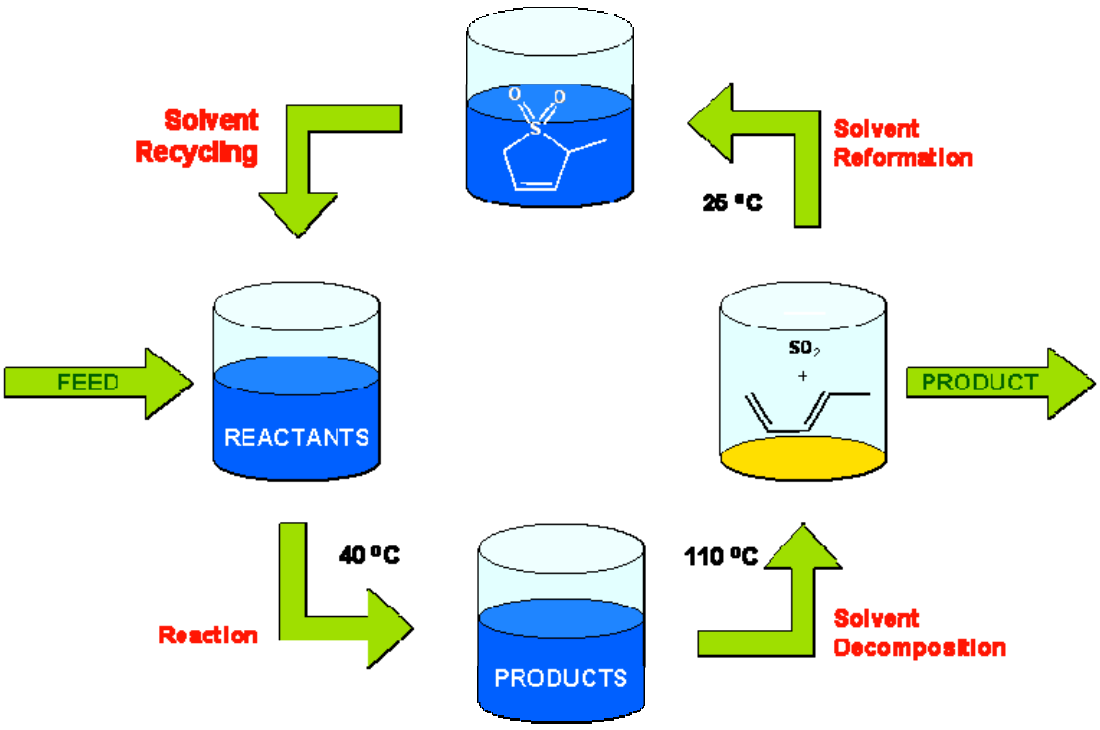

Figure 2-2. Schematic showing the use of piperylene sulfone as a reaction media, the separation from products, and subsequent reformation and recycle.

The cheletropic reaction is a cycloaddition reaction, and specifically a type of a pericyclic reaction where a reorganization of σ and π bonds of the diene and SO_2 occurs resulting in a 5-membered sulfur containing ring. In the transition state, the SO_2 donates two electrons to the 1,3-diene involving the formation of a cyclic array of interacting atoms and orbitals where two new bonds are being made on the diene. Although similar studies [12] have shown that there are two possible products that could be formed, the cheletropic reaction that yields the five-membered ring thermodynamic product is more stable than the Diels-Alder reaction yielding the kinetic product.

Although we focus on the development of piperylene sulfone in this chapter, there are several other sulfones, including butadiene sulfone and isoprene sulfone that undergo the same retro-cheletropic decomposition pathway to form a conjugated diene and SO_2.

The physical properties can be changed depending on the structure of the sulfone, as can be seen in Figure 2-3. Here we show the influence the structure of the sulfone on the melting point, where PS has the lowest melting point of all the sulfones at -12 ^{O}C, enabling its use as a liquid solvent at room temperature.

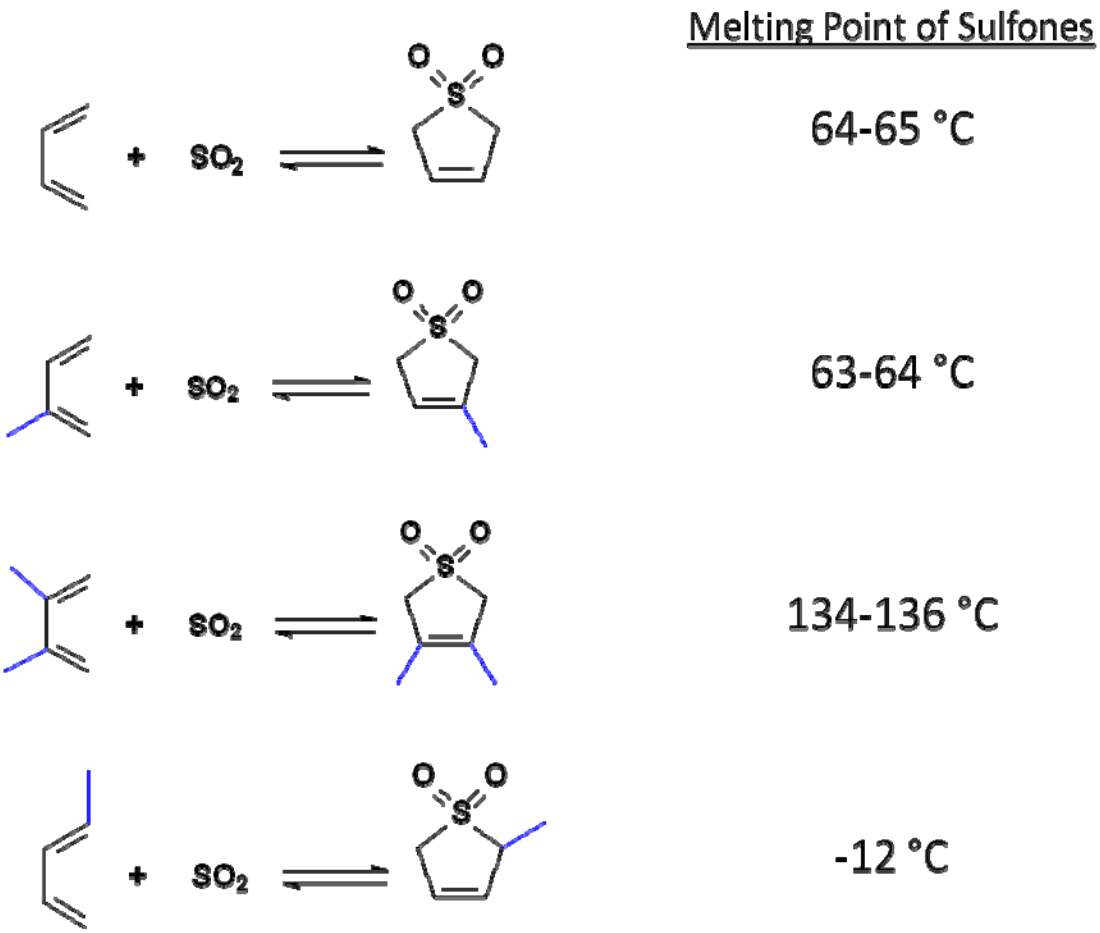

Figure 2-3. Influence of sulfone structure on melting point (butadiene sulfone [13], isoprene sulfone [14], 2,3-dimethylbutadiene [13], and piperylene sulfone [15]).

The structure of the sulfone not only influences the melting point, but also the tendency of the molecule to convert to volatile species upon elevated temperature, as we illustrate in Figure 2-4. Here, we are showing the decomposition half-lives as a function of temperature for several sulfones. It can be seen from this plot that PS has the lowest

decomposition half-life by comparison, enabling an easily accessed decomposition point and requiring less energy to convert to volatile species than its sulfone counterparts.

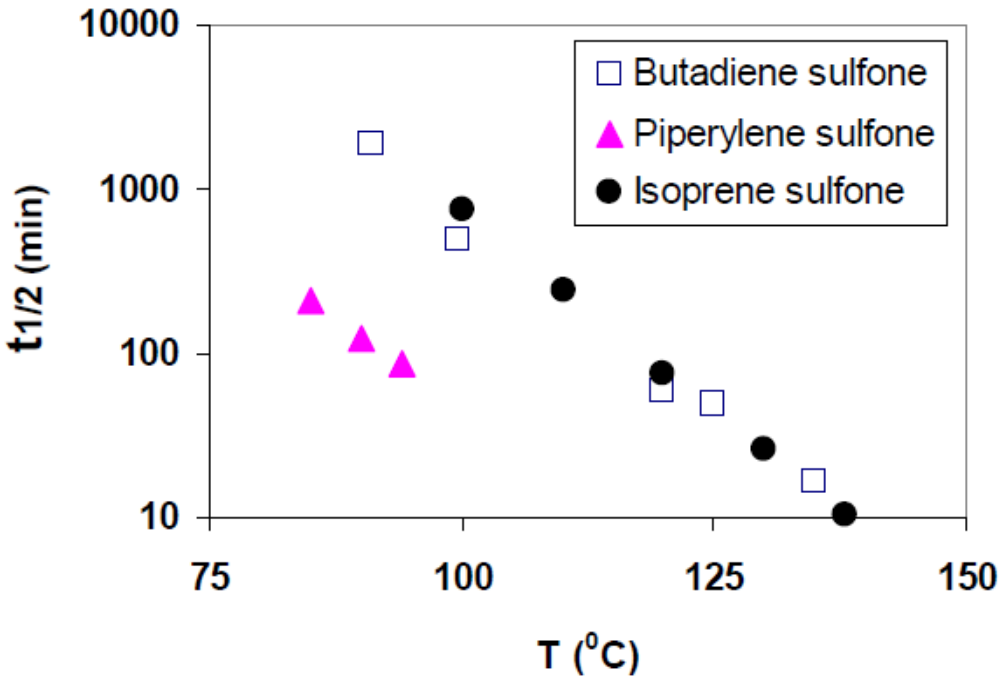

Figure 2-4. Plot of sulfone half-life as a function of temperature [16].

To show the complete decomposition of piperylene sulfone, we use Thermal Gravimetric Analysis (TGA) where we can monitor the mass loss as a function of time. In Figure 2-5, we demonstrate this complete decomposition where the sample is linearly heated to just under 120 °C in 21 minutes, and the temperature is then held constant. The corresponding mass loss is plotted and indicates that we can achieve complete decomposition in less than 1 hour, without side reaction and residual mass remaining. This is critical for an industrial process, as it is essential that the reversal of the solvent is quantitative.

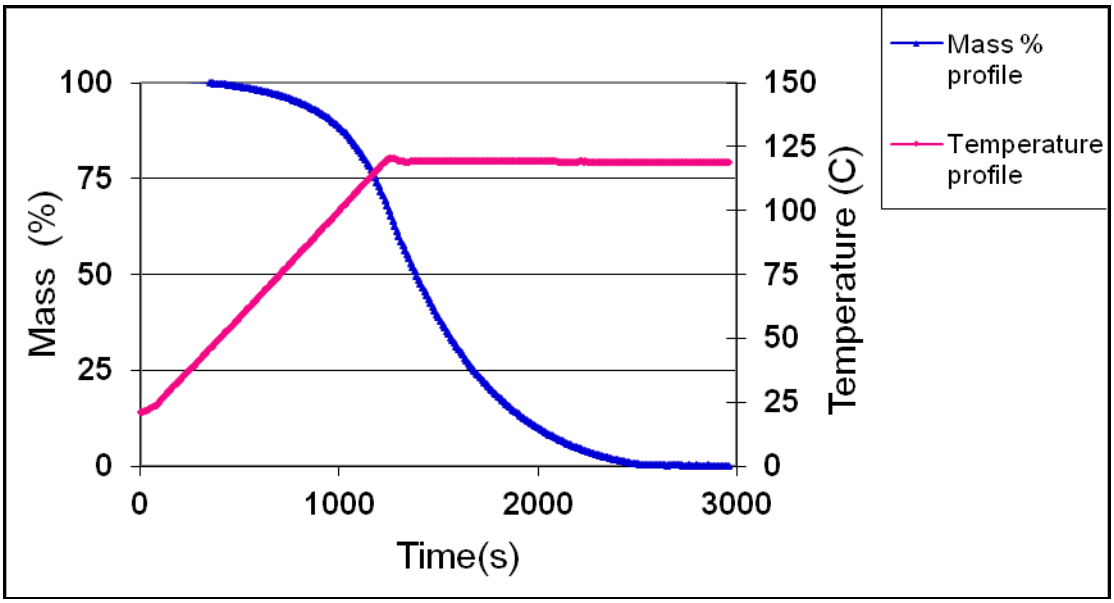

Figure 2-5. TGA of the decomposition of piperylene sulfone.

We identified solvatochromic properties of piperylene sulfone including the Kamlet-Taft parameters as well as the $E_T(30)$ and the dielectric constant. For comparison, the solvatochromic properties of DMSO are listed alongside PS in Figure 2-6. Each of these parameters can be determined spectroscopically based on the shift in wavelength at maximum absorbance using probe dyes (except the dielectric constant and the α parameter, the latter of which can be determined by measuring the π*and $E_T(30)$). The α parameter represents the ability of the solvent to donate hydrogen bonds, which specifies the acidity. The β parameter represents the ability of the solvent to accept hydrogen bonds, specifying the basicity. The parameter with the principal difference between the two solvents is the β parameter, indicating that DMSO can accept hydrogen bonds more readily and lead to better solvation of the cation and greater ion-pair separation. The

transition energy required to raise one mole of dye to its excited state is the $E_T(30)$, and it indicates the dipolarity of the solvent. Finally, the dielectric constant, ε, is a measure of the permittivity of the solvent relative to a vacuum, which provides us with another indicator of solvent polarity. The dye used to measure π* is N,N-dimethyl-4-nitroaniline, β is N,N-dimethyl-4-nitrosoaniline, and $E_T(30)$ is Reichardt's dye (2,6-diphenyl-4 (2,4,6-triphenylpyridinium-1-yl) phenolate dehydrate. The similar solvatochromic properties indicate similar solvent strength.

Property	***DMSO*** 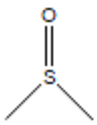	***Piperylene Sulfone*** 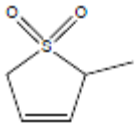
Boiling Point (°C)	189	decomposes
Melting Point (°C)	16-19	-12
α	0	0 ± 0.1
β	0.76	0.46 ± 0.08
π^*	1.00	0.87 ± 0.04
$E_t(30)$ (kJ/mol)	189	189 ± 0.3
ε	46.7	42.6

Figure 2-6. Comparison of the solvatochromic properties of DMSO and PS.

In addition to the solvatochromic properties, we demonstrate the benefits of PS as the first recyclable dipolar, aprotic solvent [17]. PS has been used at the laboratory scale as a recyclable and volatile dipolar aprotic solvent for nucleophilic substitution[17], aerobic alcohol oxidations [19], and the in-situ acid catalyzed hydrolysis of β-pinene [15]. In the nucleophillic substitution reactions, benzyl chloride was reacted with potassium thiocyanate to test piperylene sulfone's ability to react an organic compound and a salt. The rate constants of the reactions run in PS were only slightly lower than those run in DMSO illustrating that PS is an effective dipolar, aprotic solvent for nucleophilic displacement reactions [17]. Additionally, copper-catalyzed aerobic alcohol oxidations were performed at room temperature in PS. Several primary alcohols were converted to aldehydes in high yields (90-98% yield) and with exceptional turnover frequency (31 h^{-1}), and the catalytic system was recycled three times without significant loss in activity.

Lastly, the hydrolysis of β-pinene to alpha-terpineol was utilized to test the ability of either piperylene sulfone or butadiene sulfone to generate sufficient in-situ acid catalyst to catalyze a reaction that is traditionally carried out with strong acids, e.g. sulfuric acid. The equilibrium of piperylene sulfone with its decomposition products was utilized in combination with the equilibrium of water and SO_2 in order to generate sulfurous acid for in-situ catalysis. The products of this reaction are important to the flavor and fragrance industry, with applications in perfumes and cleaning materials. Several effects were studied, including the length of time to reach equilibrium, concentration of water, reaction temperature, time, and recycle-ability. The results showed competitive reaction in both solvents, even at mild reaction conditions, where

similar activity and slight improvements in selectivity were observed as compared to the strong acid systems.

To use PS in any commercial system, large quantities would be needed, and the methods used for small-scale preparation in the laboratory are not readily scalable. What we present here is a potential route to scale-up for kilogram to tonnage production of piperylene sulfone.

2.2 Experimental:

Materials.

All chemicals were used as received, unless noted otherwise. Sulfur dioxide, anhydrous (99.9+%) was purchased from Sigma-Aldrich (for kinetics), sulfur dioxide, anhydrous (99.98%) was purchased from Airgas (for scale-up), *trans*-1,3-pentadiene (94%) purchased from Sigma-Aldrich (for kinetics), 1,3-pentadiene, degassed prior to use (90%+ mixture of isomers, approximately 50% *trans* isomer, impurities – cyclopentene, 2-methyl-e-butene) was purchased from Monomer-Polymer and Dajac Labs (for scale-up), argon gas (ultra high purity) purchased from Airgas, benzene (99.9+%) was purchased from Sigma-Aldrich, deuterated benzene-D6 (D, 99.5%) was purchased from Cambridge Isotope Laboratories, Inc, N-phenyl-2-naphthylamine (97%) was purchased from Sigma-Aldrich, 8-anilino-1-naphthalenesulfonic acid magnesium salt was purchased from TCI (Japan), dichloromethane was purchased from EMD (99.97%), dimethyl sulfoxide was purchased from Baker (99.9%), carbon dioxide was purchased from Airgas (99.999%), and 7-inch medium wall NMR tubes rated for 100 psi of pressure were purchased from Wilmad Lab Glass.

Kinetic ^{1}H NMR Procedure.

Kinetic investigations of the conversion of *trans*-piperylene to PS were conducted in-situ and monitored by ^{1}H NMR for real time analysis. The NMR tubes were first loaded with the selected inhibitor (depending on experiment). The inhibitor mole fraction was maintained constant (0.05 based on *trans*-piperylene content). Under an argon gas stream, benzene, deuterated benzene, and 94% *trans*-piperylene were added in this order and weighed to six significant figures.

The benzene was a calibration standard to normalize the peak intensities. The deuterated benzene was a ^{2}H NMR lock, preventing baseline drift. Next the tube was placed in a dry-ice and acetone temperature bath (195K) such that SO_2 was condensed into the NMR tube. Due to the low temperatures, we assumed that no reaction took place during the loading of SO_2. After sulfur dioxide addition, the tube was sealed, warmed to 295K and immediately analyzed by ^{1}H NMR. At the end of the experiment, the NMR tube was weighted to determine the amount of liquid SO_2 that had been added. The ^{1}H NMR instrument used was a Bruker DMX 400 using TopSpin software.

Conversion to PS was calculated by using the NMR integrals of both piperylene and piperylene sulfone, and concentration was calculated by using the recorded weight of each component loaded into the NMR tube. The relative integration of each signal was used to monitor the progression of the reaction as a function of time. Reaction kinetics are not affected by the presence or absence of inhibitor. We used the Arrhenius equation where reactions were run at a second lower temperature of 283K (in-situ ^{1}H NMR), and

the rate constant obtained from the integral method was used in this analysis to determine an approximate activation energy.

Reactors.

The scale-up reaction vessel was a 5-liter glass round-bottom flask custom made by Ace-Glass (maximum working pressure of 45 psig). Five Teflon screw plugs were fitted and adapted for the following connections: a 316 stainless steel dip tube to add degassed piperylene, add/purge SO_2, relief valve (set at 45 psig), graphite burst disc (rated at 65 psig as fluctuations in pressure due to use over time weaken and therefore lower the burst disc pressure), and pressure gauge. A custom-made ethylene glycol temperature bath connected to a chiller was used to condense SO_2. Stirring was provided using a Teflon coated magnetic stir bar.

For the inhibitor separation experiments, a 48-milliliter glass round-bottom tube reactor (from Ace-Glass) was used with Teflon screw plug and the same connections described for the 5-liter glass vessel. The scale-up procedure described below was used to synthesize PS in both the 5-liter reactor and the 48-milliliter reactor, with all ratios adjusted accordingly.

Scale-up procedure.

We synthesized PS for scale-up reactions [20] in a 5-liter glass pressure vessel, where we add 0.05 mole fraction inhibitor (neutral or ionic). The reactor is filled then purged with sulfur dioxide gas at least three times to displace air. We remove air, oxygen, and moisture through displacement with either an inert gas (argon in the kinetic

experiments) or SO_2 (scale-up experiments) in order to standardize the reaction conditions and minimize experimental variation. The temperature bath is cooled to 263K in order to reduce the vapor pressure of sulfur dioxide and approximately 200 milliliters of liquid sulfur dioxide are added. Next, 25 milliliters of degassed 1,3-pentadiene (mixture of isomers) is then slowly pumped directly to the liquid sulfur dioxide via a dip tube and HPLC pump. The piperylene used for all scale-up and separation experiments was degassed prior to each use by three freeze-thaw cycles with liquid nitrogen. The reactor is then sealed, stirred, and allowed to react for 12 hours at 295K. Due to the large excess of SO_2 used, both the initial and final pressures are very close to the vapor pressure of SO_2 (about 35 psig) at the given reaction temperature.

After reaction completion, we extracted PS [20]. The vessel was slowly purged, to remove the excess sulfur dioxide. The crude PS was mixed with 175 milliliters of water saturated with sodium chloride for at least 30 minutes. The aqueous layer was transferred to a separate flask, extracted with 70 milliliters of dichloromethane, and mixed for at least 30 minutes. The organic extraction was repeated at least once, confirming that all PS was removed from the water. The dichloromethane was removed under reduced pressure, and then filtered over a short path of activated carbon and SiO_2. The PS was analyzed by ^{1}H and ^{13}C NMR (^{1}H NMR (ppm): δ=1.36 (d, 3H), 3.69 (m, 3H), 5.96 (m, 2H); ^{13}C NMR (ppm): δ=12.9, 54.8, 59.4, 122.5, 131.4).

For the inhibitor separation experiments, the same procedure was used to synthesize PS as described for the 5-liter reaction vessel. After reaction completion the vessel was slowly purged to remove the excess sulfur dioxide, and then placed under rotary evaporation to remove the low boiling impurities, and weighed. The isolated yield

from the unoptimized reaction was on average 92%, based on the *trans*-isomer content. Incomplete measured yield is attributed to transferring losses due to the relatively small scale. A 1 microliter sample was taken from the resulting product and analyzed for inhibitor concentration via UV-visible spectroscopy (determined by comparing the absorbance to known calibration curves). Then a windowed Parr reactor was cleaned, put under vacuum, and approximately 5 milliliters of PS was injected into the reactor. Approximately 180 milliliters of CO_2 was added using an ISCO syringe pump (volume recorded from ISCO). Due to the excess of liquid CO_2, the initial and final reaction pressures are very similar to the vapor pressure of CO_2 at the given temperature. The Parr reactor was stirred for at least 15 minutes, and equilibrated for 15 minutes (with no change in equilibrium compared to 12 hours). A sample loop was connected to the windowed Parr to sample the liquid carbon dioxide and PS phase. Upon sampling, the liquid carbon dioxide was vented and PS collected (about 0.25 milliliters). The PS was analyzed for inhibitor concentration via UV-visible spectroscopy and analyzed by ^{1}H and ^{13}C NMR (^{1}H NMR (ppm): δ=1.36 (d, 3H), 3.69 (m, 3H), 5.95 (m, 2H); ^{13}C NMR (ppm): δ=13.1, 54.9, 59.5, 122.7, 131.6). Additionally, the ionic inhibitor is over an order of magnitude less soluble in sulfur dioxide than the mole fraction initially used with the neutral analog. Therefore, we tested a reduction in inhibitor mole fraction from 0.05 to 0.001 and demonstrated the synthesis of PS using the same method on a 48mL scale. Due to the commercial unavailability of PS, we first tested the proof-of-principal separation of DMSO (an analog of PS) from a soluble mixture of DMSO and ionic inhibitor. The solution was loaded into a Parr reactor where we then added liquid CO_2 to the reactor while stirring. The ionic inhibitor separated from the mixed DMSO and CO_2

phase. We could separate the phases, and depressurize the CO_2 and recover the DMSO, which we analyzed using UV-vis spectroscopy. The separation results in a reduction from 3.70 ± 0.17 weight% inhibitor to 0.07 ± 0.04 weight% inhibitor in the DMSO.

2.3 Results:

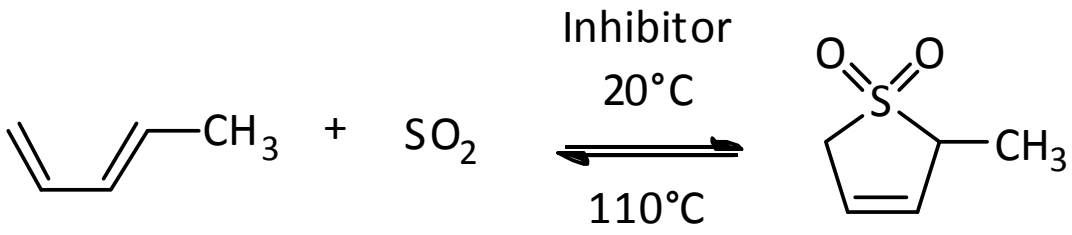

Figure 2-7. Synthesis of PS with an inhibitor from *trans*-1,3-pentadiene and SO_2.

In this section, we achieve a more fundamental understanding of the synthesis of PS in order to improve the reaction performances and develop a more sustainable purification strategy. From a process standpoint, we were especially interested in developing a process that can be readily scalable and viable on an industrial scale, thus contributing to make PS usage a reality. We initially synthesized PS according to the method described in literature [15] and shown in Figure 2-7. The procedure involves addition of piperylene, a radical inhibitor (typically either hydroquinone, p-t-butyl-catechol, or phenyl-β-naphthylamine, the structure of the latter is shown in Figure 2-

10A and is the inhibitor we used), [16, 20, 21] and an excess of liquid sulfur dioxide to a high pressure bomb. Only the *trans* isomer of piperylene reacts to form PS; thus, yield is calculated based on the *trans* isomer content where it is important to note that the *trans* content varies with the commercial source and even within the batch. Furthermore, decomposition of the PS yields solely *trans*-piperylene. In fact, this method can be used to purify the raw piperylene to the *trans*-isomer [22]. An excess of sulfur dioxide is commonly used in the literature [15, 20, 22] to maximize PS yield and minimize undesired polymerization of *trans*-piperylene, a reaction that is often observed with conjugated dienes [23]. After addition of all reactants, the reactor was sealed and shaken for 2 days at room temperature (20^{O}C). The synthesis reaction is shown in Figure 2-7. After the inhibitor was removed, the yields ranged from 45% to 55%,[19, 20, 24] and PS is then purified by distillation at reduced pressure. More recently, other researchers have adopted this procedure to synthesize PS [19]. Numerous physical properties of PS have been determined (including the density and refractive index [25], equilibrium constants and decomposition [16], rates of thermal dissociation [24], and heat of formation [16]) as well as a method of enriching the *trans*-isomer [22] and characterization studies including optical activity and purification [20].

The literature method previously developed to separate the inhibitor from the PS involved an extraction into water saturated with sodium chloride, followed by a back-extraction into dichloromethane, then removal of the dichloromethane and filtration [20]. The major disadvantage of this separation method is significant waste generation (over 100 moles of waste per mole of PS purified. Unquestionably, this method is not optimized and is inadequate from a large scale perspective. In order to make the

separation of the inhibitor less waste intensive for large scale production, a more efficient separation strategy than the method used in literature [20] was devised. This new separation strategy is aimed at significantly reducing the waste generation.

Toward a Scalable Synthesis of PS.

Steps we have taken to make the synthesis of PS more feasible on a large scale:

1. Determination of the kinetics of PS formation from piperylene and sulfur dioxide.
2. Minimization of undesirable side reactions by adjusting dilution and the structure of the inhibitors.
3. Development of a sustainable method of separating the inhibitor from PS.
4. Use of the kinetic information to develop a scale-up design.
5. Validation of the scale-up design on a laboratory scale using raw industrial material (mixtures of *cis*- and *trans*-piperylene).
6. Development of a HYSYS simulation demonstrating the complete synthesis, separation, and purification of PS on an industrial scale.

PS is synthesized by the cheletropic reaction of *trans*-1,3-pentadiene (*trans*-piperylene) and sulfur dioxide, as illustrated in Figure 2-7. Although the reaction of conjugated dienes is known in the literature [16], critical scale-up data such as kinetics of the synthesis reaction, side product formation, etc. are scarce. We used in-situ proton NMR (via use of high-pressure NMR tubes) to monitor the real-time conversion to PS from 94% *trans*-piperylene and SO_2 with respect to time. By monitoring in-situ reaction

progress, we determined that the time to reach completion occurs within 12 hours at 295K (as can be seen from the constant value of conversion in Figure 2-9 and 2-10, discussed later).

Kinetics.

We used in-situ proton NMR measurements to obtain the kinetic parameters for PS formation. TopSpin, a software package, was utilized for the acquisition, processing, and analysis of the NMR data that we collected from the Bruker DMX 400. By using the NMR integrals obtained from both piperylene and piperylene sulfone, we calculated the relative conversion of each component. As each signal was in reference to the integral of the relative benzene peak, we could determine the reaction progression as a function of time. Thus the characteristic NMR absorptions from piperylene and PS were used to calculate the conversion of the reaction, and gravimetric measurements were used to calculate exact concentration of each component in the NMR tube and used for conversion calculations.

The NMR tubes are treated as batch reactors where concentration data are collected at defined time intervals during the course of the reaction. The concentration was calculated from the recorded weight of each component loaded into the NMR tube prior to NMR analysis. Using the relative conversion to piperylene sulfone in conjunction with the calculated concentrations, we determined the relative concentration of each component as a function of time. Analysis of the concentration rate data using the integral and differential method allowed for determination of the parameters for the

kinetic expression, including the rate constant and reaction orders. The combined mole balance and rate law yields the kinetic expression for the formation of PS (Figure 2-8):

$$\frac{dC_{PS}}{dt} = kC^{n}_{Piperylene}C^{m}_{SO_2}$$

Figure 2-8. Kinetic expression for the formation of piperylene sulfone (PS).

The reaction is first order with respect to each reactant, n=1 and m=1, as determined by the integral method where the R^2 is greater than 98%.Through analysis of the rate data, we determined the function of concentration corresponding to a particular rate law that was linear with respect to time. A sensitivity analysis confirms first order behavior by comparison of the regression coefficients for other reaction orders.

We used both the differential and the integral method to find the rate constant. From the average of our experiments, the kinetic rate constant is k=0.022 ± 0.003 L/(mol*hr) at 295K. Using the differential method, we took the natural log of the combined mole balance and found the rate of reaction from concentration versus time data acquired from the NMR. By plotting the natural log of the differentiated concentration-time data versus the natural log of the concentration, we determined the reaction order which is the slope of the line fitting the data and the rate constant from the y-intercept. For the integral method, the guess and check method was used where the

reaction order was first guessed and then the differential equation used to model the batch system was integrated. When the concentration was plotted as a function of time, and the data followed linear behavior, the guessed reaction order value was correct, and the slope of the line gives the rate constant. Using the dependence of the rate constant on temperature as expressed by the Arrhenius equation, we have determined the specific rate constants at two temperatures, 283K and 295K, and estimated an approximate activation energy of 40 ± 5 KJ/mol from the slope of the line on a plot of the natural log of the rate constant versus inverse time.

Dilution.

Two significant products can be formed: (1) PS from the cheletropic reaction of *trans*-piperylene with SO_2 and (2) undesired polymeric products from piperylene polymerization. Complete conversion of *trans*-piperylene is observed in all cases, as confirmed by NMR.

Although dilution of the *trans*-piperylene with excess sulfur dioxide is known to increase PS yield, we seek to achieve a deeper understanding; although dilution has previously been used to increase yields, in order to develop a larger scale process with higher yields, a more thorough comprehension of the dilution effect is obtained. By in-situ proton NMR measurements, we measured the formation of PS at a range of dilute piperylene concentrations, as shown in Figure 2-9. The relative concentration of *trans*-piperylene was varied from 26 mole % to 2.73 mole %. At the highest concentration of piperylene tested (26 mole % piperylene), the PS yield was 48% (the remaining piperylene polymerized). At the lowest concentration (2.73 mole % piperylene), the PS

yield increased to 76%. Figure 2-9 shows that as the concentration of piperylene decreases (relative sulfur dioxide concentration increases), PS yield increases, but polymerization still occurs at all conditions tested.

These results indicate that dilution alone is insufficient to achieve complete conversion to PS. Although dilution does have a substantial effect on reduction of polymer formation, the use of an inhibitor can further increase yield and make the synthesis more practical for industrial use.

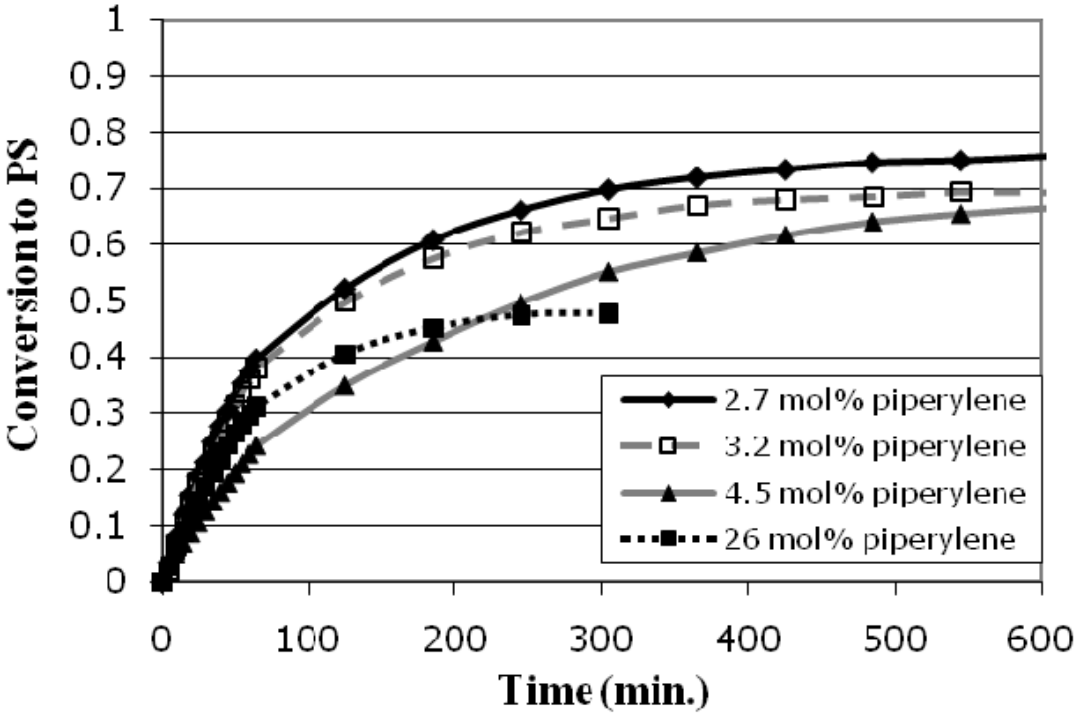

Figure 2-9. Effect of diluting piperylene with excess sulfur dioxide.

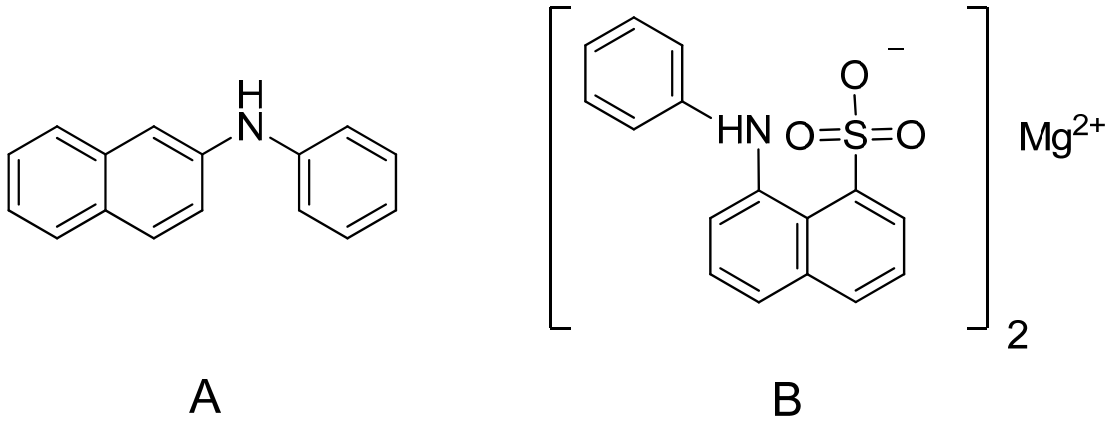

Figure 2-10. Structures of inhibitors: (A) neutral inhibitor and (B) ionic inhibitor.

Inhibitor Effect.

Two radical inhibitors, *N*-phenyl-2 naphthylamine (neutral inhibitor) and 8-anilino-1-naphtalenesulfonic acid magnesium salt (ionic inhibitor), shown in Figure 2-10, were investigated over a range of piperylene concentrations, in all cases at an inhibitor mole fraction of 0.05. When using the neutral inhibitor, 100% PS yield was not obtained, yet an increase in dilution increases PS yield and decreases polymerization (Figure 2-11).

The neutral inhibitor is more effective at preventing polymerization than dilution alone. A comparison between 4.5 mole% piperylene in Figure 3 and 8.8 mole % piperylene with neutral inhibitor in Figure 2-11, shows a difference from 68% PS yield as opposed to 83% PS yield, respectively. However, even at dilute piperylene concentrations (8.8 mole%) with the *N*-phenyl-2 naphthylamine inhibitor, complete conversion to PS is not achieved (only 83% conversion to PS, as illustrated in Figure 2-11).

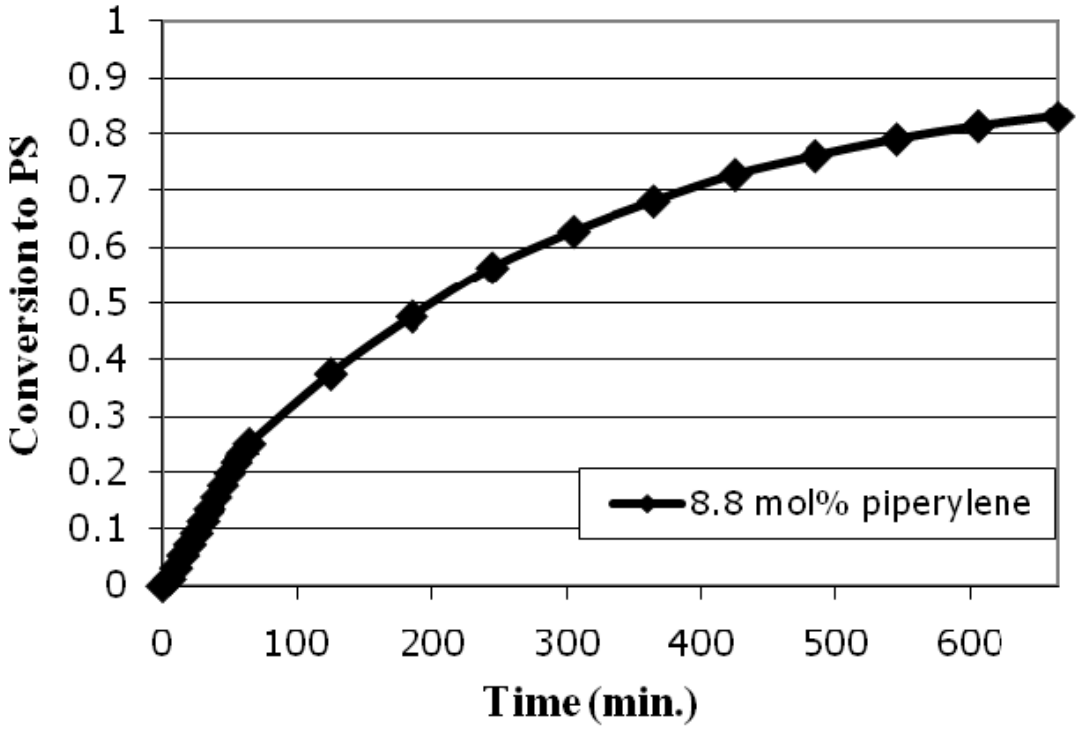

Figure 2-11. Effect of neutral inhibitor (*N*-phenyl-2 naphthylamine) on PS yield at 295K.

The ionic inhibitor gave quantitative yield of PS, with no polymer formation detected by ^{1}H NMR analysis. Thus, the ionic inhibitor appears superior to the neutral inhibitor for constant mole fractions of inhibitor used in our experiments, as shown in Figure 2-11 and Figure 2-12. Several experiments have been conducted under analogous conditions with the use of ionic inhibitor and demonstrate reproducibility of these results. Additionally, the ionic inhibitor allows enhanced separation from the product, PS, as discussed below in the separation section below.

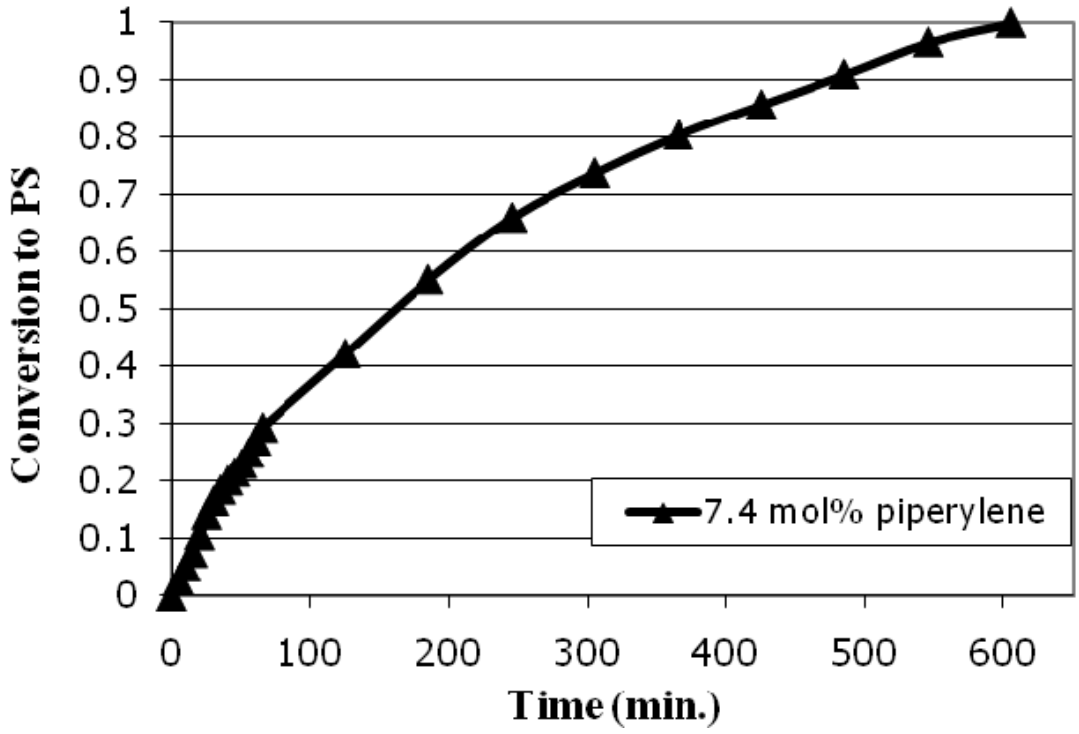

Figure 2-12. Effect of the ionic inhibitor (8-anilino-1-naphtalenesulfonic acid magnesium salt) on PS yield at 295K.

We then proceeded from PS synthesis on the milligram scale in NMR tubes to synthesis on the multi-gram scale (25 milliliters piperylene added to at least 200 milliliters liquid SO_2 and 2.75 grams neutral inhibitor), a scale still suitable for an academic laboratory. The use of expensive and highly concentrated 94% pure *trans*-piperylene is not feasible for large-scale industrial production; thus, we used the kinetic information found to synthesize larger amounts of PS from an industrial source of piperylene that is available in bulk quantities. The raw industrial piperylene we used was composed of a mixture of *cis*- and *trans*- isomers (approximately 50% *trans*, 40% *cis*) as well as other impurities. After 15 hours, we attained an isolated 75% yield of PS (based on the *trans* isomer content) due to the dilution with excess SO_2, then separated the PS

from the inhibitor using a literature method [20]. Under similar conditions of temperature, dilution with excess SO_2, and constant mole fraction of inhibitor, the non-isolated yield from the NMR reactions and isolated yield from the scale-up reactions were less than 10% apart. The list of chemical shifts from the ^{1}H NMR and ^{13}C NMR verify pure production as follows: ^{1}H NMR (ppm): δ=1.36 (d, 3H), 3.69 (m, 3H), 5.95 (m, 2H); ^{13}C NMR (ppm): δ=13.1, 54.9, 59.5, 122.7, 131.6.

Separation.

The literature method [20] involves an extraction of piperylene sulfone into water saturated with sodium chloride, followed by a back-extraction of the PS into dichloromethane, filtration of the impurities over a short pad of silica, and subsequent removal of the dichloromethane. This separation strategy is undesirable for three reasons:

1. The separation method is waste intensive because over 100 moles of waste are generated for each mole of PS produced (over 55 kilograms of waste per kilogram of PS, assuming equal volume of aqueous and organic, and the organic is regarded as waste after the separation),

2. It is expensive due to a large amount of solvents involving extractions and back extractions, and

3. This process uses a halogenated solvent, dichloromethane.

From a process standpoint, the method used in literature was not one that could be easily scaled in regard to minimizing waste generation. We needed a method to separate the inhibitor from piperylene sulfone that could be easily scaled up without the

corresponding increase in waste generation that was currently required. Thus, in order to facilitate a sustainable and scalable process, we developed a new method to purify PS and separate the inhibitor without (1) the use of halogenated solvents, and (2) without generating significant amounts of waste.

The method that we used was an anti-solvent precipitation, where we could take advantage of piperylene sulfones miscibility with nonpolar phases. Specifically, with the addition of a nonpolar liquid CO_2 phase to PS, we leveraged the low solubility of the ionic inhibitor in the nonpolar liquid CO_2.

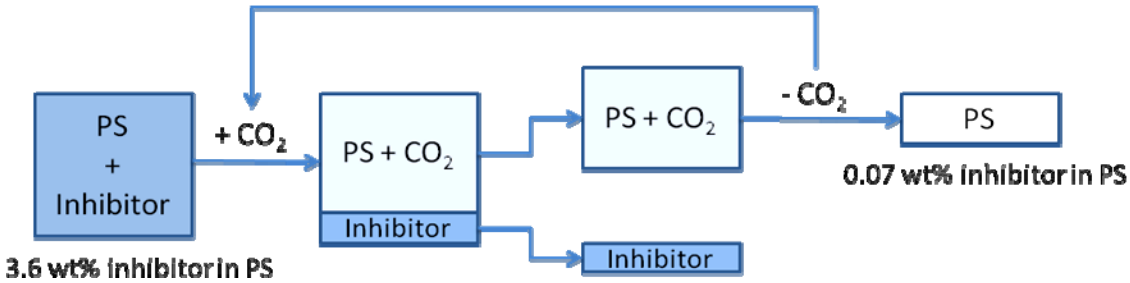

Figure 2-13. Schematic of sustainable CO_2 separation of ionic inhibitor.

As shown in Figure 2-13, we loaded piperylene sulfone containing 3.6 wt% dissolved inhibitor into a windowed Parr reactor. The initial concentration of inhibitor in PS was found using ultraviolet-visible (UV-vis) spectroscopy, as described below. We then added liquid CO_2 to the reactor while stirring. The ionic inhibitor then precipitated out of the mixed PS and CO_2 phase. We could separate the phases, and depressurize the

CO_2 and recover the PS. The PS was analyzed via UV-vis spectroscopy and indicated a reduction in the inhibitor concentration from 3.56 ± 0.05 weight% to 0.07 ±0.02 weight%. The CO_2 experiment was performed at the temperature of 294K and pressure of about 59 bar.

Ultraviolet-visible spectroscopy (UV-vis) is a type of absorption spectroscopy that uses light in the visible and adjacent (ultraviolet) regions to measure electronic transitions from the ground state to their excited state. Through the Beer-Lambert law, shown in Figure 2-14, the concentration of an absorbing species can be directly correlated to the absorbance, as in our experiments the path length and molar absorptivity are constant. A is the absorbance, I_o is the intensity of the incident light, I is transmitted intensity, ε is the molar absorptivity, L is the path length, and C is the concentration. Calibration curves were established to determine absorbances from samples to those of known standards.

$$A = \log(\frac{I_o}{I}) = \varepsilon * L * C$$

Figure 2-14. Beer-Lambert law used to correlate the measured absorbance to concentration.

This method would eliminate the need for a halogenated solvent. Additionally, we assume that the purged CO_2 can be recovered and recycled. It is also important to note here that carbon dioxide is only being used --not generated-- in the separation process and will be recycled in a scaled up process. Assuming recovery and recycle of CO_2, the only

waste generated using this separation method is the inhibitor, which may be able to be recycled. In addition to UV-vis spectroscopy, the PS was analyzed after the separation, using ^{1}H NMR and ^{13}C NMR, as shown in Figure 2-15 and Figure 2-16, and was verified according to literature sources [26, 27]. The presence of ionic inhibitor was not detected in either NMR spectrum.

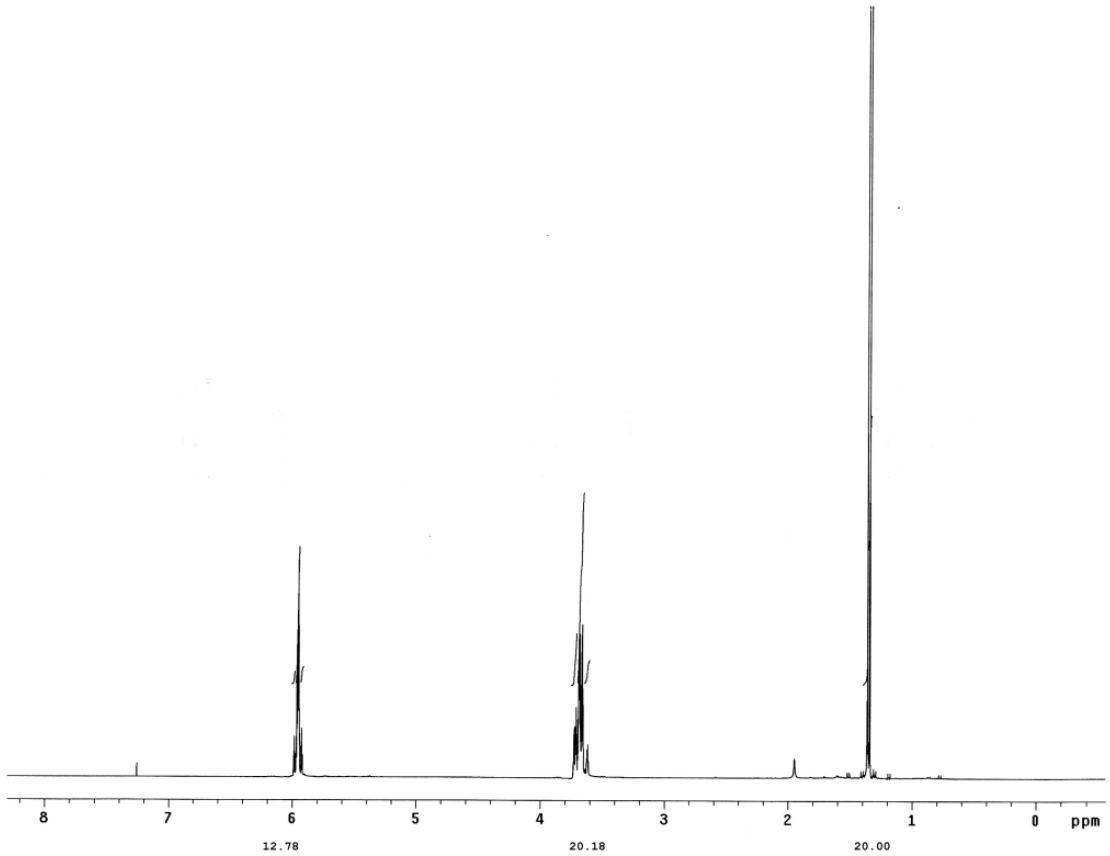

Figure 2-15. ^{1}H NMR of PS after sustainable CO_2 separation.

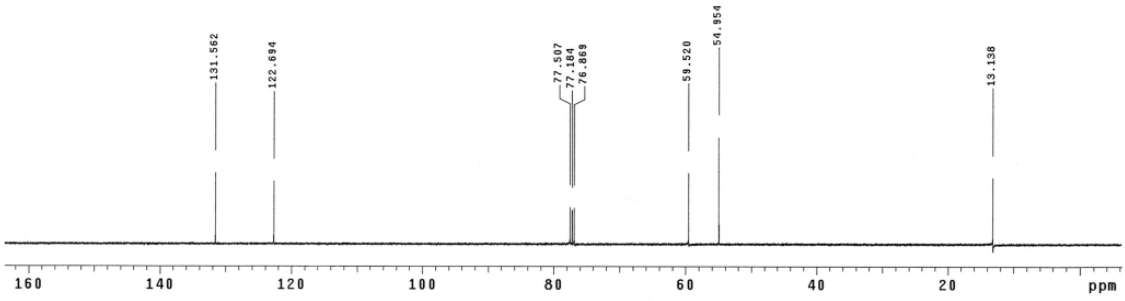

Figure 2-16. ^{13}C NMR of PS after sustainable CO_2 separation.

In Appendix II, we supplement the work we have developed here and construct a HYSYS simulation based on the parameters we acquired regarding the synthesis of PS. This simulation is then used to perform an economic analysis on the piperylene sulfone process from a materials and energy perspective.

2.4 Conclusions

Smart solvents undergo drastic changes in chemical or physical properties upon the induction of a stimulus, and it is this switch that enables facile separation from the product. Piperylene sulfone can be thermally switched from a dipolar aprotic liquid to volatile components. In its liquid form, piperylene sulfone has solvent properties similar to DMSO. Furthermore, once separated from products, these volatile components can be recombined to form the piperylene sulfone molecule, allowing for complete solvent recycle.

We have demonstrated a method for transitioning from a laboratory synthesis to a less waste intensive and sustainable method for the industrial scale production, where we have overcome previous barriers, including low yields and significant waste generation. This chapter has shown the scalable synthesis of the fully recyclable dipolar aprotic solvent, piperylene sulfone. For this reaction, we attained the kinetic parameters of PS formation and shown that the synthesis reaction reaches completion in less than one-quarter of the original time given. Additionally, we have demonstrated suppression of undesirable polymerization, allowing for quantitative yields of product to be attained. Furthermore, we have developed a novel separation method utilizing non-toxic materials to overcome the use of halogenated solvents in minimizing waste. Lastly, we have

completed a HYSYS simulation for the industrial scale synthesis, separation, and purification of piperylene sulfone. It should be noted that SO_2 is a hazardous gas and small amounts of water present during processing could lead to material corrosion, and we recognize these potential drawbacks in its use. However, processing SO_2 is common in the refining industry, and the expertise is established to handle it. In summary, the production of piperylene sulfone demonstrates the innovative progression of novel techniques and laboratory discoveries to a more useful form. This research is a critical first step towards the implementation into industry.

2.5 References

[1] Jimenez-Gonzalez, Concepcion; Poechlauer, Peter; Broxterman, Quirinus B.; et al., *Key Green Engineering Research Areas for Sustainable Manufacturing: A perspective from Pharmaceutical and Fine Chemicals Manufacturers*, Organic Process R&D, 2011. **15**: p. 900.

[2] Sheldon, RA., *Green Solvents for sustainable organic synthesis: state of the art,* Green Chemistry, 2005. **7**: p. 267.

[3] Beckman, E.J., *Supercritical and near-critical CO2 in green chemical synthesis and processing*. Journal of Supercritical Fluids, 2004. 28: p. 121-191.

[4] Jessop, P.G. and B. Subramaniam, *Gas-Expanded Liquids*. Chemical Reviews, 2007. **107:** p. 2666-2694.

[5] Kruse, A.D., E., *Hot compressed water as reaction medium and reactant: Properties and synthesis reactions*. Journal of Supercritical Fluids, 2007. **39:** p. 362-380.

[6] West, K.N.H., Jason P.; Jones, Rebecca S.; Bush, David; Liotta, Charles L.; Eckert, Charles A., *CO2-Induced Miscibility of Fluorous and Organic Solvents*

for Recycling Homogeneous Catalysts. Industrial and Engineering Chemistry Research, 2004. **43:** p. 4827-4832.

[7] Welton, T., *Room-Temperature Ionic Liquids*. Solvents for Synthesis and *Catalysis*. Chemical Reviews, 1999. **99:** p. 2071-2083.

[8] Constable David J. C.; Dunn Peter J.; Hayler John D.; et al., *Key green chemistry research areas–a perspective from pharmaceutical manufacturers*, Green Chem., 2007. **9:** p. 411.

[9] Raymond Michael J.; Slater C. Stewart; Savelski Mariano J., *LCA approach to the analysis of solvent waste issues in the pharmaceutical industry*, Green Chem., 2010. **12:** p. 1826.

[10] Lapkin, A., and Constable, D., *Green Chemistry Metrics. Measuring and Monitoring Sustainable Processes*, Wiley, 2008.

[11] Dunn, P.J., in 10th Green Chemistry and Engineering 2006: Washington D.C.

[12] Suarez, D.; Sordo, T. L.; Sordo, J. A., *A Comparative Analysis of the Mechanisms of Cheletropic and Diels-Alder Reactions of 1,3-dienes with Sulfur Dioxide – Kinetic and Thermodynamic Controls.* J. Org. Chem., 1995. **60:** p. 2848-2852.

[13] Staudinger, H.; Ritzenthaler, B., *High polymers links, 104 Announcement - On the adsorption of sulphur dioxide on ethylene-derivatives.* Berichte Der Deutschen Chemischen Gesellschaft 1935. **68:** p. 455-471.

[14] Frank R.; Adams C.; Blegen J.; Deanin R.; and Smith P., *Effects of Impurities on Copolymerization of Isoprene and Styrene.* Ind. Eng. Chem., 1947. **39:** p. 887.

[15] Craig, D., *The Geometric Isomers of Piperylene*. Journal of the American Chemical Society 1943. **65:** p. 1006-1013.

[16] Drake, L. R.; Stowe, S. C.; and Partanksy, A. M., *Kinetics of the Diene Sulfur Dioxide Reaction*, J. Am. Chem. Soc., 1946. **68:** p. 2521-2524.

[17] Vinci, D.; Donaldson, M.; Hallett, J. P.; John, E. A.; Pollet, P.; Thomas, C. A.; Grilly, J. D.; Jessop, P. G.; Liotta, C. L.; Eckert, C. A., *Piperylene sulfone: a labile and recyclable DMSO substitute.* Chemical Communications 2007. **14**: p. 1427-1429.

[18] Donaldson, M. E.; Mestre, V. L.; Vinci, D.; Liotta, C. L.; Eckert, C. A., *Switchable Solvents for in-Situ Acid-Catalyzed Hydrolysis of beta-Pinene.* Industrial & Engineering Chemistry Research 2009. **48**: p. 2542-2547.

[19] Jiang, N.; Vinci, D.; Liotta, C. L.; Eckert, C. A.; Ragauskas, A. J., *Piperylene sulfone: A recyclable dimethyl sulfoxide substitute for copper-catalyzed aerobic alcohol oxidation.* Industrial & Engineering Chemistry Research 2008. **47:** p. 627-631.

[20] Krug, R. C.; Rigney, J. A., *Unsaturated Cyclic Sulfones. 4. Isomeric 2-Methyldihydrothiophene 1,1-Dioxides.* Journal of Organic Chemistry **1958.** 23: p. 1697-1699.

[21] Frey, F. E. *Process of Separating Geometric Isomers of Piperylene from Each Other.* US Patent 2430395, November 4, 1947.

[22] Frank, R. L.; Emmick, R. D.; Johnson, R. S., *Cis-Piperylenes and Trans-Piperylenes.* Journal of the American Chemical Society 1947. **69:** p. 2313-2317.

[23] Fried, J. R., Polymer Science and Technology. Prentice Hall: 1995.

[24] Grummitt, O.; Ardis, A. E.; Fick, J., *Thermal Dissociation of Methyldihydrothiophene-1-Dioxides.* Journal of the American Chemical Society 1950. **72:** p. 5167-5170.

[25] Morris, R. C.; Finch, H. deV. Separation of Diolefins. US Patent 2373329, 1945.

[26] Yamada, S.; Ohsawa, H.; Suzuki, T.; Takayama, H., *Stereoselective Synthesis of (E)-Conjugated, (E,Z)-Conjugated, and (E,E)-Conjugated Dienes via Alkylation of 3-Sulfolenes as the Key Step.* Journal of Organic Chemistry 1986. **51**: p. 4934-4940.

[27] Chou, T. S. T., His Hua; Chang, Lee Jean, *Study of the alkylation reactions of sulfol-3-enes.* Journal of the Chemical Society- Perkin Transactions 1 1985. **3:** p. 515-519.

CHAPTER III

CONTINUOUS FLOW PROCESSING

3.1 Introduction:

The pharmaceutical industry is dedicated to the development of drugs that can allow patients to live longer, healthier, and more productive lives; they also seek to bring these drugs to the patient with a minimal impact on the environment [1]. However, historically the pharmaceutical and fine chemical industries were shown to have the highest E-factors in the chemical industry, with ranges commonly from 25-100 and 5-50, respectively [2]. The E-factor is simply a measure of the mass (kilograms) of waste divided by the mass of product produced, and was originally published in 1992 [2]. The manufacture of fine chemicals is typically performed in batch reactors where annual production quantities range from 50-5000 tons. The pharmaceutical industry also employs batch reactors with even smaller annual productions, usually from 5-100 tons. Combine these annual production quantities with the high E-factors, and one can see the significant amount of waste that is being generated for the relatively low amount of high-value product being produced. Since the introduction of the E-factor metric nearly 20 years ago, the pharmaceutical and fine chemical industries have shifted from a focus on increasing process efficiency to the elimination of waste and maximizing use of raw materials [3].

In 2005, the American Chemical Society (ACS) Green Chemistry Institute and several major pharmaceutical firms established the Pharmaceutical Roundtable in order to implement green chemistry and engineering into pharmaceutical research, development,

and production practices. To this end, the Roundtable has identified several priorities and methods with which to implement their agenda. Then in 2007, the Roundtable published a list of key green chemistry research areas [1]. This was followed by the publication of the key green engineering research areas as from the viewpoint of pharmaceutical and fine chemical manufacturers [4]. The process in order to determine these key green engineering research areas is given in Figure 3-1. The results of their collaboration are shown in Figure 3-2.

Figure 3-1. Process used by the Roundtable to identify the key green engineering areas.

Rank	Main Key Areas	Sub-areas/aspects	Votes
1	Continuous Processing	Primary, Secondary, Semi-continuous, etc.	12
2	Bioprocesses	Biotechnology, Fermentations, Biocatalysis, GMOs,	11
3	Separation and Reaction Technologies	Membranes, crystallizations, etc.	11
4	Solvent Selection, Recycle and Optimization	Property modeling, volume optimization, recycling technologies, in process recycle, regulatory aspects etc.	10
5	Process Intensification	Technology, process, hybrid systems, etc	9
6	Integration of Life Cycle Assessment (LCA)	Life cycle thinking, Total Cost Assessment, carbon / eco-footprinting, Social LCA, streamlined tools	4
7	Integration of Chemistry and Engineering	Business strategy, links with education, etc.	4
8	Scale up aspects	Mass and energy transfer, Kinetics, and others	3
9	Process Energy Intensity	Baseline for pharmaceuticals, estimation, energy optimization	1
10	Mass and Energy Integration	Process integration, Process Synthesis, Combined Heat and Power, etc	0

Figure 3-2. Key green engineering research areas as identified by the Pharmaceutical Roundtable.

At the top of the list of green engineering research areas is continuous processing. Batch processing is the current method of conducting reactions for the vast majority of the pharmaceutical industry, as long has been this case [1]. In fact, traditional manufacturing designs used in the pharmaceutical and fine chemical industries utilize multipurpose batch plants for active pharmaceutical ingredients (API) and formulated drugs. However, there are challenges in scaling up a process using batch technology including the discrepancy between macro and meso mixing within large and small reactors, the time at which to transfer heat into or out of a reactor-as these transfer rates are typically not the same, and the variations in separation and filtration as isolation times or crystal formation may be affected.

As the pharmaceutical industry is currently undergoing significant changes in response to increased cost pressures, business and market demands, and a changing environment, they have carefully considered improvements in productivity, reductions in waste, and quality/control improvement [4].

In order to address these challenging issues and remain competitively positioned, the notion and implementation of process intensification is rapidly gaining interest. In brief, process intensification focuses on the optimization of energy, capital, environmental footprint, and safety combined with a reduction in physical size of the plant. The implementation of this idea requires a significant shift in culture which may be an equal if not greater challenge than the technical implementation. According to Dr. Ramshaw, Chair of Chemical Engineering at Newcastle University and pioneer in the field of process intensification, “a strategy of process intensification requires a step

change in the philosophy of plant and process design. If effectively implemented, it will lead to major improvements in environmental acceptability, energy efficiency, intrinsic safety and capital cost. A major cultural change is required on behalf of chemists, engineers and managers and it is this, rather than technical difficulty which represents the main obstacle to progress" [5]; once the traditional batch reaction approach is taken in the initial development process, transitioning to a continuous approach is much more difficult to implement.

Process intensification is a very recent subject of attention in the chemical field, as the notion is only about three decades old. It consists of any development in the chemical engineering field – via novel techniques, equipment and methods – to bring about significant improvements in manufacturing and production processes that result in smaller, cleaner, and more energy efficient technology. New technologies have been motivated by improved chemistry, safety, processing energy and environmental benefits, lower inventories, capitol cost reduction, enhanced corporate image, enhanced products, and value to customers [6]. In fact, the cost of main plant equipment, such as the reactors separators, and other vessels, accounts for 20% of the initial capital, whereas the remaining 80% accounts for piping, structural support, installation, etc.

Continuous processing is one part of process intensification where the objective several fold: the reduction of costs, reduction in the size of equipment, improving quality of product, reduction of energy consumed, and reduction of solvent and waste which result in a reduction of the environmental footprint [4]. Through improved mass and heat transfer coefficients, the continuous process may be operated more intensely at higher temperatures resulting in more economic reactions with higher atom efficiency and

increased product quality. This product quality is also more consistent when the continuous flow reactor is operated continuously at steady state as compared to dynamically run batch reactions, which have batch-to-batch variability. Using batch reaction technology, a number of scale up steps are required before reaching production scale, whereas fewer, if any scale up steps are required for continuous processing.

Additional processing benefits realized when using continuous flow include greater safety due to lower holdup volumes of hazardous reagents or solvents. Therefore, the risks when dealing with hazardous chemistry are decreased as the gaseous headspace is eliminated in continuous flow, whereas the gaseous components in the headspace of a batch reactor can lead to explosive conditions which is a barrier in commercialization [7]. The concentration of solvent can be reduced in a flow reactor, allowing for higher concentration reactions, or even neat reactions to be run. This will also reduce the emissions associated with solvent processing and operation.

Continuous flow technology is especially superior for reactions involving a temperature sensitive and/or a highly reactive intermediate [8], reactions with hazardous reagents [9], and reactions of biphasic systems, preventing thermal degradation or explosive evolution [10] through improving mass and heat transfer[11, 12]. The pharmaceutical industry is continually searching for controllable, information-rich, high-throughput and environmentally friendly methods of producing compounds with a high degree of chemical selectivity [13]. Indeed, small scale continuous flow technology offers a different approach that allows for expeditious technology transfer from laboratory to manufacture scale [9, 14, 15].

One metric critical to the pharmaceutical industry is the ability to bring drugs to market in the shortest time possible in order to take full advantage of the patent, widely known as time-to-market. Given the continuous production of a compound at the laboratory scale as opposed to batch processing, the time required for the regulatory authority to approve of a new process will be drastically reduced in the transition to full scale processing. This is due to the use of already proven equipment as the laboratory scale is the full scale, where this type of processing is referred to as scale out as opposed to scale up pertaining to traditional batch reaction technology.

To demonstrate the benefits of changing from batch to continuous flow technology, we use as an example the Meerwein-Ponndorf-Verley (MPV) reduction [16]. This is an important reaction in both industry and academia as a method for the reduction of carbonyls to their respective alcohols and specifically its use in the pharmaceutical industry as a key transformation makes it a valuable reaction to implement. This reaction is a commonly used pathway in the production of pharmaceutical intermediates, such as HIV protease inhibitors. For example, the production of Saquenavir®, Amprenavir® and Atazanavir® are formed through the (2S, 3S)-CMA* **(2)** and (2R, 3S)-CMA† **(3)** intermediate. They are prepared through an MPV reduction of (S)-CMK‡ **(1)**, generally using a high loading and commonly stoichiometric quantities (50 mole%) of the $Al(O\textit{i}Pr)_3$ catalyst in isopropanol at 50°C for about 2 hours. Our objectives were to

---

* N-(*tert*-butoxycarbonyl)-(3S)-3-amino-1-chloro-4-phenyl-(2S)-butanol
† N-(*tert*-butoxycarbonyl)-(3S)-3-amino-1-chloro-4-phenyl-(2R)-butanol
‡ N-(*tert*-butoxycarbonyl)-(3S)-3-amino-1-chloro-4-phenyl-2-butanone

improve the current MPV reduction and enable the use of the MPV reduction in continuous flow.

MPV reductions are chemoselective and use mild reaction conditions. The catalyst that is typically used is $Al(OiPr)_3$ in isopropanol, functioning as both the reagent and the solvent. The $Al(OiPr)_3$ catalyzed reductions take several hours to reach completion [16]. The MPV reduction is a reversible reaction, and in fact the reverse reaction is the Oppenauer oxidation [17], hence the formation of the alcohol reduction products is favored by optimizing temperatures, using large excess of the metal catalyst, and/or a secondary alcohol (in our case here, this is isopropanol) which functions as both the reagent and the solvent.

In order to define and demonstrate the applicability of MPV reduction processes in continuous flow technology, our primary objective was to established a more active catalyst for shorter reaction time. In addition to the optimization of reaction conditions, many catalysts [18] have been developed to enhance the MPV reduction with respect to rate as well as the yield for the reductions of aldehydes and ketones, including bidentate aluminum reagents [19], alkylboranes [20], and lanthanide based systems [21]. For example, bidentate aluminum species have been used successfully to improve the reduction of benzaldehyde; however, the formation of the bidentate ligands requires in-situ synthesis from reactive, highly air-sensitive trimethylaluminum. Although improvements were made to the reaction performances, practical industrial applications remain limited by the reactive nature of alkylaluminum species.

Alternatively, aluminum alkoxide catalysts such as $Al(OtBu)_3$ have not been studied extensively. $Al(OtBu)_3$ for instance does not have an α-proton available to

perform the reduction to proceed, making it intuitively a poor choice for MPV reduction. Few reports have documented the use of $Al(OtBu)_3$ in the MPV reduction including its use as an aluminum catalyst to assist in the stereochemical outcome of one particular reduction [22] and the in situ formation of TFA-$Al(OtBu)_3$ adducts [23] which reduce benzaldehyde at an enhanced rate compared to the conventional reduction but suffer from competing aldol reactions.

In this chapter, we show how our use of $Al(OtBu)_3$ has enabled the transition to continuous flow as an highly active, efficient and cost-effective catalyst for MPV reductions of aldehydes and ketones to their corresponding alcohols, and then we show the successful MPV reductions of benzaldehyde and acetophenone in continuous mode.

3.2 Experimental:

Methods and Materials.

All solvents were purchased in their anhydrous form from Sigma Aldrich. Acetophenone and benzaldehyde were distilled before using. All other chemicals were purchased from Sigma Aldrich and used as received.

Batch Reactions.

For purposes of comparisons we ran batch reactions in a Brinkmann 12-reaction carousel apparatus equipped with a heating and reflux block, integrated temperature controller, and simultaneous stirring of all 12 glass reaction vessels (1 to 20 mL total volume). This apparatus allowed for excellent control temperature, mixing, and reaction under an inert atmosphere. All solutions and reagents were prepared under anhydrous

conditions. The integrated reflux head of the carousel system is controlled by a heat exchanger (Thermo Election Corp., NESLAB RTE7).

MPV batch reactions were reductions of benzalydehyde or acetophenone: $Al(O\textit{t}Bu)_3$ (0.11 mmol/mL for 20 mol% catalyst loading) was stirred in anhydrous toluene at reaction temperature under argon atmosphere. A 0.75mmol/mL stock solution of benzaldehyde (or 0.78 mmol/mL acetophenone) in isopropanol was added to start the reaction. The batch reactions all had a total reaction volume per vessel of 5 mL, and, unless otherwise stated, a 3:2 volume ratio of toluene/isopropanol. Upon reaching the desired reaction time, each reaction vessel was placed in an ice bath, quenched with 2 mL of 2 M HCl, stirred for 5 minutes, and diluted with 30 mL of Methanol. Two samples were taken for subsequent HPLC analysis. The quenched reaction solution was then diluted 10:1 for HPLC analysis. The organic content was quantified using the calibration curves. The batch MPV reductions using benzaldehyde conducted at the 40°C temperature allowed us to more easily obtain kinetic information on the progression of the reaction. On the other hand, the reduction of acetophenone was carried out at 50°C.

Continuous Reactions.

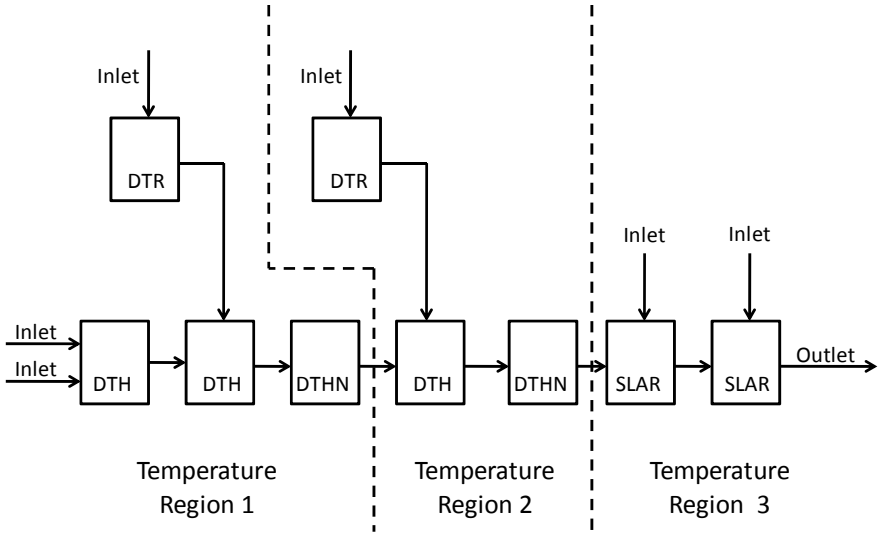

Figure 3-3. Schematic of the Corning continuous flow reactor.

We employed a Corning Advanced-Flow Reactor (AFR), as illustrated in Figure 3-3. This reactor is a versatile glass continuous flow reactor constructed of standard borosilicate glass and is compatible with a wide range of chemicals and solvents over a wide range of temperatures (-60^{o}C to 200^{o}C) and pressures (up to 18 bar). Corning has specifically engineered these mixing reactor modules for heterogeneous systems. Linear reactor modules are used for heating or cooling and residence time. All of the reactor modules are jacketed for enhanced thermal control (-60^{o}C to 200^{o}C, up to 3 bar) and has three possible temperature regions and six possible inlets. Of the 9 total modules, 8 modules were used for the MPV reduction. Two modules are used to preheat the reagents to the specified reaction temperature, and 6 more modules are used for reaction: 4 modules are of the mixing type (DTH for 2 inlets and DTHN for one inlet, which is the designation used by Corning), and 2 modules are of the linear type (SLAR for two inlets and DTR for one inlet) and were used to extend the residence time, as shown in Figure 3-4.

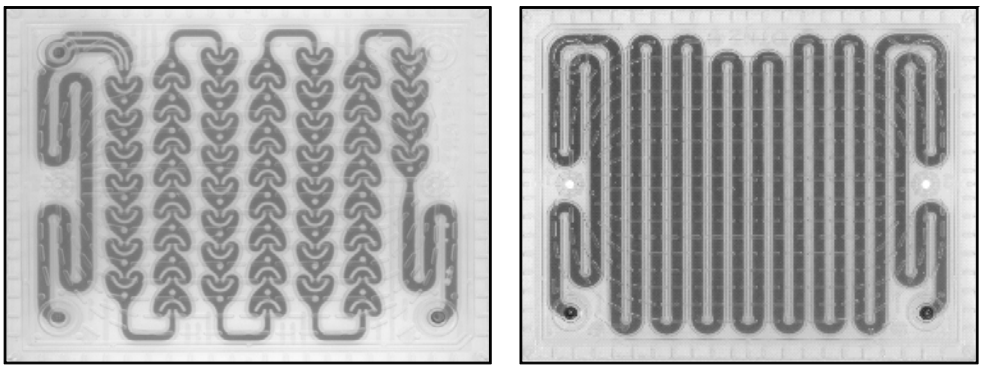

Mixing module (DTH) Linear module (DTR)

Figure 3-4. The mixing and linear reactor modules of the Corning® glass reactor.

The reagents were stored in two separate solution reservoirs. They were pumped into the flow reactor with ISCO syringe pumps in a ratio of 3:2 toluene/isopropanol and the residence time was defined by setting the flow rates. Rotameters at the inlet of the reactor were installed to verify the flow rates. Our system, which includes two ISCO 500D Syringe Pumps and two heat exchangers (a LAUDA Integral XT150 and a Thermo Election Corp. NESLAB RTE7), is contained in a floor-to-ceiling hood in our laboratory. We monitored the temperatures by thermocouples that were installed into the heat exchanger fluid modules. Pump flow rates are monitored using flow meters (Omega, PTFE construction and sapphire float). The system pressure is measured using pressure gauges (Matheson, 316 stainless steel, 0-30psig) and both inlets to the reactor have pressure relief valves (Swaglok, 316 stainless steel).

All continuous flow reactions were performed using the Corning system. Stock solutions of the reagents were prepared under anhydrous conditions. A 0.75 mmol/mL solution of benzaldehyde in isopropanol was made and 1.0 vol% dodecane was added to

the solution to make the final stock solution. For 20 mol% catalyst loading experiments, a 0.11 mmol/mL solution of $Al(OtBu)_3$ in toluene was made and 1.0 vol% nonane was add to the solution to make the final stock solution. For 5 mol% catalyst loading experiments, a 0.03mmol/mL solution of $Al(OtBu)_3$ in toluene was made and 1.0 vol% nonane was add to the solution to make the final stock solution. The hydrocarbons dodecane and nonane are added as internal standards; they do not participate in the reaction. Solids were weighed out using a balance (Mettler Toledo, AT21 DeltaRage ®, ± 0.001g). Liquid compounds were measured using NORM-JECT luer lock syringes and Eppendorf research pipettes.

One ISCO is used to deliver the catalyst in toluene, and the other ISCO is used to deliver the substrate in alcohol. Before initializing the flow experiments, the piston pumps were loaded with the reagent and catalyst stock solutions. A filter (Swagelok, 140 micron) was used when loading the catalyst stock solution. The ISCO reservoirs do not have mixing, so before each flow rate experiment an initial sample of the reagent solutions was collected after the flow meter to account for any concentration gradient in the reservoir. The ISCO pumps continuously delivered the stock solutions to the Corning reactor at a 2:3 volume ratio of reagent to catalyst. The system was allowed to equilibrate for two reactor volumes at the set flow rate before collecting samples. After equilibrium, three reaction samples were collected, one reactor volume apart, and averaged to calculate experimental error.

For organic content analysis, 1.0 mL of the collected reaction sample was cooled in an ice bath, quenched with 0.4 mL of 2M HCl for 5 min and then diluted with 16 mL of methanol. The quenched reaction solutions were then diluted 10:1 for HPLC analysis.

This dilution was repeated twice. The disappearance of starting material for conversion and appearance of product for yield calculations was quantified using calibration curves as follow: benzaldehyde at 254 λ and 2.64 min, R^2= 0.999; benzyl alcohol at 210 λ and 1.73 min, R^2 = 0.999; acetophenone at 210 λ and 2.72 min, R^2 = 0.994; and 1-phenylethanol at 210 λ and 2.03 min, R^2 = 0.987.

The internal standards, nonane and dodecane were monitored by GC from a 1.0 mL sample collected from reaction (nonane at 2.9 min, dodecane at 7.9 min). The ratio of the internal standard peak area after reaction to that before reaction, as initial samples, allows us to monitor accurately the volume ratio from the two piston pumps. This ratio was used to calculate the amount of benzaldehyde available for reaction and accurately calculate yield and conversion when combined with the HPLC data.

Analysis.

The reaction streams were quenched in the same molar proportions as batch reactions with 2M HCl, diluted with methanol, and quantified using HPLC. To verify the flow rates and concentrations, we used two internal standards: dodecane and nonane, and performed a GC analysis. The internal standards were added in 1 vol% to the isopropanol solution and to the toluene/catalyst solution, respectively. The homogenous reaction mixture (reactants, products, and internal standards) was collected upon exiting the reactor, and analyzed using a HP 6890 Series GC equipped with an FID detector and a HP-5 capillary column (30m x 0.25 mm and 0.25 μm). By comparing the ratio of the internal standards in the reaction mixture to that in the stock solutions via GC, we were able to confirm flow rates.

HPLC/GC analysis method.

Reaction samples were run on an HP 1100 series HPLC equipped with a UV detector, and used a Phenomenex Luna 5μ C18(2) reverse phase column. A guard column was used to prevent clogging. An isocratic HPLC method using water (0.1 vol% trifluoroacetic acid in water) and acetonitrile as the mobile phases at 1.5mL/min was used for the analysis. For continuous flow experiments, the internal standards nonane and dodecane were analyzed using an Agilent 6890 series GC with FID detector. A HP-5 column 30m x 0.25 mm and 0.25 μm was used and helium was the carrier gas. Calibration curves were performed in order to determine the concentration of the compounds: benzaldehyde and acetophenone and their corresponding alcohols, benzyl alcohol and 1-phenylethanol, respectively.

3.3 Results

We demonstrated the first continuous Meerwein-Ponndorf-Verley (MPV) reduction in a Corning® Advanced-Flow Reactor (AFR) using two model compounds, benzaldehyde and acetophenone. With the development of a more active catalyst, $Al(O\textit{t}Bu)_3$, for MPV reductions, we have enabled the transition from batch to continuous flow mode for this pharmaceutically significant reaction.

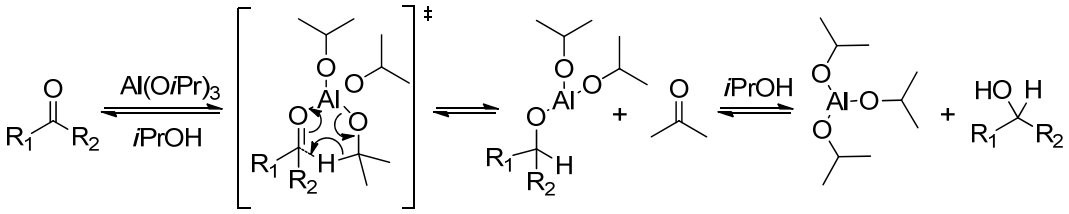

Figure 3-5: Six-membered transition state of the aluminum complex during reduction.

The accepted MPV mechanism [25], shown in Figure 3-5, first requires coordination of the Al(O*i*Pr)$_3$ catalyst with the carbonyl containing substrate through a Lewis interaction. Next, a hydride transfer (the α- hydrogen) from the methylene carbon on the isopropoxide ligand proceeds through a 6-membered transition state, forming acetone and the desired alcohol product. In the presence of excess isopropanol, displacement of the alcohol product with isopropanol regenerates the active the catalyst. Although Al(O*t*Bu)$_3$ does not have α-hydrogens for MPV reduction, it is known that aluminum alkoxide ligands can undergo ligand exchange in the presence of isopropanol [25]. As a result, not only did the MPV reductions of all three carbonyl substrates we have investigated proceed to high yields using Al(O*t*Bu)$_3$, significant rate enhancements were achieved.

The Al(O*t*Bu)$_3$ catalyst gives superior activity, as we first demonstrated with two model compounds: benzaldehyde **1** and acetophenone **2**. The reduction of *N*-(*tert*-butyloxycarbonyl)-(3*S*)-3-amino-1-chloro-4-phenyl-2-butanone **3** or (S)-CMK, a key intermediate in HIV-protease inhibitor synthesis [24] was also investigated (in Table 3-1). All three compounds were investigated as a function of catalyst type (Al(O*t*Bu)$_3$ *vs*. Al(O*i*Pr)$_3$), time, and solvent. Table 3-1 displays the yields of the reaction for each model compound with Al(O*t*Bu)$_3$ *vs*. Al(O*i*Pr)$_3$ at selected reaction times. In the reduction of **1** as shown in Figure 3-6, 30 minutes was found to be a sufficient time for complete

reduction with 50 mol% Al(O*t*Bu)$_3$ whereas Al(O*i*Pr)$_3$ under the same conditions only reached 32% yield. The reduction of **2** (Figure 3-7) and **3** (Figure 3-8) both follow the same trend in rate enhancement from 31% yield compared to 75% yield in the reduction of **2** and 31% to 100% in the reduction of **3** with Al(O*t*Bu)$_3$ compared with Al(O*i*Pr)$_3$, respectively. The current industrial scale production of the product alcohols from 3 is performed through an MPV reduction using a 50 mol% loading of Al(O*i*Pr)$_3$ in isopropanol at 50^{o}C [26].Using those same conditions, the reduction using Al(O*t*Bu)$_3$ was complete after 40 minutes, as compared to only 32% complete in 40 minutes with the conventional Al(O*i*Pr)$_3$ catalyst. The reduction of **3** was faster than **2** most likely due to the precipitation of alcohol products as the reaction progressed.

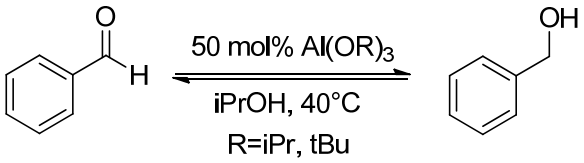

1

Figure 3-6. MPV reduction of benzaldehyde with 50 mol% catalyst in isopropanol.

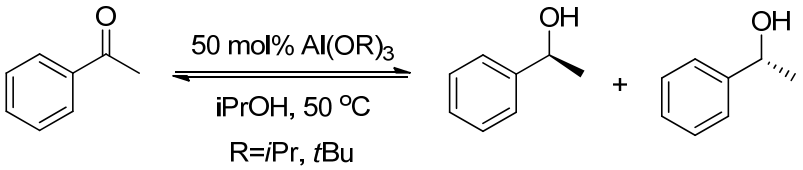

2

Figure 3-7. MPV reduction of acetophenone with 50 mol% catalyst in isopropanol.

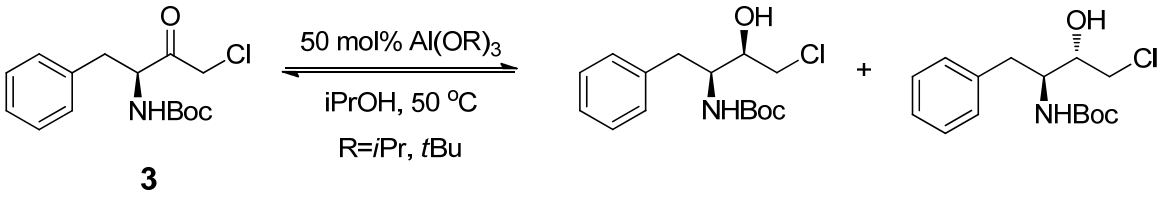

Figure 3-8. MPV reduction of (S)-CMK with 50 mol% catalyst in isopropanol.

Table 3-1. MPV Reductions of benzaldehyde, acetophenone, and (S)-CMK

Entry Number	Reaction Temp[a]	% Yield (HPLC)[b] $Al(OiPr)_3$ 50mol%	% Yield (HPLC)[b] $Al(OtBu)_3$ 50mol%
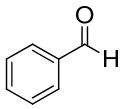	40	32	100
		85	100
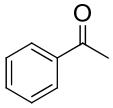	50	5	25
		31	75
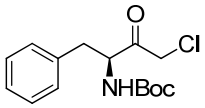	50	5	80
		32	100

[a]Reactions were conducted in a glass tube at the selected temperature (5 mL isopropanol and 50 mol% catalyst were stirred under inert atmosphere). Carbonyl substrate was added to begin the reaction and quenched with 2M HCl and methanol at desired time. Reactions were run in triplicate. [b]HPLC/ UV-Vis analysis was conducted to determine the yields of the reductions.

The difference in aggregation state is suspected to contribute to the superior activity of aluminum tert-butoxide. In fact, aluminum isopropoxide (as shown in Figure 3-9) is known to exist as a tetramer while the aluminum tertbutoxide (as shown in Figure 3-10) is a cyclic dimer [27] in a solvent such as benzene. The dimeric structure has two bridging t-butoxide ligands and four exchangeable ligands. In order for reduction to occur using $Al(O\mathit{t}Bu)_3$, exchange of non-bridging (the only one participating in the reaction) [27] tert-butoxy ligands by the nonreactive isopropoxide ligands from isopropanol is paramount. The dimeric and tetrameric states of the two aluminum species conducted in our laboratories were consistent with the literature report, confirming the exchange of isopropoxide ligands in $Al(OtBu)_3$ while the state of aggregation remains the same.

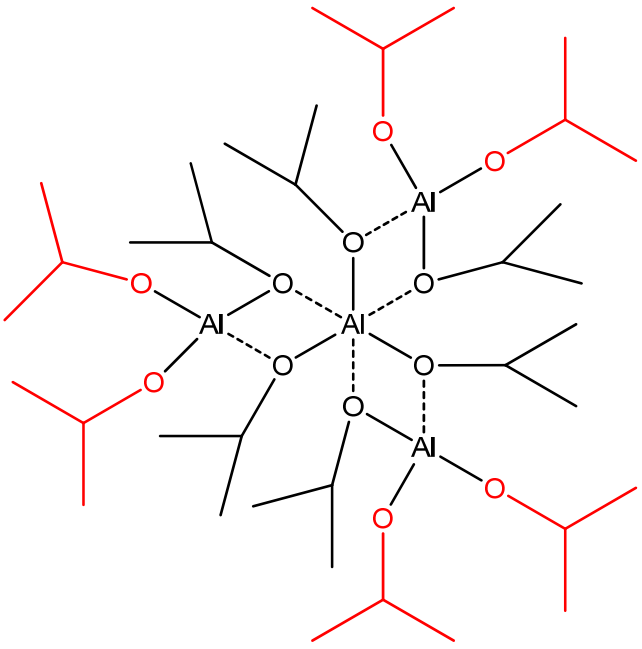

Figure 3-9: Tetrameric State of Aggregation in $Al(OiPr)_3$

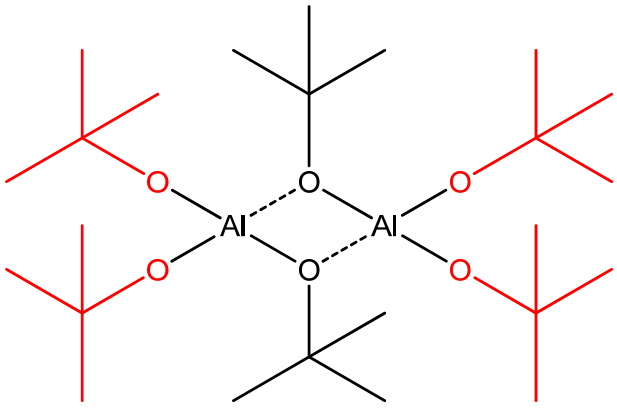

Figure 3-10: Dimeric State of Aggregation in $Al(OtBu)_3$

Next, a better understanding of the reaction variables was explored in order for optimization and subsequent implementation to continuous flow. We investigated both catalyst loading and solvent system in the MPV reduction. Comparison of catalyst loadings from 50 to 5 mol% were conducted on the reduction of (S)-CMK. Additionally, we investigated this rate enhancement in mixed solvent systems. This is necessary for transition to a continuous flow system to ensure solubility of reactants, catalyst, and products formed through the residence time allocated. We began by using a 9:1 ratio of toluene:isopropanol in the reduction of benzaldehyde at 40°C with 50 mol% loading of $Al(O\textit{t}Bu)_3$. It is noted in Figure 3-11 that the rate enhancement is still obvious when using $Al(O\textit{t}Bu)_3$. We have connected the points with a curve to aid in a visual understanding of the data. Upon optimization of the reduction of benzaldehyde using catalyst loadings 20 mol% and lower and increasing the reaction temperature in a mixed solvent system of toluene and isopropanol an investigation into the implementation of the MPV reduction of benzaldehyde to continuous flow was realized. Additionally, other

members of the group verified these results using (S)-CMK in batch reactions at 50 °C using both Al(O*t*Bu)$_3$ and Al(O*i*Pr)$_3$, as shown in Figure 3-12.

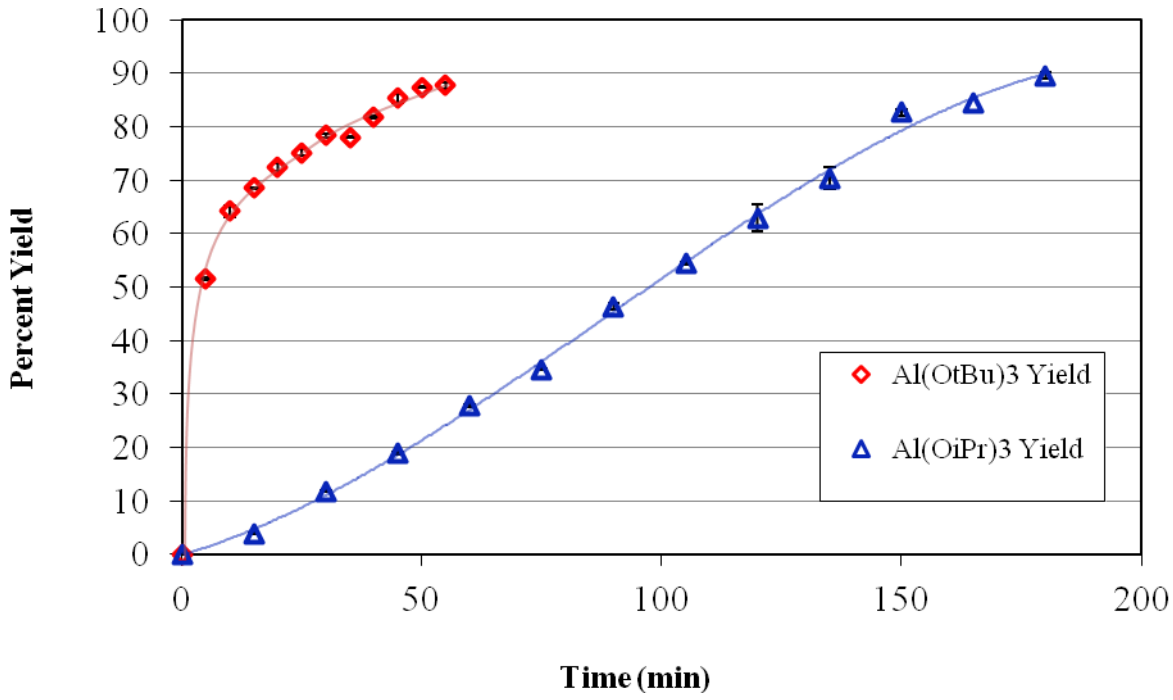

Figure 3-11. Reaction yield as a function of time for the MPV reduction of benzaldehyde.

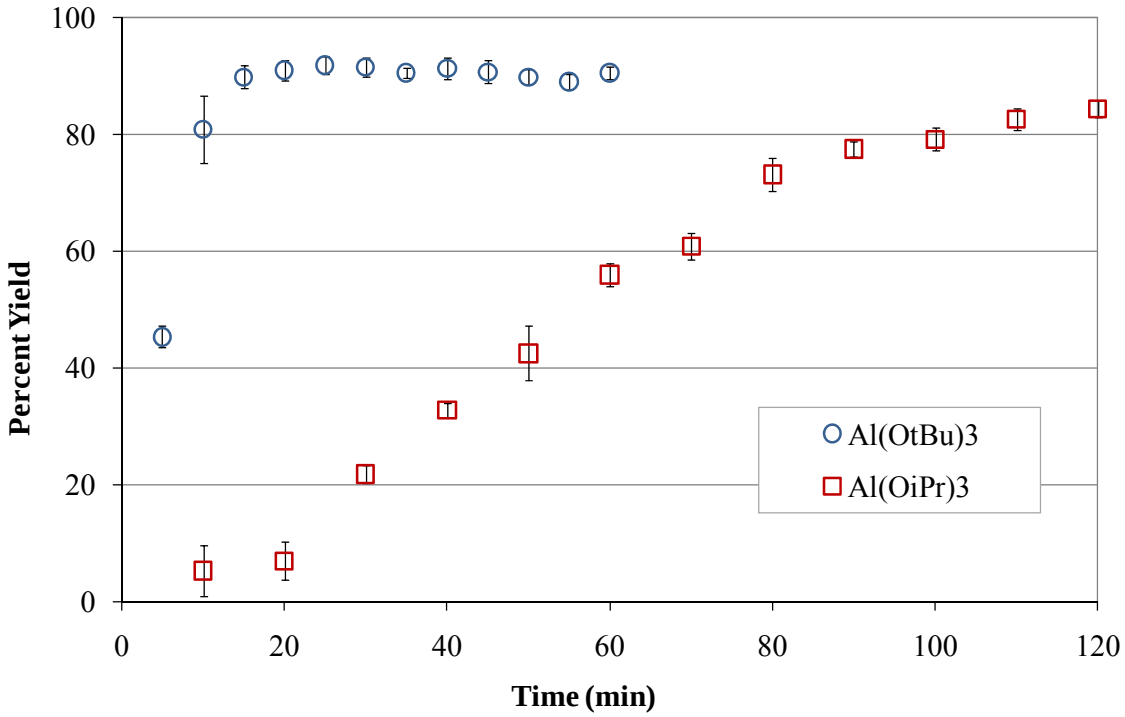

Figure 3-12. Reaction yield as a function of time for the MPV reduction of (S)-CMK.

By increasing the rate of reaction, we have decreased not only the reaction time necessary to achieve a given yield, but we have also decreased the energy requirements to heat a reaction vessel over an extended period of time. Additionally, we can decrease the $Al(O\textit{t}Bu)_3$ catalyst loading to significantly lower loadings, e.g. 20 mol% and even 5 mol%, without impacting reaction time and efficiency. In Figure 3-13, we plot benzyl alcohol yield as a function of reaction time for the two catalyst loadings of 5 mol% and 20 mol% where the MPV reduction is conducted at 65°C. The Figure shows that 85% yield of benzyl alcohol from the MPV reduction of benzaldehyde is achieved in less than 15 minutes with 20 mol% $Al(O\textit{t}Bu)_3$; yet when the catalyst is decreased to 5 mol%, the reaction reaches nearly similar completion in about one hour. This is important if the

objective is to minimize the amount of metal catalyst used and in considering its subsequent disposal. The MPV reduction of acetophenone to 1-phenylethanol in both isopropanol and toluene/isopropanol as catalyzed by 50 mol% $Al(OiPr)_3$ and $Al(OtBu)_3$ at 50°C provides a comparable trend, as indicated in Table 3-1.

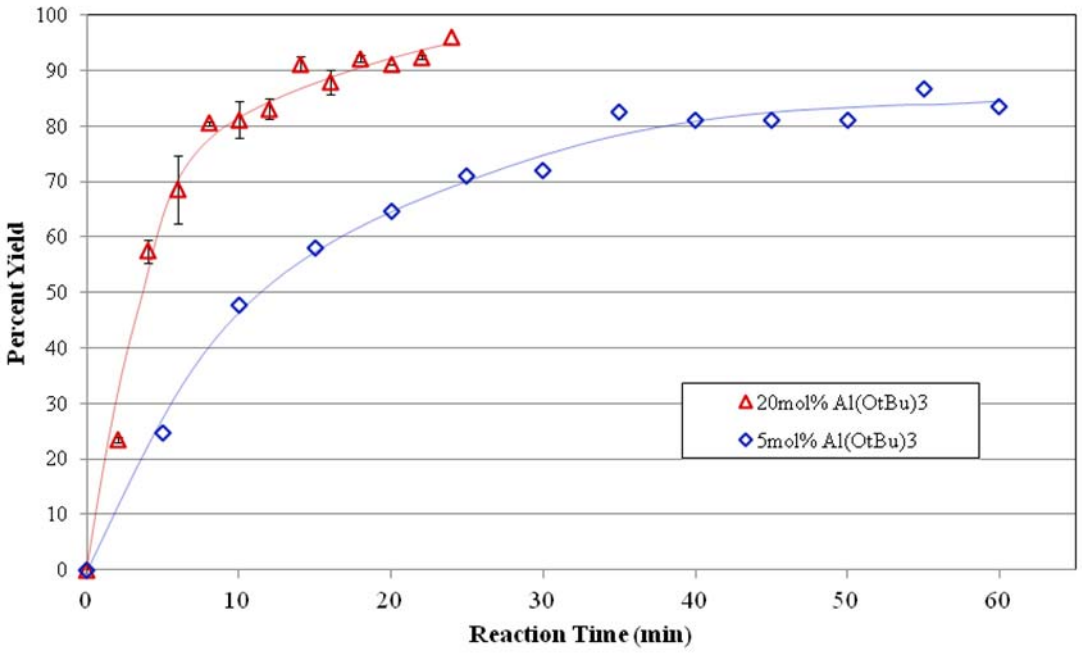

Figure 3-13. MPV reduction of benzaldehyde in batch reactors at 65°C.

(S)-CMK: A Key Example Relevant to the Pharmaceutical Industry.

The MPV reduction of (S)-CMK is currently conducted on an industrial scale with the conventional catalyst system, $Al(OiPr)_3$. As demonstrated with model compounds benzaldehyde and acetophenone, rate enhancements were achieved when

using $Al(OtBu)_3$ and in mixed solvent systems. An important consideration in the pharmaceutical industry is time and money. In the case of (S)-CMK, we showed that the reaction time could be lowered by using $Al(OtBu)_3$. Lowering the cost of a process is also essential and we have demonstrated one way to do that is by lowering the catalyst loading. Comparison of catalyst loadings from 50 to 5 mol% were conducted on the reduction of (S)-CMK. Shown in Figure 3-14, the rate of the reduction differs only slightly from 50 mol% to 20 mol%. Decreasing the catalyst loading to 10 mol% slowed the reaction down by an order of magnitude from 20 mol% and 5 mol% slowed it down by about two orders of magnitude. Because the reduction products precipitate out of solution as the reaction proceeds, implementation of (S)-CMK reduction to continuous flow was not viable without further optimization. However, reductions in batch can now be done faster or cheaper with lower catalyst loading, which is a significant improvement to the current industrial processes.

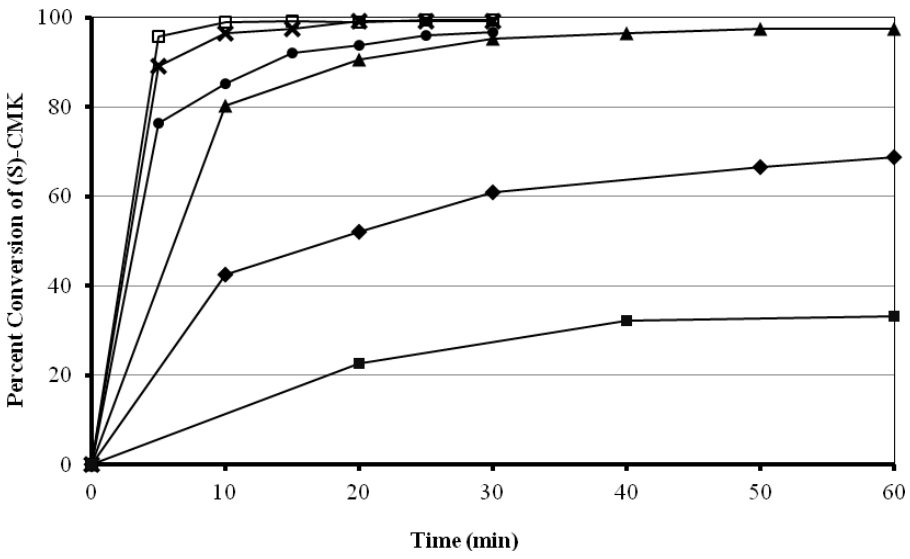

Figure 3-14. Conversion of (S)-CMK to (S,S) and (S,R)-CMA at various Al(O*t*Bu)$_3$ catalyst loadings in isopropanol. Key: ■ 5mol%, ♦ 10mol%, ▲20mol%, ● 30mol%, **x** 40mol%, □ 50mol%

Implementation to Continuous Flow.

As mentioned in the introduction, one of the advantages of continuous flow versus batch processes is the ability to scale-out instead of scaling-up. We saw the MPV reduction as a perfect candidate for this conversion because of its wide usage in the pharmaceutical industry. To demonstrate the power of continuous flow processes, we implemented the MPV reductions of benzaldehyde and acetophenone using the new catalyst, Al(O*t*Bu)$_3$, into the Corning Advanced-Flow Glass® Reactor (AFR).

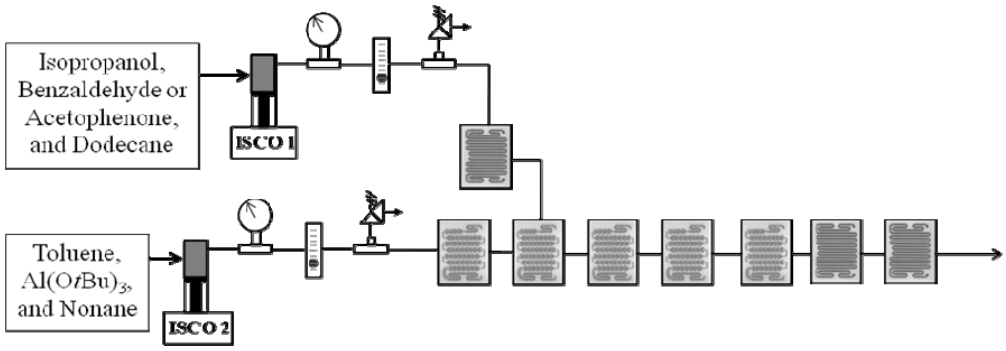

Figure 3-15. Continuous flow reactor schematic.

Our device had 8 reactor modules, and was equipped with pressure gauges, rotameters, thermocouples, and pressure relief valves, as represented in Figure 3-15. ISCO syringe pumps deliver reactant flow through pressure gauges, rotameters, pressure relief valves, then to the reactor utilizing preheating modules for each reactant prior to mixing of the separate reactant. Flow was delivered to the reactor using parallel solenoid controlled ISCO syringe pumps, where each pump contained separate solutions; one ISCO contained a mixture of toluene, the catalyst, and nonane; the second contained a solution of isopropanol, the starting material (ketone or aldehyde) and dodecane. Nonane and dodecane were added to the reactants in small quantity and served as internal standards. For all continuous flow reactions, we used a mixed solvent system of 3:2 toluene and isopropanol in order to enable storage and transport of the reactants without precipitation or gradients in composition. We controlled the concentration of reactants and catalyst in the IPA and toluene; additionally, we controlled the residence time by setting flow rate. We took samples at the reactor exit, which were quenched with HCl, diluted with methanol, and analyzed via HPLC and GC.

The implementation of the MPV reduction of benzaldehyde in the continuous flow reactor was done at two temperatures, 65°C and 80°C, two catalyst loadings, 5

mol% and 20 mol% Al(O*t*Bu)$_3$, and three residence times (1.87 minutes, 3.73 minutes, and 11.2 minutes) at each set of conditions, for a total of twelve reaction points, as shown in Figure 3-16. Higher yields of benzyl alcohol were obtained at the higher catalyst concentrations for both temperatures; the yield is 98% using 20 mol% Al(O*t*Bu)$_3$ at 80°C after 11.2 minutes of residence time. At 5 mol% catalyst and 80°C, we obtain a 74% yield after 11.2 minutes of residence time, showing the trade-off between catalyst loading, yield, selection of reaction temperature, and residence time. In Figure 3-17, we show the batch and continuous flow reduction of benzaldehyde at 20 mol% Al(OtBu)$_3$ and 80°C.

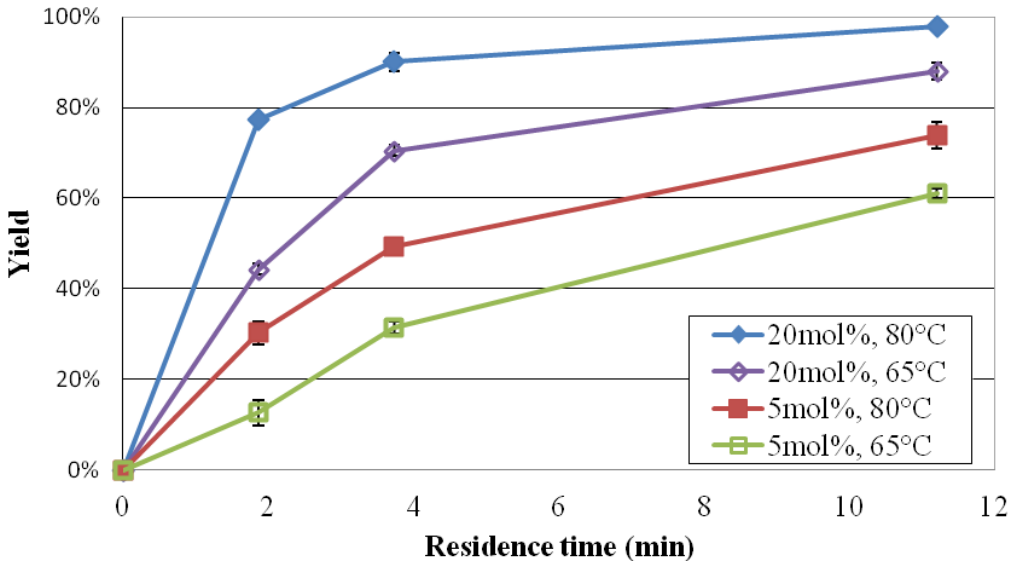

Figure 3-16. MPV Reduction of benzaldehyde in the continuous flow reactor.

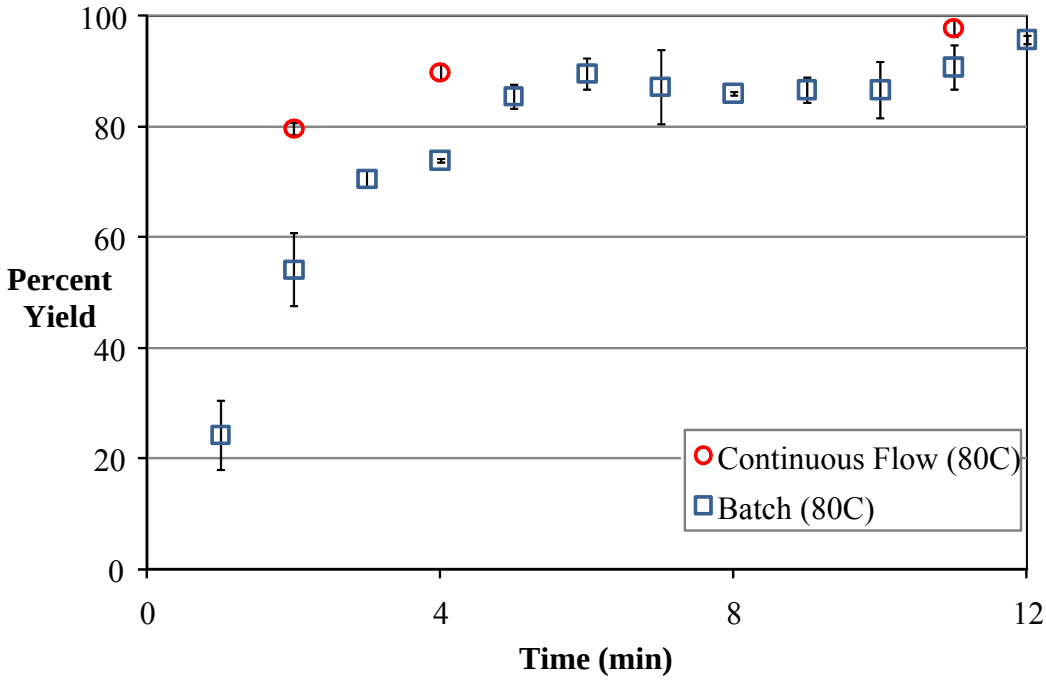

Figure 3-17. Batch and continuous flow MPV reduction of benzaldehyde.

We extend our investigation by implementing acetophenone as the starting material. Using the optimized conditions for benzaldehyde, we conducted the MPV reduction of acetophenone to 1-phenylethanol at 20 mol% $Al(O\textit{t}Bu)_3$ and at 80°C, as it is well known that the MPV-mediated reduction of ketones are slower than their aldehyde counter-parts. In Figure 3-18, yield of 1-phenylethanol is plotted as a function of reaction time, and nearly linear behavior is observed in this range of residence times. It was realized that under these conditions, the yield only reached 18% with the longest residence time but by increasing the residence time using additional reactor modules, a complete reaction may be observed.

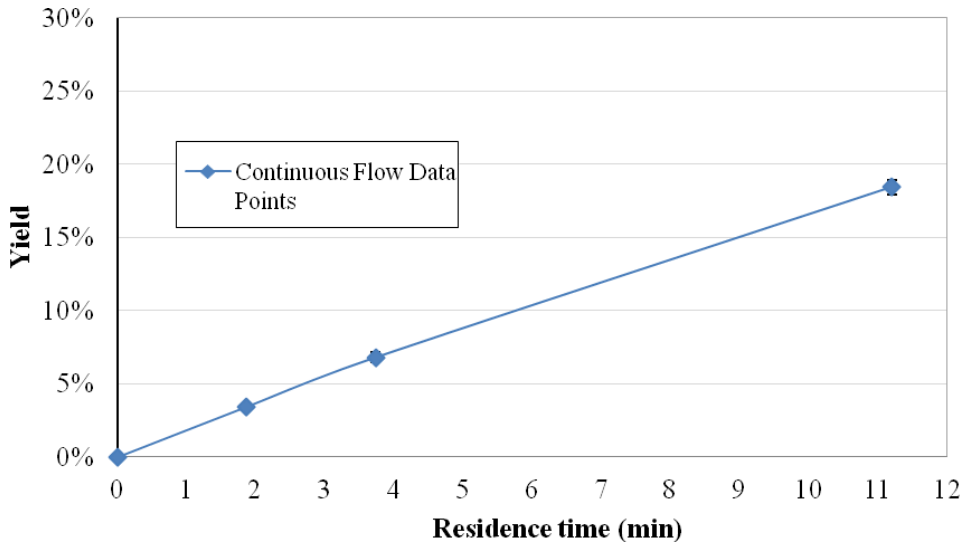

Figure 3-18. MPV Reduction of acetophenone in the continuous flow reactor.

The MPV reductions of benzaldehyde and acetophenone were converted to a continuous flow process after optimization with $Al(OtBu)_3$. The reduction of (S)-CMK to the alcohol products was impractical for use in the Corning® reactor merely due to the insolubility of the products formed. With optimization of solvent system used, the reduction of (S)-CMK has potential for use in the continuous flow reactor.

3.4 Conclusions

The MPV reduction is a commonly-used pathway in the synthesis of important pharmaceutical intermediates. We demonstrate the first MPV reductions to be run in continuous flow mode. By developing a highly active catalyst and establishing reaction conditions adequate for continuous flow technology, we were able to implement a continuous flow protocol for the MPV reductions on two model compounds. Previously, the MPV reduction reaction has industrially been limited to being run in only batch

reactors, yet process development in this way suffer from several issues including the need to redesign the process for each scale up and modifications to the chemistry. Process development using batch technology has dominated in the pharmaceutical industry; but, in the interest of improvements in productivity, reductions in waste and the E-factor, and quality/control improvement, the use of continuous flow processing as part to a process intensification operation has accumulated interest. It should be noted, however, that the pharmaceutical industry can be reluctant to make processing changes, as FDA approval is required. Utilizing continuous flow technology from the onset can offer a number of advantages including reduction of costs, reduction in the size of equipment, reduction of time-to-market, improving quality of product, reduction of energy consumed, and reduction of solvent and waste. Recommendations on a path forward to this work are provided in Chapter V.

3.5 References

[1] Constable, David J.C.; Dunn, Peter J.; Hayler, John D.; et al, *Key green chemistry research areas–a perspective from pharmaceutical manufacturers*. Green Chem., 2007. **9**: p. 411.

[2] Sheldon, R.A., *Organic-Synthesis – Past, Present, and Future.* Chem. & Ind. (London), 1992. **23**: p. 903-6.

[3] Sheldon, R.A., *The E Factor: fifteen years on*. Green Chem., 2007, **9**: p. 1273.

[4] Jimenez-Gonzalez, Concepcion; Poechlauer, Peter; Broxterman, Quirinus B.; et al, *Key Green Engineering Research areas for Sustainable Manufacturing: A Perspective from Pharmaceutical and Fine Chemical Manufacturers*. Org. Process Res. Dev., 2011. **15**: p. 900.

[5] Ramshaw C., *Process Intensification and Green Chemistry*. Green Chem., 1999. **1**: p. G15.

[6] Charpentier, J.C., *Process Intensification by Miniaturization*. Chem. Eng. Technol., 2005. **8**, p. 255.

[7] Kopach, Michael E.; Murray, Michael, M,; Braden, Timothy M.; et al., *Improved Synthesis of 1-(Azidomethyl)-3,5-bis-(trifluoromethyl)benzene: Development of Batch and Microflow Azide Processes*. Org. Process Res. Dev., 2009. **13**: p. 152.

[8] Pollet, P.; et al., *Production of (S)-1-Benzyl-3-diazo-2-oxopropylcarbamic Acid tert Butyl Ester, a Diazoketone Pharmaceutical Intermediate, Employing a Small Scale Continuous Reactor*. Industrial & Engineering Chemistry Research, 2009. **48**(15): p. 7032-6.

[9] Delville, M.M.E.; et al., *Continuous flow azide formation: Optimization and scale-up.* Chemical Engineering Journal, 2011. **167**(2-3): p. 556-9.

[10] O'Brien, A.G.; Levesque, F.; Seeberger, P.H., *Continuous flow thermolysis of azidoacrylates for the synthesis of heterocycles and pharmaceutical intermediates*. Chemical Communications, 2011. **47**(9): p. 2688-90.

[11] Watts, P. and Haswell, S.J., *The application of microreactors for small scale organic synthesis.* Chemical Engineering & Technology, 2005. **28**(3): p. 290-301.

[12] Fletcher, P.D.I.; et al., *Micro reactors: principles and applications in organic synthesis*. Tetrahedron, 2002. **58**(24): p. 4735-57.

[13] Watts, P. and Haswell, S.J., *Continuous flow reactors for drug discovery*. Drug Discovery Today, 2003. **8**(13): p. 586-93.

[14] McMullen, J.P. and Jensen, K.F., *Rapid Determination of Reaction Kinetics with an Automated Microfluidic System*. Organic Process Research & Development, 2011. **15**(2): p. 398-407.

[15] McMullen, J.P. and Jensen, K.F., *An Automated Microfluidic System for Online Optimization in Chemical Synthesis*. Organic Process Research & Development, 2010. **14**(5): p. 1169-76.

[16] (a) Wilds, A., Organic Reactions, 1944. **2**: p. 178. John Wiley and Sons, New York
(b) Degraauw, C. F.; Peters, J. A.; Vanbekkum, H.; Huskens, J., *Meerwein-Ponndorf Verly Reductions and Oppenauer Oxidations – An Intergrated Approach*. Synthesis-Stuttgart, 1994. **10**, p. 1007.

[17] Oppenauer, R. V., *A dehydrogenation method from secondary alcohols to ketones 1. On the preperation of stearine ketones and sexual hormones.* Recueil Des Travaux Chimiques Des Pays-Bas, 1937. **56**: p. 137.

[18] Cha, J.S. Bull. Korean Chem. Soc. 2007. **28**: p. 2162.

[19] Ooi, T.; Miura, T.; Maruoka, K., *Highly efficient, catalytic Meerwein-Ponndorf-Verley reduction with a novel bidentate aluminum catalyst.* Angew. Chem. Int. Ed., 1998. **37**: p. 2347.

[20] Chandrasekharan, J.; Ramachandran, P. V.; Brown, H. C. *Diisopinocampheylcchloroborane A Remarkabaly Efficient Chiral Reducing Agent for Aromatic Prochiral Ketones*, J. Org. Chem. 1985. **50:** p. 5446.

[21] Fukuzawa, S.; Nakano, N.; Saitoh, T. *Reduction of carbonyl compounds by lanthanide metal/2-propanol: In-situ generation of samarium isopropyloxide for stereoselective Meerwein-Ponndorf-Verley reduction,* Eur. J. Org. Chem. 2004. p. 2863.

[22] (a) Bach,G.; Capitaine, J.; Engel, C.R. *Can. J.Chem.* **1968**, 46, 733. (b) Bouchard, R. ; Engel, C.R. *Can. J.Chem.* **1968**, 46, 2201.

[23] Kow,R.; Nygren, R.; Rathke, M.W. *Rate Enhancement of the Meerwein-Ponndorf-Verley Oppenhaur Reaction in Presence of Proton Acids*. J. Org. Chem. 1977. **42** (5): p. 826.

[24] Gills, J.; Lo Piccolo, J.; Tsurutani, J.; Shoemaker, R. H.; Best, C. J. M.; Abu-Asab, M. S.; et al. *Nelfinavir, a lead HIV protease inhibitor, is a broad-spectrum, anticancer agent that induces endoplasmic reticulum stress, autophagy, and apoptosis in vitro and in vivo* Clin. Cancer Res. 2007. **13:** p. 5183.

[25] Shiner, V. J.; Whittaker, D. *Mechanism of the Meerwein-Ponndorf-Verley Reaction*, J. Am. Chem.Soc. 1963, **85:** p. 2337

[26] Malik, A.A.; et al., US Patent 6,852,887. 2005.

[27] Shiner, V. J.; Whittaker, D.; Fernande, V. P., *Mechanism of Meerwein-Ponndorf-Verley Reaction*. J. Am. Chem. Soc., 1963. **85**: p. 2337.

CHAPTER IV

BIOMASS-BASED PROCESSING IN NOVEL SWITCHABLE SOLVENTS

4.1 Introduction

Economics dictate that as the accessible petroleum reserves contract, the price of petroleum and petroleum-based products will increase in accordance with increasing demand. Thus, the production of chemicals from biologically based resources can not only reduce our dependence on limited supplies of foreign oil, but also ensures that we maintain our competitive edge in using green chemistry and engineering to innovate new products and processes.

One high-value chemical product that has rapidly ignited interest in both academic researchers and the chemical industry is 5-(hydroxymethyl)-2-furaldehyde (abbreviated as 5-HMF, or just HMF). First characterized in the early 1900's [1], HMF (as shown in Figure 4-1) has continually accumulated momentum due in part to its vast field of application, demonstrated by the fact that there are now well over 1000 papers published on this compound.

5-HMF is an organic molecule containing both aldehyde and alcohol functional groups, and is obtained from the dehydration of simple carbohydrate or sugar molecules. HMF has been described as "a versatile intermediate and its derivatives could potentially replace voluminously consumed petroleum-based building blocks, which are currently used to make plastics and fine chemicals." [2]. Hence, both 5-HMF and its reaction

products have wide application and usefulness. A few of the highly useful compounds that can be derived from 5-HMF include 2,5-furfuryldiamine, 2,5-furfuryldiisocyanate, and 5-hydroxymethyl furfurylidenester, all of which are useful starting materials in the synthesis of polymers such as polyesters, polyamides, and polyurethane [3]. In Figure 4-1, we show the general reaction scheme of a hexose to form HMF (1).

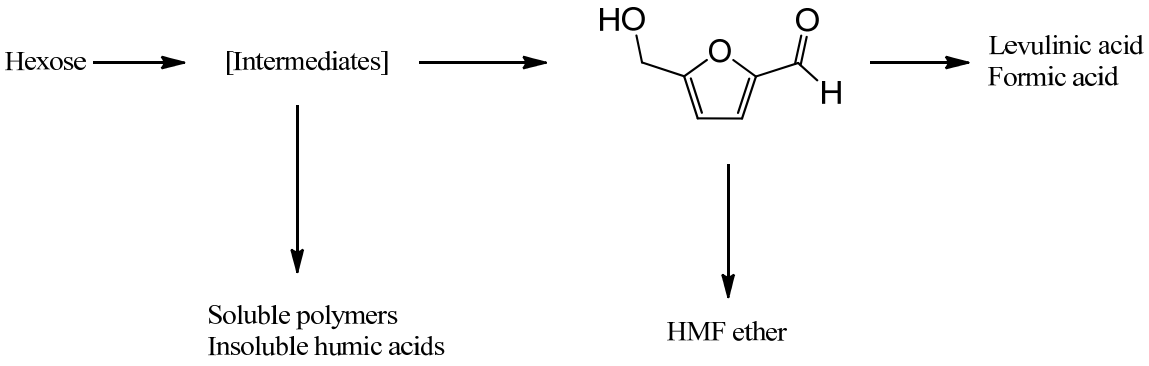

Figure 4-1. Simplified reaction scheme for the production of HMF and subsequent derivatives.

The preparation of these types of polymers is, importantly, derived from renewable resources that are capable of replacing traditional petroleum based conventional and other high-tech materials [3]. Additionally, levulinic acid can be produced under acidic conditions via hydrolysis of the furan ring. Levulinic acid and its derivatives are considered an important building block for a range of materials with applications in fuel production and additives, as well as polymers. The selective reduction of the formyl group gives 2,5-bis(hydroxymethyl)furan, which is considered to be another significant building block in polymers and polyurethane foams.

In Figure 4-2, we show the structure of HMF and a few of the many useful monomers derived from HMF [4]. Importantly, HMF can be further processed to produce chemicals that are useful in a wide range of fields, including polymers, biofuels, and fine chemicals.

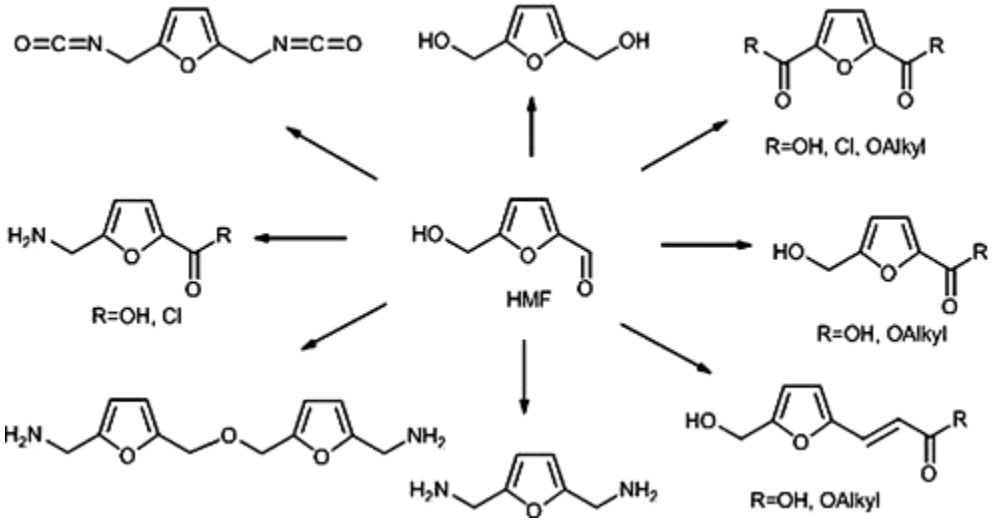

Figure 4-2. Structure of HMF (center) and a few of the many useful monomers derived from HMF [4].

Two named derivatives of interest are the molecules 2,5-furandicarbaldehyde (FDC) and 2,5-furandicarboxylic acid (FDCA), which are the starting materials for the synthesis of complex macromolecules, a variety of pharmaceutical precursors, and thermo-resistant polymers [5]. In fact, 2,5-furandicarboxylic acid has significant potential as a biorenewable replacement monomer for terephthalic acid, a major component in the synthesis of various polyesters, such as polyethylene terephthalate (PET). The PET industry is a 4 billion pound per year business, with applications in films and

thermoplastic engineering polymers. The main production challenge of FDCA is the selective and controlled dehydration of simple carbohydrates [6]. The transformation to FDCA, which is mentioned as a building block of the future [6], via oxidation of the formyl and the hydroxyl groups of HMF results in the formation of a highly stable molecule and very valuable potential monomer [4]. As an example of recent research in this area, the reaction of HMF to FDCA has been reported to occur in 71% yield at 30 °C using water as a solvent and a supported gold-nanoparticle catalyst [7].

In fact, HMF has even been considered a 'sleeping giant' in the field of intermediates derived from renewable resources [8]. 5-HMF can be used as a precursor in the production of biologically derived polymers, plastic processing, and as a building block in biofuel development. It is cited in literature that furanic compounds, such as 5-HMF, are promising as alternative precursor sources for sustainable liquid transportation fuels and chemicals [9]. A few polyester building blocks include 2,5-furandicarboxylic acid, 2,5 bis(hydroxymethyl)furan, and 2,5-bis(hydroxymethyl)tetra-hydrofuran, as well as 2,5-di- methylfuran, the compound specified as an alternative liquid transportation fuel. Moreover, greater quantities of 5-HMF are needed for pharmaceutical and disease related research, as it is being studied in a number of cases involving metabolic syndrome, hypertension, diabetes, and sickle cell anemia [9].

The Preparation of 5-HMF.

The efficient preparation of pure 5-HMF continues to be a challenge to researchers, reflected in its cost, as it remains to be a specialty chemical. The bulk cost of HMF is $1,240/kg at a 25 kg purchase amount and 96% purity [10].

The synthesis of HMF used today is based on the developments of Haworth and Jones [11]. The basic procedure is to treat sucrose with oxalic acid (0.25%) in an aqueous solution at elevated temperature (ranging from 120 to 160 °C) under the vapor pressure of water at the given temperature. The maximum yield of the HMF product was about 50% based on the fructose unit. The product could be isolated by distillation with only a small amount of decomposition. It was postulated early on that the acid catalyzed decomposition to form HMF occurred through the furanose form of the fructose, which exists in equilibrium with the pyranose form. Later studies showed that the dehydration reaction proceeds through one of two pathways, either through the transformation of ring systems or through acyclic compounds, as shown in Figure 4-3, where path (a) represents the transformation through the ring system, where as path (b) represents the transformation via acyclic compounds [5]. The acid was neutralized with calcium carbonate (creating a salt), then extracted with ethyl acetate, dried, then distilled.

Forty years later, it was shown that the acid catalyzed reaction occurs in both aqueous and organic media, where more degradation of the HMF occurs in the aqueous media, but polymerization occurring in both solvents [9a]. Degradation occurs in the aqueous media occurs after HMF is formed; the hydrolysis reaction consumes two water molecules then forming levulinic acid and formic acid. However, the polymerization reactions occur in both solvents forming soluble polymers and insoluble humins [5].

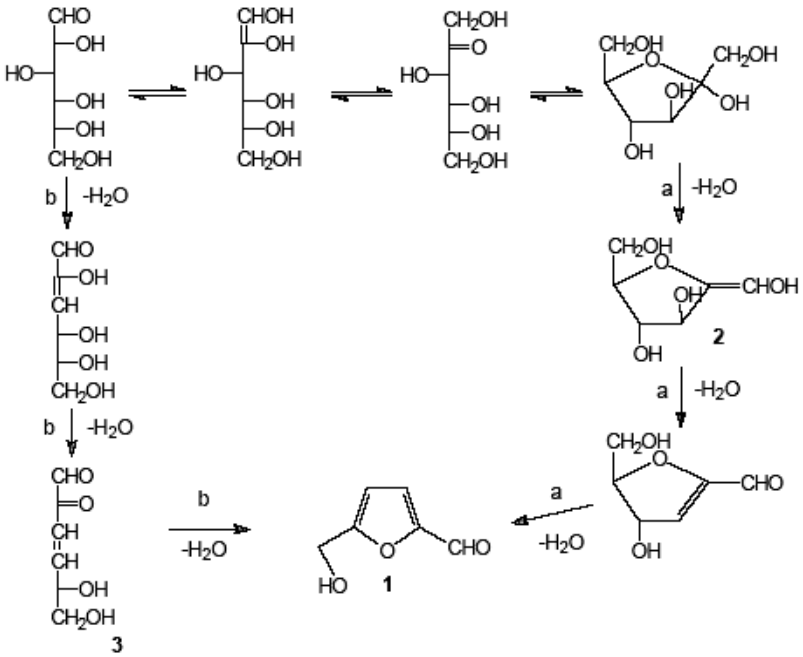

Figure 4-3. Pathways for the acid catalyzed dehydration of hexoses to yield HMF [5].

Sugar chemistry.

Monosaccharides, e.g. fructose, in solution exist as equilibrium mixtures of the linear chain and cyclic forms. More specifically, fructose exists as a ratio of five different structures in water, each in equilibrium with each other [11]; two structures are of the pyranose form (alpha-D-fructopyranose and beta-D-fructopyranose), two structures are of the furanose form (beta-D-fructofuranose and alpha-D-fructofuranose), as well as the linear chain D-fructoketose. For example, fructose is 67% in the pyranose form and 31% in the furanose form in water [13]. Although the alpha- and beta-d-fructofuranose are the most reactive, it may be important to consider all molecular isomers of the starting material. The glucose molecule (an aldose) is lower in reactivity than fructose (a ketose), as fructose has a more abundant acyclic form. Because the ring structures of glucose are more stable, fructose has a higher rate of enolisation, which is the rate determining step in

HMF formation [14]. An illustrative example of the cyclization of D-fructose to the furanose and pyranose forms is shown in Figure 4-4. Once the carbohydrate forms the furanose structure, an enolisation occurs with the loss of the first water molecule. Early preparations of HMF use fructose as a starting material [11]. Although glucose can be used, yields are traditionally lower.

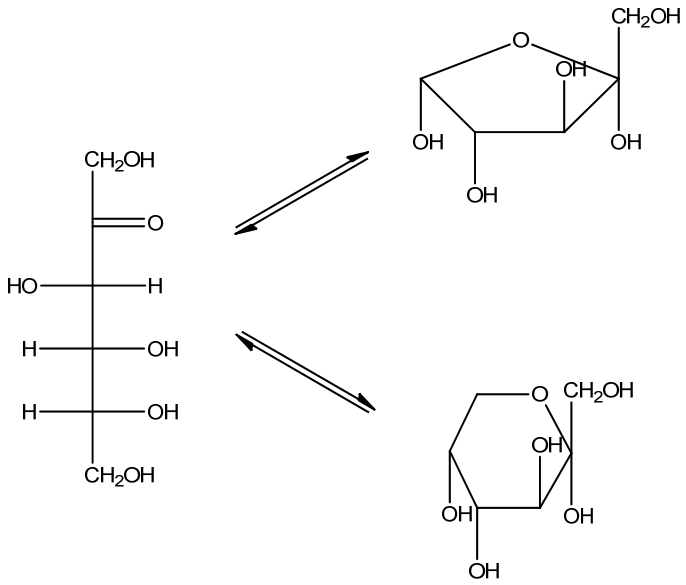

Figure 4-4. Illustrative example of the cyclization of D-fructose.

Literature overview of current approaches to HMF production.

Presently, the innovative approaches include a wide range of solvents employed in the dehydration of D-fructose and other carbohydrates to HMF, including but not limited to acidified water at less than 200 °C [15], aqueous systems at greater than 200 °C [12], organic solvents [16], mixed solvent systems [17], and ionic liquids [18]. There are advantages of each solvent type; for example: Organic solvents and ionic liquids favor the cyclic fructose molecular isomers, those most reactive to form the desired product, and thus generally have higher yields. The acyclic fructose can polymerize along with

HMF forming humins, insoluble amorphous polymers [19]. By also limiting the water content using organic based solvents or ionic liquids (IL's), the decomposition of HMF to either levulinic or formic acid can be lessened. However, IL's are not only currently expensive but can be difficult to separate from reaction products and starting material. Polar aprotic organic solvents like DMSO have high boiling points (189 °C) which is energy intensive and costly to separate.

In place of DMSO, sulfolane (tetramethylene sulfone) has been cited as a better solvent alternative to DMSO. It has advantageous properties, including strength as a polar aprotic solvent and miscibility with both water and hydrocarbons, and is nonvolatile [20]. The authors report obtaining a high yield at >90% under moderate conditions of 100 °C for 1 hour, using 5 wt% of a HBr catalyst and other catalyst types were tested as well. Another group reports using sulfolane for the catalytic steam pyrolysis of cellulose in the presence of sulfuric acid, where they achieve a yield of 9 mol% HMF based on the glucose unit. In another reaction system, d-fructose is used as the substrate in DMSO/H_2O and $LaCl_3$ as a catalyst [21]. It has been shown in the DMSO system that the presence of water in up to 10% does not affect the HMF yields.

Both heterogeneous and homogenous catalysts are widely used to enhance HMF yields, with no one method clearly leading the effort. Researchers have used mineral acids, where H_2SO_4 and HCl are commonly employed due to their low cost and availability. Other researchers have used ion exchange resins, such as Amberlyst-15 as the catalyst in a choline chloride system with fructose as the starting material, where HMF yields were about 40% [22]. One group reports using the Amberlyst-15 catalyst in DMSO, and even with 50 wt% fructose, they achieve 100% conversion and selectivity.

The catalyst particle size used was 0.15 to 0.053 mm, and time was reported to be two hours at 120 °C. However, because of the use of DMSO, isolation of the products from solvent is problematic [23].

One recent and highly cited approach was developed by Dumesic [9c, d]. In this two-phase production method (shown in Figure 4-5), an organic phase of methyl isobutyl ketone, MIBK, is the product extracting phase (modified with 2-butanol to improve yield in the organic phase), and an acid catalyzed aqueous reaction phase containing DMSO and PVP (polyvinylpyrrolidone), improves the desired yield. The DMSO is also speculated to help stabilize the furanose form of the hexoses. Conversion is 77%, with 50% partitioning of 5-HMF into organic extracting phase. However, subsequent removal of the DMSO is problematic. Small amounts of the DMSO (5-8 wt%) are carried into the extraction phase, causing difficulty in product isolation.

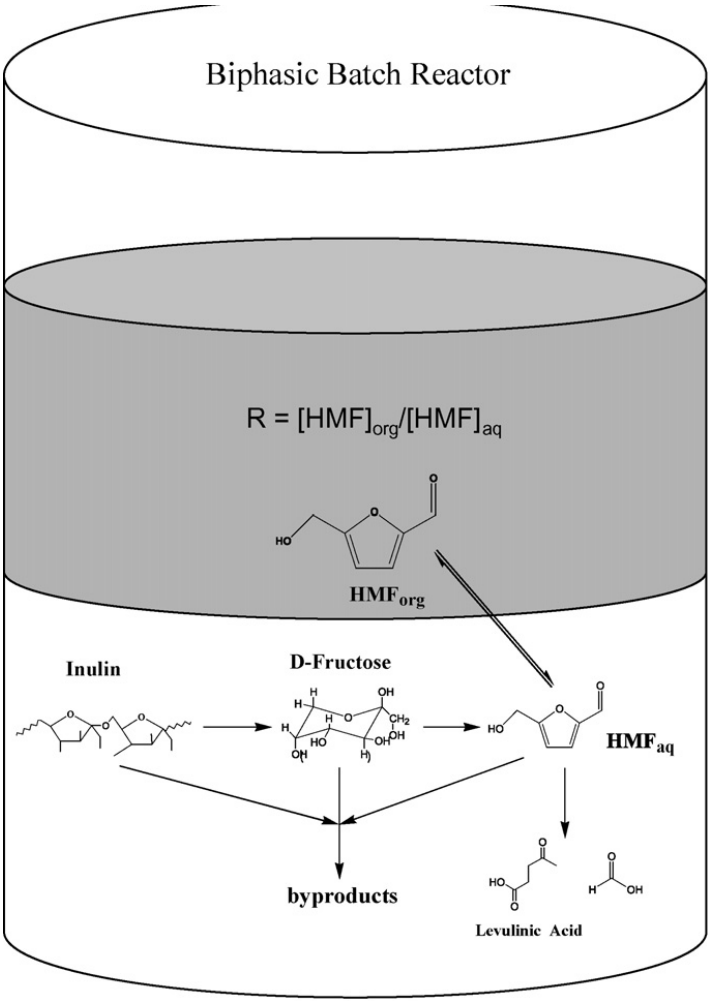

Figure 4-5. Schematic of the two phase method employed by Dumesic [9c,d].

We need to develop more efficient product separation methods to make the synthesis of HMF economically viable. DMSO is difficult to remove via distillation, and, it decomposes to organic products including CH_3SO_3H and H_2SO_4 at temperatures 130 °C and higher [24]. On the other hand, our smart solvent, piperylene sulfone, has a thermal mechanism allowing for separation at relatively low temperatures (110 °C) at ambient pressure, contrary to other common similar polar organic solvents. This is extremely useful in separation of the solvent and the reaction product, HMF, as traditional distillation is undesirable due to the reactive nature of HMF. In this chapter, we report on the application of piperylene sulfone to these reactions.

4.2 Experimental

Materials.

All chemicals were used as received, unless noted otherwise. Piperylene sulfone was synthesized in our laboratories as described in Chapter 2. Dimethyl sulfoxide was purchased from Baker (99.9%) argon gas (ultra high purity) purchased from Airgas, deuterated benzene-D6 (D, 99.5%) was purchased from Cambridge Isotope Laboratories, Inc., butadiene sulfone (98%) was purchase from Sigma Aldrich, fructose (99%+) was purchased from Sigma Aldrich, 5-(hydroxymethyl)furfural (>99%) was purchased from Sigma Aldrich, and Amberlyst-15 (<1.5% moisture) was purchased from Sigma Aldrich.

HMF Separation from Butadiene Sulfone.

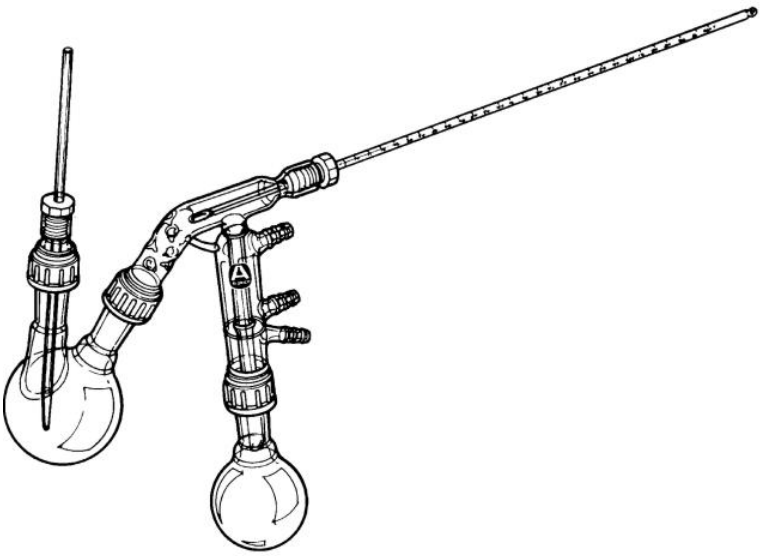

Figure 4-6. Short-path distillation apparatus for the thermal separation of butadiene sulfone.

We first attempted to separate 5-hydroxymethylfurfural (5-HMF) from butadiene sulfone and water initially using short path distillation, as shown in Figure 4-6. However, we encountered contamination issues and switched to a kugelrohr (Buchi Glass Oven B585) as shown in Figure 4-7. For this separation, $4*10^{-4}$ mol HMF, $4.5*10^{-3}$ mol butadiene sulfone, and a variable amount of water (0-100 vol%) was used. A mass balance was performed after separation to ensure conservation of mass during the separation.

Figure 4-7. Buchi kugelrohr used for the separation of butadiene sulfone from HMF.

The components were loaded into the final bulb of the kugelrohr, mixed, heated, and placed under vacuum. The temperature was varied between 80 °C and 100 °C to determine the reasonable temperatures for separation, where 95 °C was selected as an optimum based upon the potential reactivity or charring nature of product at higher temperatures. We also varied the water volume percent, at settings of 0 vol%, 10 vol%, and 20 vol%. The mixtures were separated under the same temperatures. The resulting mass balances and H NMR's confirm that separation was effective in the presence of up to 20% water by volume, with no charring or side products observed, which indicates that the thermal separation route is effective in separation of the sulfone from the HMF.

Piperylene sulfone was also used to perform the separation. We used a nitrogen flow to remove volatile components (*trans*-piperylene and sulfur dioxide). We used the same concentration as with the butadiene sulfone separation, and 20 vol% water. The temperature was set to 95 °C.

HMF Reactions in Butadiene Sulfone and Piperylene Sulfone.

Reactions were run using both butadiene sulfone and piperylene sulfone in an effort to produce HMF from fructose. In order to establish a consistent reactor set-up, we used sealed glass vessels under an inert atmosphere of argon, PTFE stir bars, and an oil bath to maintain uniform temperature control. 0.02 moles of butadiene sulfone were combined with 0.001 moles of fructose in the presence of 20 vol% water in a 10 mL round bottom flask. These reactors allowed for high temperature reactions where the volatile gases could be contained. Additionally, we used 10 mL round bottom glassware connected to a water condenser which was later replaced with a septa in order to contain all components for the purpose of mass balance calculations. The vessels were stirred using Teflon coated magnetic stir bars. We weighed the solvent and reactant using a Mettler Toledo mass balance and measured the water using an Eppendorf pipette. After loading the butadiene sulfone, fructose, and water, if specified, the vessels were flushed with an inert atmosphere of either argon or nitrogen. The vessels were then placed in an oil bath which had been set to the desired reaction temperature. The oil baths were heated at 65-90 °C. HPLC and ^{1}H NMR samples were taken. Once we confirmed successful reaction to produce HMF, butadiene sulfone was replaced with piperylene sulfone. 0.002 moles of piperylene sulfone was combined with 0.0001 moles of fructose in the presence of 20 vol% water, giving a 0.47 mol/L concentration of fructose. The mixture was added to the round bottom, sealed with a septa, flushed with argon gas, and placed into an oil bath where reaction took place at a temperature which was varied between 65-90 °C. The reaction time was also varied between 2-24 hours. After reaction completion, the vessels

were cooled, and diluted with a 90/10 vol% ratio of water/acetonitrile solution for analysis. HPLC and ^{1}H NMR samples were taken for each reaction.

The samples were analyzed by HPLC (High Performance Liquid Chromatography). The solutes were gradient eluted using a mobile phase that consisted of a starting gradient of 95 % water and 5 % acetonitrile and a column temperature of 40 °C. At 5 minutes, the gradient linearly changed to reach 95% acetonitrile and 5% water at 36 minutes. A Hewlett Packard 1100 Series LC equipped with an Agilent Technologies 1200 Series UV-vis Refractive Index Detector (RID) set to 210 λ and 254 λ and a C18 Galaxy RP1 column at a flow rate of 1.000 mL/min and UV-vis detection was used. A guard column was used to prevent clogging. A calibration curve was generated from standard solutions of HMF prepared in HPLC-grade water. Selected samples were also analyzed by ^{1}H NMR spectroscopy (Varian 400 MHz) in $CDCl_3$. The HPLC calibration curves in conjunction with the response areas allowed for direct determination of the concentrations, which were used to determine yield.

HMF Reactions in Butadiene Sulfone Using Amberlyst-15.

We used a standard reaction volume of 5 mL, 5.5E-2 mol, of butadiene sulfone which was added to a 10 mL round bottom flask. Next, the individual carbohydrate from a concentration of 0.1-0.5 mol/L and catalyst with a concentration of 2-4 mg/mL was added to the round bottom. The catalyst, Amberlyst-15 was sized down to <63 micrometers via crushing and a series of metal filters. 10 mg of N-phenyl-2-naphthylamine inhibitor was added to each flask. Each reaction was heated to a temperature from 100-120 °C using a mineral oil bath and was maintained under an inert

nitrogen environment. The reactions were quenched with 20 mL of distilled water, giving a 20:1 dilution, and allowed to cool to room temperature. 15 mL samples were taken in 6 dram vials and centrifuged for 10 minutes. Samples were analyzed using both LCMS and HPLC. With a 1:1 conversion, the relative order of measured concentration at 200:1 dilution for the LCMS is 10^{-4} M, and a measured concentration at 50:1 dilution of 10^{-3} M for HPLC. A calibration curve was prepared for pure 5-HMF in distilled water ranging in concentration from 0.1M to 0.00001M.

A solid acid resin catalyst, Amberlyst-15 was used as the catalyst for the triple dehydration of D-fructose [25]. A fractional factorial design of experiments was constructed in order to explore the effects and possible interactions of six variables: temperature, time, catalyst loading, catalyst diameter, sugar concentration, and mixing rate. Following the procedure outlined by Louvar [26], 16 experiments were set up corresponding to the typical one-quarter fractional-factorial design of a two level, six factor full factorial design, with an additional 8 experimental runs and the center point in order to deconfound the results.

4.3 Results

Separation.

In the production of HMF, current solvent systems are limited by the inefficient separation of the desired HMF product from the solvent. The route in the separation method used by Dumesic [9c, d] relies on the extraction of HMF into an organic phase, where partitioning is typically observed to be 50%. After extraction, the organic solvent is removed, which is typically performed under reduced pressure. Dumesic's approach is

to balance the optimization of reaction yields, via the use or aqueous phase modifiers- namely DMSO, with the optimal separation, where the organic phase is enhanced with its own modifiers. DMSO has been shown to significantly enhance conversion and selectivity– by 2-3 times, but the existence of DMSO in the aqueous phase leads to carryover into the organic phase, causing separation difficulties. More specifically, DMSO is speculated to help stabilize the furanose form of the hexoses. In addition, DMSO has been shown to catalyze the dehydration of fructose at elevated temperature, where the proposed mechanism is shown in Figure 4-8 [27].

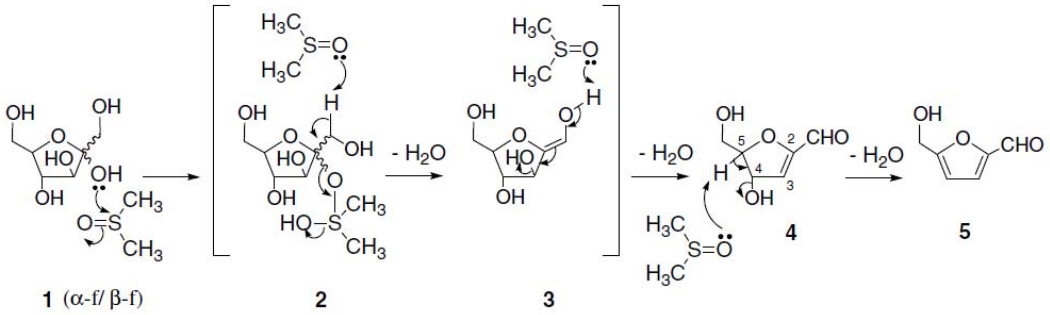

Figure 4-8. Proposed mechanism for the DMSO catalyzed dehydration of fructose to HMF [27].

In order to show this thermally triggered separation route, we used both piperylene sulfone and butadiene sulfone, as they undergo the same retro-cheletropic reaction into conjugated dienes and sulfur dioxide. We show this retro-cheletropic decomposition route for both piperylene sulfone and butadiene sulfone in Figure 4-9 and Figure 4-10, respectively. For both reaction and separation purposes, we first used butadiene sulfone for several reasons: it is commercially available (opposed to piperylene

sulfone which must be synthesized in our laboratories), it is available in high purity (98% from Sigma Aldrich), and it is inexpensive on a laboratory scale ($49.90 for 500 grams).

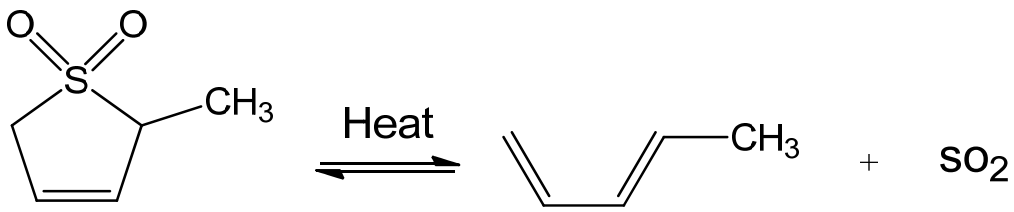

Figure 4-9. Decomposition of piperylene sulfone using the retro-cheletropic switch.

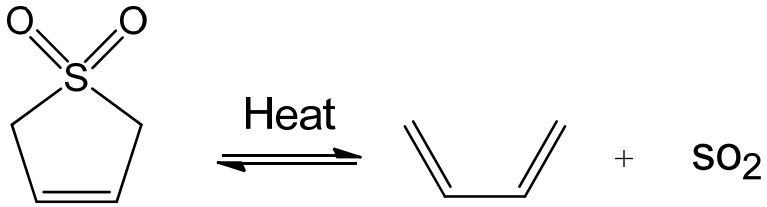

Figure 4-10. Decomposition of butadiene sulfone using the retro-cheletropic switch.

Use of the novel thermal switch of either piperylene sulfone or butadiene sulfone bypasses the need for an extraction phase, as the solvent can be separated thermally. After reaction completion, the temperature is slightly elevated to activate the decomposition switch and enable separation of the volatile components (conjugated diene and sulfur dioxide) and the solid product, HMF. At these conditions, HMF is not volatile and remains solid, as it has a vapor pressure of 1 mm Hg at 116 °C.

One primary goal here was to show the thermal separation of sulfone from HMF without any side reaction occurring at elevated temperature. In order to ensure that no

reaction was occurring between the volatile species –the conjugated diene and the SO_2– and the product, we initially added $4*10^{-4}$ moles of pure HMF and $4.5*10^{-3}$ moles of butadiene sulfone to a round bottom, melted, and stirred the mixture. We used short-path distillation with two round bottom flasks that could be temperature controlled separately. One round bottom containing the butadiene sulfone and HMF was submerged in an oil bath set from 80-85 °C, while the second round bottom was connected to a water condenser and partially submerged in a dry ice and acetone bath to collect any volatile species, in addition to a cold trap. After running the experiment at elevated temperature for one hour, no liquid butadiene sulfone appeared to remain in the round bottom. We disconnected the round bottom and added $CDCl_3$ to the remaining solid, mixed in the round bottom, and then removed a sample of the liquid for ^1H NMR analysis.

The results indicated that the HMF remained unreacted during the separation. However, the results also show the presence of butadiene sulfone using the short-path distillation set up, indicating insufficient time given for the separation of the solvent. Next, we increased the time to about 2 hours and temperature to 95-100 °C. However, in our ^1H NMR analysis, we still observed small butadiene sulfone peaks. Because the temperature of the entire round bottom could not be uniformly maintained at the desired temperature, even when well insulated, we suspect some solvent had accumulated at the neck of the vessel and lead to contamination upon sampling. See Figure 4-6 above for the schematic of the short-path distillation apparatus used.

Therefore, we used a reaction set up allowing for more control – a kugelrohr – where the entire round bottom bulb could be uniformly heated in the heating cage, and the solvent could be recovered in a separately bulb where the temperature could be

reduced. Figure 4-7 shows a schematic of the kugelrohr used. Vacuum was used in order to assist in the removal of volatile species and cold traps were installed for collection. Additionally, by reducing the pressure, the equilibrium of the reaction will shift to side with more moles, the volatile components, as by Le Chateliers principle. The results show complete separation of the butadiene sulfone with pure HMF remaining, and no trace of solvent detected by ^{1}H NMR. No detectable loss of structural integrity of HMF was detected though the NMR results, indicating that degradation of the HMF did not occur.

Next, we tested the separation at atmospheric pressure using a round bottom flask and nitrogen flow to remove the volatile components, butadiene and sulfur dioxide. For this separation, $4*10^{-4}$ moles of HMF and $4.5*10^{-3}$ moles of butadiene sulfone were heated to 95 °C in a round bottom submerged in an oil bath. After an hour, we removed the round bottom, added $CDCl_3$ to the remaining solid, mixed in the round bottom, and then removed a sample of the liquid for ^{1}H NMR analysis. In later separation experiments, 10-20 vol% water (to generate in-situ acid with the gaseous SO_2) was added to this mixture to more closely simulate the actual reaction mixture. Once again, the analysis in each case indicated that the HMF remained un-reacted during the thermally triggered removal of butadiene sulfone. Additionally, no butadiene sulfone was detected by NMR, even when water was added to the mixture before the separation.

Next, we replaced butadiene sulfone with piperylene sulfone and performed the separation under the same conditions, 20 vol% water and a temperature set to 95 $^{\circ}C$. We used a nitrogen flow to remove volatile gaseous components. Through ^{1}H NMR analysis, the spectrum showed that the HMF remained un-reacted during the thermally triggered

removal of piperylene sulfone, and only the presence of HMF was the sole product remaining. The successful separation of both butadiene sulfone and piperylene sulfone from HMF at elevated temperature indicates that the retro-cheletropic route is a useful alternative to overcoming the problematic separation when using an organic extraction phase.

Reaction.

Our next step is to use the sulfones, both butadiene sulfone and piperylene sulfone, directly as reaction solvents and as recyclable extraction media to replace the use of DMSO. Starting with butadiene sulfone, preliminary reactions were performed to determine if the solvent could be used to facilitate reaction, therefore calibration curves were not initially established to quantify yield. Reaction temperatures were varied from 65-90 °C, and 20 vol% water was added to the vessels in order to generate sulfurous acid for catalysis. The dehydration reaction is shown in Figure 4-11, where fructose, shown in its open chain form, undergoes a dehydration reaction under elevated temperature and acid catalysis to form 5-hydroxymethylfurfural (5-HMF or just HMF) and three molecules of water.

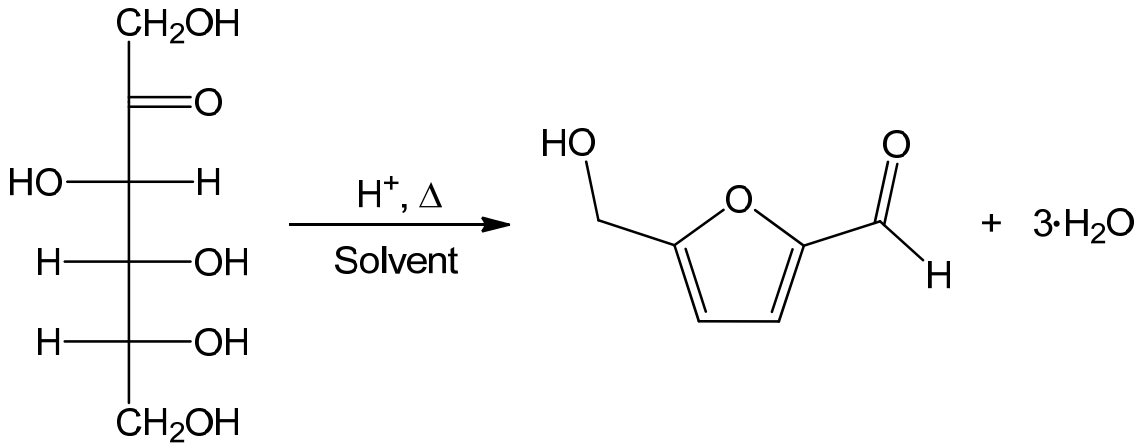

Figure 4-11. Dehydration reaction of fructose with an acid catalyst to form HMF.

Within half an hour, the solutions in butadiene sulfone changed from a translucent to a yellow color. HMF was detected using HPLC as compared with known HMF samples. Because HMF was detected, we went on to further studies.

The dehydration reaction of fructose to 5-HMF is acid catalyzed. Thus we explore two routes to provide the acid for this catalysis: we generate acid in-situ through addition of water, and we add a heterogeneous acid catalyst. First, we tested the ability of butadiene sulfone to generate acid in-situ at elevated temperatures in the presence of small amounts, <20 vol% of water. It is important to note here that sulfones cannot function as catalysts alone. The generation of acid for catalysis is obtained through the equilibrium of the retro-cheletropic reaction. As shown in Figure 4-12, butadiene sulfone is decomposed to butadiene and sulfur dioxide. The equilibrium favors the decomposition species at elevated temperatures. In the presence of water, the available sulfur dioxide can dissolve to form sulfurous acid. The acid can be removed from the solvent without

neutralization, by elevating the temperature to the decomposition point of the solvent, where the acid is unstable.

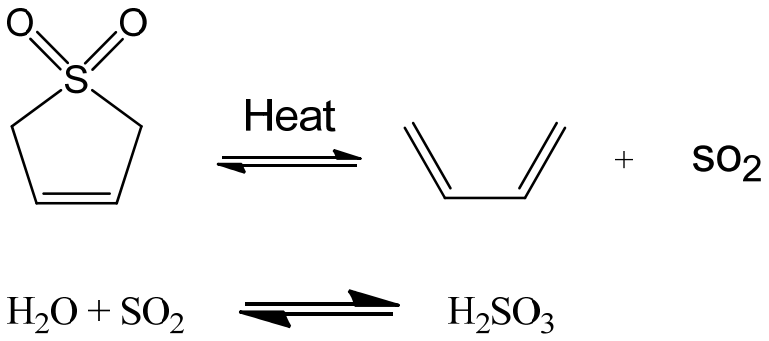

Figure 4-12. Sulfurous acid generated through leveraging the equilibrium reaction of butadiene sulfone and combination of water with sulfur dioxide.

Reaction in PS with In-Situ Acid Catalysis.

Screening reactions were performed using piperylene sulfone. 0.002 moles of piperylene sulfone was combined with 0.0001 moles of fructose, giving a 0.5 mol/L concentration of fructose. We took advantage of the equilibrium reaction of piperylene sulfone by adding 20 vol% H_2O in order to generate acid in-situ for catalysis under elevated temperature. An initial reaction was run at 65 °C for 24 hours, which resulted in a low, 1% yield. We then increased the reaction temperatures to 90 °C, for 6.5 hours reaction time, and we observed a 5% yield. As charring was observed with this reaction time, we decreased the time even further to two hours, and ran the reaction at a temperature of 85 °C; we observed an 11% yield. Carbohydrate concentration is an important variable that we did not vary here, as a constant concentration of 0.5 mol/L was

used throughout the experiments as higher carbohydrate concentrations can lead to reactions that consume the HMF that is formed, resulting in formation of larger amounts of undesirable humins. Thus, even in an un-optimized experiment the in-situ acid catalyzed dehydration reaction of fructose occurs in piperylene sulfone. Next, we choose to establish a design of experiments using a heterogeneous catalyst to work toward an optimal set of experiments.

Reaction in Butadiene Sulfone with Amberlyst-15.

The acid catalyzed dehydration of fructose to HMF has been investigated with the use of several types of catalysts, including mineral acids, ion exchange resins, and heterogeneous catalysts. Heterogeneous acid catalysts have the advantage of easy separation from solvent as well as the ability to be recycled, therefore are well suited for industrial reactions. One research group has reported the use of DMSO and Amberlyst-15 to dehydrate fructose and form HMF [25]. The Amberlyst-15 they used, of particle sizes 53-150 microns, indicated a significantly increase in reaction rate. Amberlyst-15 is a strongly acidic sulfonic acid catalyst for reaction and separation. It is a polymeric resin that is based on styrene and divinylbenzene copolymers. The catalyst is used in a very wide variety of aqueous and organic solvents, when an aqueous miscible solvent is present, and organic reactions including esterification, etherification, and hydration reactions. Additionally, the catalyst has been reported to replace traditional acids and bases in various synthesis including condensation of aldehydes and ketones, or phenol alkylation.

A reaction was run in DMSO as a control experiment and to verify the results reported in the literature. We duplicated the literature conditions of 120 °C, 2 hours

reaction time, and use of the heterogeneous Amberlyst-15 catalyst in a slightly narrower particle size range, 67-125 microns. HMF was obtained in a 90% yield, consistent with literature's report. Next, preliminary reactions were run at a temperature of 120 °C for 2 hours time, the same conditions as those used in literature with DMSO [25], except using butadiene sulfone as the solvent. Significant charring was observed and yields were observed to be less than 10%. As we observed changes in solution color at the 30 minute interval, we decided to decrease reaction time, and analyze yield. Upon decreasing the time from 120 minutes to 30 minutes, we observed an increase in yield to 18%.

With the implementation of the heterogeneous catalyst, additional variables were introduced to the system, including catalyst size and concentration, creating too many variables to efficiently vary independently. Thus, we decided to employ a statistical design of experiments where another group member is working on varying several independent variables simultaneously and exploring the effects and possible interactions. Design of experiments is routinely used in the process development industry to address major processing issues and optimize performance. The independent variables of interest are time, temperature, catalyst loading, catalyst size, sugar concentration, and rate of mixing. The dependant variable is HMF yield. Each of these factors has two levels as well as the center point. Designed in this way, the factorial design of experiments allows for the effects of several factors and the interactions between them to be determined with the same number of experiments that would be required to determine the effect of any one variable by itself. As we are interested in a relatively high number of variables (6), using the standard 2^k factorial design method would require 64 experiments even without any replications; thus we chose a fractional factorial design. In this statistical method, a

subset of the experimental runs of the full factorial design was selected in order to bring out the most important interactions of the considered variables. With the fractional factorial design, we did not need to dedicate the full time and resources required for a full design. The number of runs is expressed by I^{k-p}, where I is the number of levels considered, k is the number of factors, and p is the number of generators and describes the size of the full factorial design used. We select two levels, six factors, and two generators. Thus the number of combinations is expressed by $2^{6-2} = 16$ experimental combinations. As we have two generators, the fraction of the full factorial design is expressed by $\frac{1}{I^p} = \frac{1}{2^2} = \frac{1}{4}$, thus we are using a one-quarter fractional-factorial design of a two level, six factor full factorial design. The experimental runs were randomized in order to reduce the impact that an external bias could have on the results. The first step was to prepare a design table, as seen in Figure 4-13, containing the independent variables and preliminary ranges for these variables which are selected based on those reported in literature [26].

Table 4-1. Factorial design table containing the independent variables and ranges used.

Symbol	Variables and Units		Low	High	Center
X_1	T	Temperature (°C)	100	120	110
X_2	t	Time (minutes)	30	60	45
X_3	C	Catalyst Loading (mg/mL)	2	4	3
X_4	D	Catalyst Diameter (mm)	<0.063	.063 - .125	50% of each
X_5	S	Sugar Concentration (mol/L)	0.1	0.5	0.3
X_6	R	Mixing Rate (rpm)	120	180	150

The next step is to apply regression analysis to the experimental combinations to determine the relationship between the dependant variable (yield) and the independent variables. Yet, due to confounding of variables, an additional set of 8 experiments is employed [26] in addition to a center point in order to completely deconfound the results. Thus, a total of 25 experimental runs are required before continuing. The fractional factorial design table containing each of the 25 experimental design settings is shown in Figure 4-14.

Table 4-2. Fractional factorial design table showing design points for each experiment.

Independent Variables: High(+), low(-), or center(o)							
Run #	**X_1**	**X_2**	**X_3**	**X_4**	**X_5**	**X_6**	**Order**
1	-	-	-	-	-	-	10
2	+	-	-	-	+	-	8
3	-	+	-	-	+	+	2
4	+	+	-	-	-	+	14
5	-	-	+	-	-	+	25
6	+	-	+	-	+	+	13
7	-	+	+	-	+	-	15
8	+	+	+	-	-	-	7
9	-	-	-	+	+	+	4
10	+	-	-	+	-	+	9
11	-	+	-	+	-	-	5
12	+	+	-	+	+	-	1
13	-	-	+	+	+	-	12
14	+	-	+	+	-	-	22
15	-	+	+	+	-	+	3
16	+	+	+	+	+	+	17
17	o	o	o	+	+	o	6
18	o	o	o	+	o	+	16
19	o	+	o	o	+	o	23
20	+	o	o	o	+	o	18
21	o	o	+	o	o	+	24
22	o	+	o	o	o	+	21
23	o	o	o	o	+	+	11
24	+	o	o	o	o	+	19
25	o	o	o	o	o	o	20

The next step is a residual analysis, where the residuals are plotted against each independent variable. If the residuals are evenly distributed, indicating a normal distribution, then no additional terms are required, and a response surface method can be applied and optimal experimental conditions determined. The response surface method

indicates experimental conditions yielding optimal results in the dependant variable. Another group member is currently completing the acquisition of the remaining design points. Several points already obtained indicate that high yields (85%) are expected. Recommendations on a path forward are given in Chapter V.

4.4 Conclusions

In conclusion, we have demonstrated the use of a thermally switchable solvent to replace DMSO in the production of 5-hydroxymethlfurfural, a high-value compound. Literature has cited the need for more efficient product separation methods to be developed in order to make the synthesis of HMF economically viable. We have shown the effective separation of piperylene sulfone and butadiene sulfone to overcome the traditionally problematic separation involved in using DMSO. This separation route utilizes a novel retro-cheletropic switch that can be activated at moderate temperatures. We have also used these sulfones as reaction media in the production of HMF. Although optimization of reaction conditions is needed, we have shown that reaction can be facilitated in these media with the assistance of easily separated acid catalysts.

This is a step towards the production of high-value compounds from renewable resources. HMF is a versatile intermediate that could replace heavily consumed petroleum-based compounds currently used in the production of plastics and fine chemicals, and has sparked the interest of academic researchers and the chemical industry alike. It is essential that we develop new strategies and processes to produce chemicals from biologically based resources opposed to traditional petroleum-based resources; this ensures that we maintain our competitive edge and align ourselves ahead of the shifting trend of seeking independence on foreign sources of oil and petroleum-based products.

4.5 References

[1] Fenton, H. J. H.; Gostling, M. J., *Derivatives of Methylfurfural.* Chem. Soc. 1901. **79:** p. 807.

[2] Zhao, H.; Holladay, J. E.; Brown, H.; and Zhang, C., *Metal chlorides in ionic liquid solvents convert sugars to 5-hydroxymethylfurfural*. Science, 2007. **316:** p. 1597.

[3] Gandini, A.; Belgacem, M.N., *Recent contributions to the preparation of polymers derived from renewable resources*, J. Polym. Environ. 2002. **10:** p. 105.

[4] Gandini, A., *Furans as offspring of sugars and polysaccharides and progenitors of a family of remarkable polymers: a review of recent progress.* Polym. Chem., 2010. **1:** p. 245.

[5] J. Lewkowski, *Synthesis, chemistry and applications of 5-hydroxymethyl-furfural and its derivatives.* Arkivoc, 2001. 1: p. 17-54.

[6] T. Werpy and G. Petersen, *Volume I: Results of Screening for Potential Candidates from Sugars and Synthesis Gas*, Top Value Added Chemicals From Biomass, Pacific Northwest National Laboratory (PNNL) and the National Renewable Energy Laboratory (NREL).

[7] Gorbanev Y.; Klitgaard, S.; Woodley, J.; Christensen, C.; and Riisager, A.; *Gold Catalyzed Aerobic Oxidation of 5-Hydroxymethyl-furfural in Water at Ambient Temperature*, ChemSusChem. 2009. **2:** p. 672 – 675.

[8] M. Bicker; J. Hirth; H. Vogel; *Dehydration of fructose to 5-hydroxymethylfurfural in sub- and supercritical Acetone,* Green Chem. 2003. **5:** p. 280–284.

[9] (a) M. J. Antal, Jr. , W. S. L. Mok, G. N. Richards, *Kinetic Studies of the Reactions of Ketoses and Aldoses in Water at High-Temperature 1. Mechanism of Formation of 5-HMF from D-Glucose and Sucrose,* Carbohydr. Res. 1990. **199:** p. 91 – 109;
b) J. Lewkowski, *Synthesis, chemistry and applications of 5-hydroxymethyl-furfural and its derivatives.* Arkivoc, 2001. 1: p. 17-54;
c) G. W. Huber, J. N. Chheda, C. J. Barrett, J. A. Dumesic, *Production of liquid alkanes by aqueous-phase processing of biomass-derived carbohydrates*, Science 2005. **308;** p.1446 – 1450;
d) Chheda, J. N.; Huber, G. W.; and Dumesic, J. A., *Liquid-phase catalytic processing of biomass-derived oxygenated hydrocarbons to fuels and chemicals,* Angew. Chem. Int. Ed. 2007. **46:** p. 7164 – 7183.

[10] Quoted from Dr. Tony Tianbao Huang, President, Proactive Molecular Research (July 2011).

[11] W.N. Haworth, W.G.M. Jones, *The Conversion of Sucrose into Furan Compounds. Part I. 5-hydroxymethylfurfuraldehyde and Some Derivatives.* J. Chem. Soc. 1944. p. 667–670.

[12] Antal MJ; Mok WSL; Richards GN, *Kinetic studies of the Reactions of Ketoses and Aldoses in Water at High Temperature.2. 4. Carbon Model Compounds for the Reactions of Sugars in Water at High Temperatures,* Carbohydrate Research, 1990. **199:** p. 111.

[13] Organic Chemistry, Third edition, Maitland Jones Jr., W.W. Nortan & Company, 2005, p. 1237.

[14] Kuster, B.F.M, 5-*HMF – A Review Focusing on Its Manufacture*, Starch/Staerke, 1990. **42:** p. 314–321.

[15] De Sudipta; Dutta Saikat; Saha Basudeb, *Microwave assisted conversion of carbohydrates and biopolymers to 5-hydroxymethylfurfural with aluminium chloride catalyst in water,* Green Chem. 2011. 13: p. 2859.

[16] Bonner W.A.; and Roth M.R., *The Conversion of D-Xylose-1-C-14 Into 2-Furfuraldehyde-Alpha-C-14*, J. Am. Chem. Soc. 1959. **81:** p. 5454

[17] Kuster, B., and Vanderbaan HS., *Dehydration of D-fructose (Formation of 5-Hydroxymethyl-2-Furfaldehyde and Levulinic Acid) .2. Influence of Initial and Catalyst Concentrations on Dehydration of D-Fructose*. Carbohydr. Res., 1977. **54:** p. 165.

[18] Zhao Qian; Wang Lei; Zhao Shun; et al., *High selective production of 5-hydroymethylfurfural from fructose by a solid heteropolyacid catalyst*, Fuel, 2011. **90**: p. 2289

[19] C. Sievers, I. Musin, T. Marzialetti, M. B. V. Olarte, P. K. Agrawal, C. W. Jones, *Acid-Catalyzed Conversion of Sugars and Furfurals in an Ionic-Liquid Phase,* ChemSusChem, 2009. **2:** p. 665 – 671.

[20] B. R. Caes and R. T. Raines, *Conversion of Fructose into 5-(Hydroxymethyl)furfural in Sulfolane,* ChemSusChem, 2011 **4:** p. 353 – 356

[21] K. Seri, Y. Inoue, and H. Ishida, *Highly Efficient Catalytic Activity of Lanthanide(III) Ions for Conversion of Saccharides to 5-Hydroxymethyl-2-furfural in Organic Solvents,* Chemistry Letters, 2000, p. 22

[22] F. Ilgen, D. Ott, D. Kralisch, C. Reil, A. Palmberger, B. König, *Conversion of carbohydrates into 5-hydroxymethylfurfural in highly concentrated low melting mixtures*, Green Chem. 2009. **11:** p. 1948–1954.

[23] K. Shimizu, R. Uozumi and A. Satsuma, *Enhanced production of hydroxymethylfurfural from fructose with solid acid catalysts by simple water removal methods*, Catal. Commun., 2009. **10:** p. 1849–1853.

[24] Santosusso, T.M., Swern, D., *Chemistry of Epoxides 32. Acid Catalysis in Dimethyl-Sulfoxide Reactions - Generally Unrecognized Factor*. J. Org. Chem., 1976. **41:** p. 2763-2768.

[25] Shimizu Ken-ichi; Uozumi Rie; Satsuma Atsushi, *Enhanced production of hydroxymethylfurfural from fructose with solid acid catalysts by simple water removal methods*, Catalysis Communications, 2009. **10:** p. 1849.

[26] Louvar, J., *Simplify Experimental Design*, Chemical Engineering Progress, 2010. **106:** p. 35.

[27] Amarasekara Ananda S.; Williams LaToya D.; Ebede Chidinma C., *Mechanism of the dehydration of D-fructose to 5-hydroxymethylfurfural in dimethyl sulfoxide at 150 degrees C: an NMR study*, Carbohydrate Research, 2008. 343: p. 3021.

CHAPTER V

CONCLUSIONS AND RECOMMENDATIONS

5.1 Conclusions

Novel Switchable Solvents.

Piperylene sulfone is a smart solvent that can be easily separated from reaction products with a built-in thermal switch that enables the decomposition of the solvent to volatile components. This thermal switch causes the chemical and physical properties to undergo a step change with an increase in temperature, this is what characterizes PS as a smart solvent. Importantly, this reversible switchable property not only allows for separation of solvent, but also subsequent recycle and reuse of the solvent, making the process sustainable by design. We have shown the synthesis of this solvent and characterized the parameters of PS formation. We have achieved quantitative yields with the use of an ionic inhibitor. Furthermore, we have developed a method allowing for an effective separation of the inhibitor and a substantial reduction in waste compared to the methods used in literature.

We have successfully shown the transition from the laboratory gram scale synthesis of a specialty compound to enabling the full scale production with high yields and minimal waste generation. Through implementation of these developments into a HYSYS simulation, we simulated the full scale production of PS. An economic analysis determined the cost of PS production from a materials and energy standpoint. Indeed

further optimizations will be needed at each stage in the industrial scale-up process, but this is a critical first step to large scale production.

Continuous Flow Processing.

Batch processing has dominated the pharmaceutical industry, from research and development to manufacturing. Challenges in scaling up a process using batch technology have limited the profit margins and caused increased pressure on the industry to consider improvements in productivity, reductions in waste, and quality/control improvement. We demonstrate the first Meerwein-Ponndorf-Verley (MPV) reductions to be run in continuous flow mode, using the reductions of aldehydes and ketones to their corresponding alcohols as model components. Our use of $Al(O\textit{t}Bu)_3$ as an highly active, efficient and cost-effective catalyst has been integral to enabling the transition to continuous flow. This MPV reduction is a valuable chemoselective reaction pathway for the pharmaceutical industry and has been used in the production of several HIV protease inhibitors, commonly prepared through the MPV reduction of *N*-(*tert*-butyloxycarbonyl)-(3*S*)-3-amino-1-chloro-4-phenyl-2-butanone, or (S)-CMK.

However, in continuing forward, researchers must be cautious of the challenges in the use of continuous processing, which include the requirement of a detailed understanding of the process such that the reaction can be run at steady state and provide a high quality product. Additionally, the start-up and shut down of a reaction may not be straightforward due to operational issues such as variations in pumping rates and equipment limitations like clogging of reactor channels.

Biomass-based Processing in Novel Switchable Solvents.

The production of fuels, chemicals, and essential building blocks from renewable biological resources has captured the attention of both academic researchers and the chemical industry. Government agencies around the world have provided incentives, and several global companies have developed infrastructure for biochemical production. One specific high-value chemical produced from biological resources that has accumulated significant interest is 5-hydroxymethylfurfural, or HMF.

HMF is considered a 'sleeping giant' in the field of intermediates derived from renewable resources, as it is an intermediate in polymers synthesis, plastic processing, and referenced as a building block in biofuel development. As researchers have yet to develop an efficient separation strategy for HMF, the compound remains prohibitively expensive and a specialty chemical. The economical production of HMF is closely tied to its efficient separation from solvent. We have applied our novel switchable solvent to the reaction and separation of HMF, and demonstrated successful separation. This separation route uses the switchable piperylene sulfone, and avoids the need for a second phase for extraction. Additional research is being currently being conducted on the reaction of fructose to form HMF. We have shown that reaction can be facilitated in our solvents with either the addition of water to generate acid catalysis in-situ or through the assistance of an easily separated heterogeneous acid resin. Using piperylene sulfone as the solvent and 20 vol% water to generate acid catalysis in-situ at moderate conditions, we obtained 11% yield in an unoptimized reaction. When we used Amberlyst-15 in butadiene sulfone at the same conditions as those used with DMSO, we achieved an 18%

yield. These results are encouraging to date as both of these reactions are not yet optimized, and show that the sulfone solvents can be used to facilitate the reaction of fructose to HMF. Due to the large number of independent variables involved in this system (time, temperature, catalyst loading, catalyst size, sugar concentration, and rate of mixing) a statistical design of experiments was employed to determine optimal conditions. Although the optimizations are currently underway, preliminary results indicate that high yields can be obtained, as we have observed yields of 88%.

5.2 Recommendations

Novel Switchable Solvents.

Now that we have enabled the production of piperylene sulfone in high yields, it can be further explored and established as a solvent for reaction and/or separation. We already demonstrated it as a solvent for nucleophilic displacement reactions and the in-situ acid catalyzed hydrolysis of β–pinene. Several potentially valuable paths forward may be to:

- Apply piperylene sulfone as a solvent for complete reaction, separation, and recycle on a larger scale to show (1) the quantitative recycle of piperylene sulfone which ensures its effectiveness in an industrial scale process (2) no loss in solvent due to undesirable side reaction enabling an indefinite number of recycles.
    - The complete process has been shown with benzyl chloride and potassium thiocyanate, and upon separating the piperylene sulfone from the product and reforming the solvent, 87% of the mass was recovered, and the remainder is attributed to small scale losses. By showing the quantitative

recycle of piperylene sulfone, we ensure its use as completely recyclable solvent.

- Use of PS as a replacement to DMSO, in the single solvent reaction and separation of a high value compounds, such as HMF or its derivatives. In this process, we would demonstrate the complete reaction, separation using the thermal switch, and recycle of piperylene sulfone on a scale that is at least tens of milliliters.
- Continued identification of processes that can benefit from the thermal separation route. The case of using piperylene sulfone as a reaction and separation media will be enhanced by showing other reactions in piperylene sulfone and then subsequent separation utilizing the thermal separation route. This requires non-volatile products that are stable at reaction temperatures of about 100 °C.
- Cleaning of newly manufactured microelectronic components with piperylene sulfone as a replacement to DMSO. In this case, the thermal switch of piperylene sulfone at moderate temperatures (~ 110 °C) is leveraged to avoid the economic costs of using a high-boiling solvent. This is one example of an innovative application where a dipolar aprotic solvent is required, but separation issues constrain process development.

Continuous Flow Processing.

A multistep synthetic strategy utilizing a continuous uninterrupted reactor network is of great advantage to the pharmaceutical industry, as such a scale-out approach would eliminate the need for pilot plant engineering and reduce the time-to-market of a proprietary drug. The Corning reactor is well suited for multistep syntheses,

as it is equipped with multiple feed inlets and temperature regions which can be adapted for sequential multistep reagent injection and mixing.

The next step in this research involves continued work with the synthesis of pharmaceutically relevant compounds. More specifically, heteroaromatic-fused rings are a major component of biologically active molecules and useful building blocks for complex synthesis in the pharmaceutical industry. We aim to conduct a multistep synthesis of the Lewis-acid catalyzed homo-Nazarov reaction to produce heteroaromatic compounds, as represented in Figure 5-1. In this reaction, the cyclopropyl vinyl ketone undergoes an acid-promoted ring opening yielding a 1,3-dipole which then undergoes intramolecular attack to form the cyclic cation. The cation is quenched to form the enol and tautomerized to form the desired cyclohexenone product.

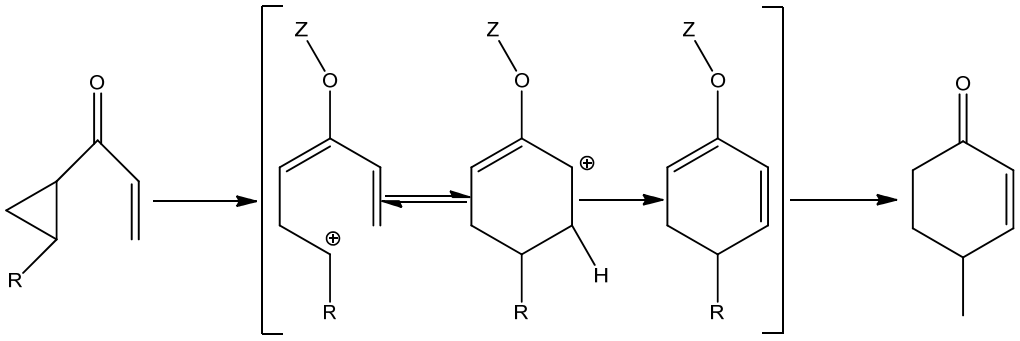

Figure 5-1. Schematic of the homo-Nazarov cyclization of cyclopropyl vinyl ketones.

Our objectives in implementing the homo-Nazarov cyclization to continuous flow are:

- Maximize reaction yield and selectivity and reduce solvent requirements, especially the use of halogenated solvents, then implement this single reaction step to continuous flow.
- Demonstrate the multistep synthesis of the reaction, where each step is individually optimized first; from an innovation stand point, it is important to implement the entire multistep synthesis into continuous flow.
- Develop a process optimization using Aspen, and perform an economic and environmental assessment.

The multistep homo-Nazarov cyclization is an important example in bringing about significant improvements in pharmaceutical manufacturing and production processes that result in smaller and more energy efficient technology, as well as higher quality product.

Biomass-based Processing in Novel Switchable Solvents

The next step in this research is:

- Analysis of the statistical design of experiments as completed by another group member and determination of the optimal reaction conditions. Next, we can confirm these statistical predictions by conducting an experiment at the optimal conditions. As high yields have already been observed, we expect that nearly quantitative yields are possible after optimization.

- Combine reaction and separation to demonstrate a complete process; we will separate the butadiene sulfone solvent away from the HMF produced, using the thermal mechanism.
- Perform a process optimization using HYSYS or Aspen, and subsequently complete an economic analysis to determine competitiveness of our method and also to facilitate the transfer of technology developed on the laboratory scale to larger production.
- The reaction conditions determined from the optimization with butadiene sulfone can be extended as a first order approximation for the use of piperylene sulfone; although more expensive, the advantages to using PS for reaction and separation are a lower melting point, a lower decomposition temperature and exclusivity.

From a longer-range perspective, the reaction of HMF from fructose represents a class of reactions where high-value products are synthesized from renewable resources. This is one example of producing such a product, where we can replace traditional petroleum-based syntheses. To enhance upon the success of this project, one potentially valuable path forward may be the use of more abundant and less expensive starting material for the HMF production, such as other monosaccharides (e.g. glucose), polysaccharides (e.g. cellulose), and then biomass. A schematic showing this process is given in Figure 5-2. Implementation of the longer chain carbohydrates will first require an acid hydrolysis step to cleave the chain into individual monomers. If the results are encouraging, we can contact Dr. Charlotte Williams, a collaborator at Imperial College in England.

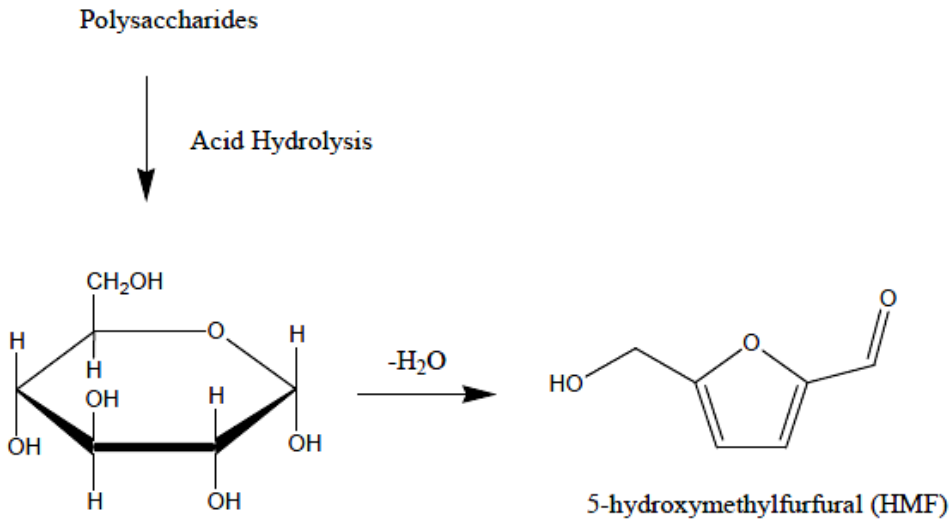

Figure 5-2. Schematic showing the acid hydrolysis of polysaccharides in the production of HMF from glucose.

APPENDIX A

CO_2-ENHANCED SUB-CRITICAL WATER AS A SUSTAINABLE BIOMASS PRETREATMENT SOLVENT

A.1 Introduction

Energy demand is expected to increase by roughly 50% in the next 20 years, attributed predominantly to growth in developing nations. In fact, the Department of Energy has specified goals by 2025 to replace 30% of the liquid petroleum transportation fuel with biofuels and 25% of industrial organic chemicals with biomass-derived chemicals [1]. An increasing demand for a finite amount of petroleum resources cannot be sustained, as alternative fuel derived from natural resources becomes a more accepted approach. Fuel production from biomass and biological resources is based on a closed carbon cycle, in contrast to fuel derived from fossil resources, where carbon reserves trapped in the earth's crust are released into the atmosphere. Currently, bioethanol in the United States is predominantly derived from corn, sparking a "food versus fuel" debate. In 2007, 5.7 billion gallons of ethanol were produced and indeed most of this production was from the starch in corn kernels [2]. After the cost of corn doubled within a year of the government releasing incentives to increase ethanol production, it became evident that bioethanol production will not be based on corn [3] (U.S. Deputy Energy Secretary, Clay Sell, 2007) and it is expected to be based on lignocellulosic biomass.

Lignocellulosic biomass is composed of three structurally distinct components: cellulose which is shown in Figure A-1 (roughly 50 wt%), hemicellulose which is shown

in Figure A-2 (roughly 25 wt%), and lignin which is shown in Figure A-3 (roughly 25 wt%) [4]. Only two of these components, cellulose and hemicellulose, can be processed to ethanol in appreciable yield by microbial fermentation. Cellulose is a polymer composed of $\beta(1 \rightarrow 4)$ linked D-glucose units, which form a crystalline structure called microfibrils, connected via hydrogen bonds. Hemicellulose is composed of a matrix of polysaccharides with an amorphous structure of mainly hexoses and pentoses. Lignin is a rigid aromatic biopolymer of phenylpropane units and has a highly heterogeneous composition. The purpose of this structure is to provide support and resistance to compression in plant cell walls, consequently hindering enzymatic access to the cellulose and hemicellulose. While lignin cannot be processed to ethanol, it is commonly used in the paper and pulp industry as a raw fuel.

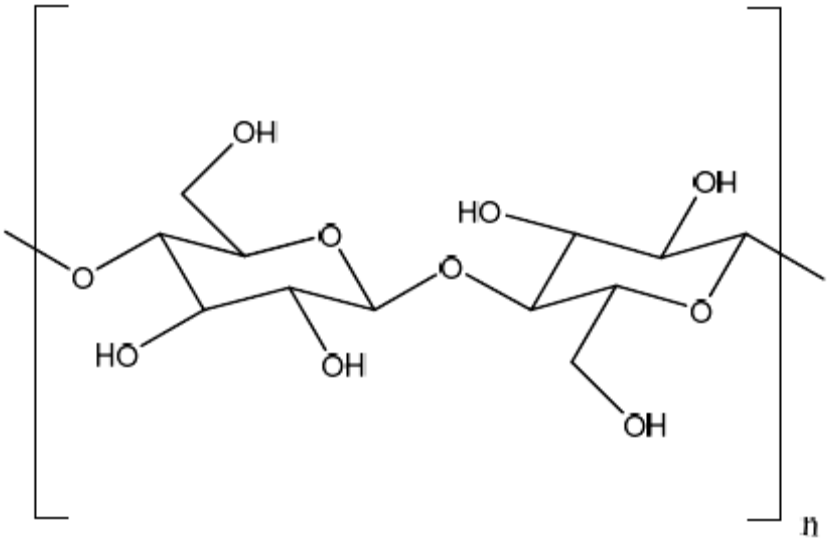

Figure A-1. A representative structure of cellulose composed of β (1 → 4) linked D-glucose units.

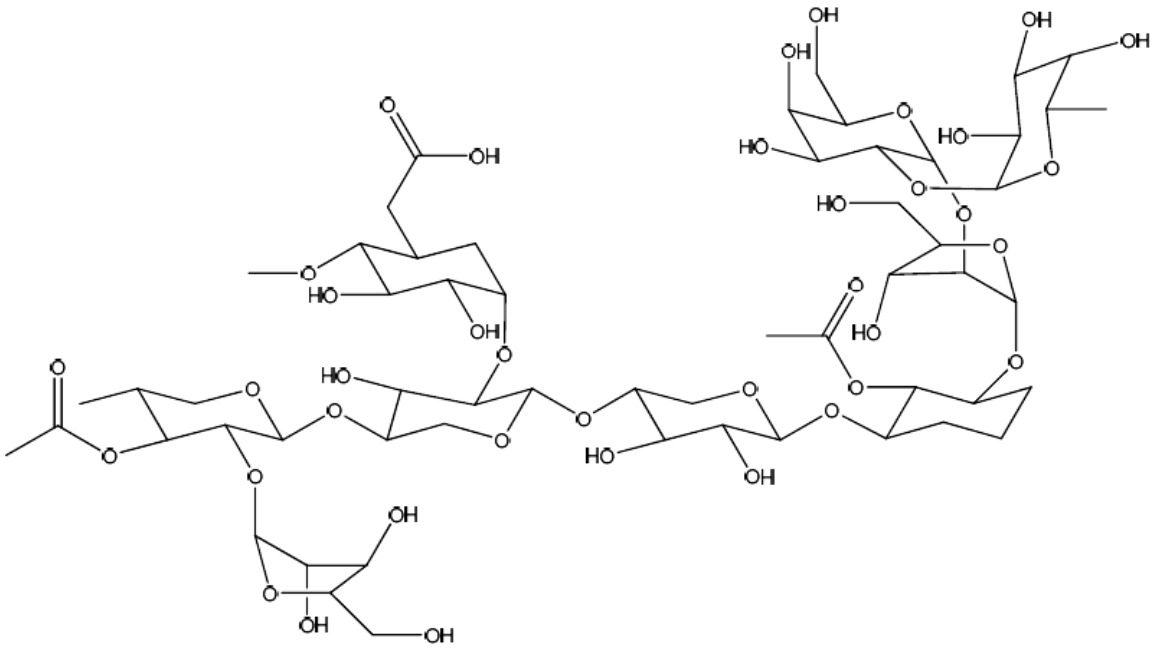

Figure A-2. A representative structure of hemicellulose.

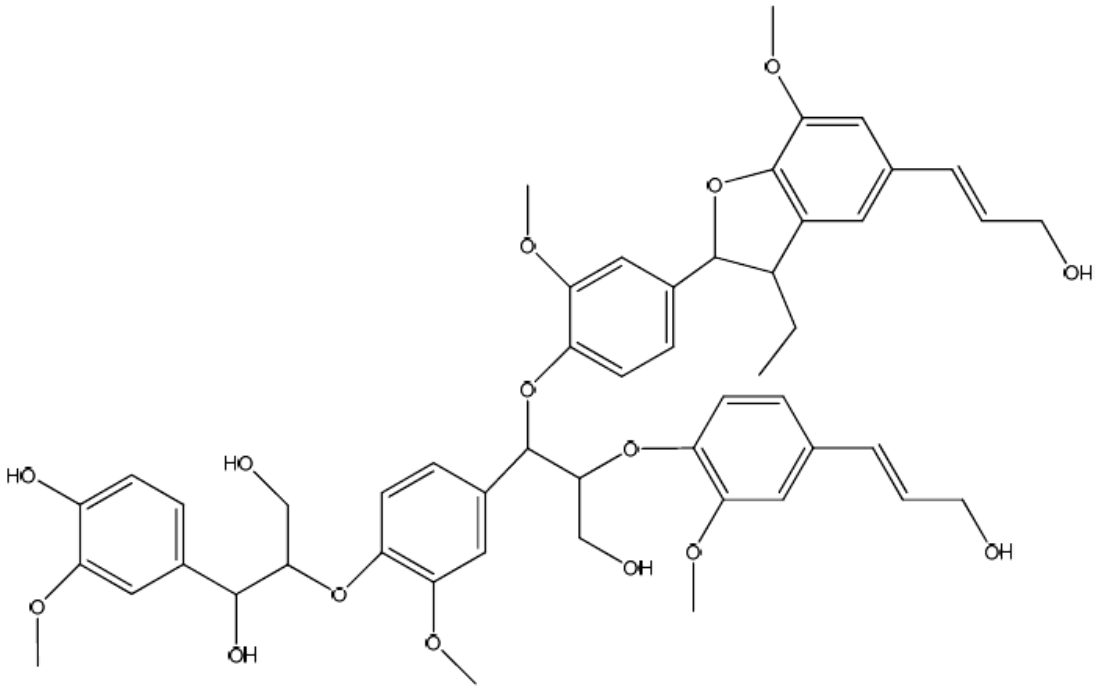

Figure A-3. A representative structure of lignin.

Given the structural rigidity of the lignin component in lignocellulosic biomass, it is necessary to pretreat the biomass using a specialized method to increase the effectiveness of the subsequent steps of enzymatic saccharification and fermentation. The other components, cellulose and hemicelluloses are broken down to simple monosaccharides, like glucose or xylose, and fermented to ethanol. However, due to the presence of the lignin barrier, a pretreatment step is necessary prior to fermentation. In fact, the pretreatment step is estimated to be the most expensive capital investment in the conversion of lignocellulosic biomass to ethanol [5]. The efficient and inexpensive depolymerization of lignocellulosic biomass in this pretreatment step is central to use of biomass as a sustainable fuel. The pretreatment must accomplish several objectives: rupturing the lignin barrier [4], interrupting the crystallinity of cellulose [4], preserving hemicelluloses [6], minimize degradation products [6], lower catalyst cost and enhance recycle [6], and minimize energy demands and costs [6]. We reference a visual schematic to show the objectives of pretreatment in Figure A-4.

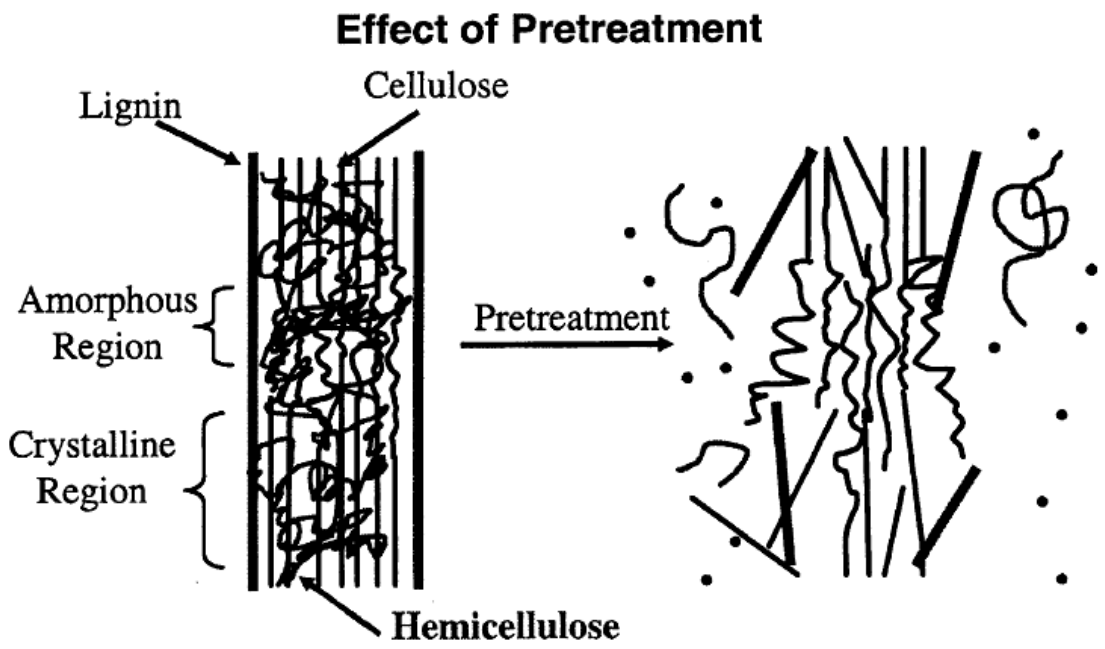

Figure A-4. Schematic showing the pretreatment objectives of lignocellulosic biomass [4]

There are many methods of pretreatment currently being investigated, including dilute acid, liquid hot water, ammonia fiber explosion, ammonia recycled percolation, and lime. Although many of these methods are effective at accomplishing the pretreatment goals, they require acid or base neutralization, many times generating a salt which then requires separation and removal. These contaminated salts cause additional separation processing challenges, increase costs, and are economically unfavorable [13]. The development of a more economically and environmentally benign lignocellulosic biomass pretreatment method is needed.

First, sub-critical water has the advantages of: an increased dissociation constant (K_w) by several orders of magnitude compared to water at standard temperature and pressure[7], facilitating both acid and base catalyzed reactions, creation of a homogenous aqueous reaction phase, and straightforward reversal upon cooling to room temperature

and returning to atmospheric pressure without the need for any additional components in neutralization. Sub-critical water is limited to moderate temperatures, as significant byproduct formation and degradation of the sugar molecules is observed at higher temperatures and for extended processing times.

However, the addition of carbon dioxide is known to accelerate the rate of acid catalyzed reactions in hot water [14, 15]. Independently, supercritical carbon dioxide offers the advantages of reduced surface tension, high diffusion coefficients, and simple separation. Furthermore, the combination these two solvents for the purpose of carbohydrate extraction from lignocellulosic biomass results in a powerful combination. CO_2 enhanced sub-critical water further facilitates acid catalyzed reactions, as the carbon dioxide is driven into the liquid phase, forming in-situ carbonic acid and reducing the pH, as shown in Figure A-5. The solvent system is environmentally benign and completely reverses upon cooling and depressurization, minimizing prohibitive separation issues commonly encountered in biomass pretreatment solvents [8] as well as reducing the processing costs. It should be noted that this process uses carbon dioxide which can be recycled in a scalable process, as opposed to generating CO_2.

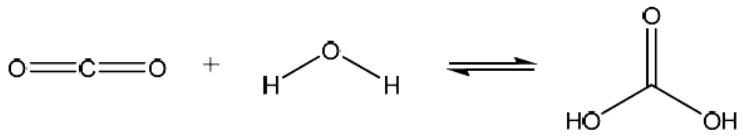

Figure A-5. The formation of carbonic acid from the reaction of CO_2 with water.

Accomplishing the pretreatment objectives discussed above requires a balance of pretreatment severity (high temperatures, times, and pressures) and effectiveness in rupturing the lignin barrier and obtaining the monosaccharide carbohydrates. At the high temperature range, greater than 250 °C, an increase in degradation products and inhibitors to fermentation is observed. Not only are these degradation products, such as HMF, prohibitive in the downstream fermentation to ethanol, but also a decrease in carbohydrate extraction is observed. On the other hand, at the low temperature range, less than 100 °C, a majority of the structure of biomass remains intact, and the oligosaccharides are not effectively broken down. In this example, reaction temperature is only one of the variables that can be influenced, considering we keep the other variables constant. The other variables include reaction time and carbon dioxide pressure. Given the number of variables, wide range of reaction conditions, and nonlinear variable interaction, a successful investigation of the pretreatment objectives necessitates a statistical design of experiments.

With a statistical design approach, several factors can be simultaneously varied, yet we can independently evaluate each factor. This is important in our case of lignocellulosic biomass pretreatment due to nonlinear and dependent variable interaction. The effect of each reaction variable can be measured, as a main effect, as well as the effect of the interaction of the variables, as interaction effects, eliminating confounding of variable effects [9]. A statistical design of experiments is planned testing prior to experiments, and it helps handle experimental error. In order to perform a statistical design of experiments, Minitab is used. Within Minitab, a Benhken-box design is employed as the statistical design for surface analysis. In brief, this is a 2^k factorial design

with 2 levels and k factors (3) where the design points are selected as the midpoints of the edges, avoiding experimental extremes.

A.2 Experimental

Materials.

The following materials were used as received: glucose (D-(+)-glucose, Sigma Aldrich, 99.5% or dextrose, BDH, anhydrous, ACS reagent), arabinose (Sigma Aldrich, 98%), xylose (Sigma Aldrich, Sigma ultra >99%), mannose (Sigma Aldrich, >99%), galactose (Sigma Aldrich, 99%), and fructose (Sigma, min 99%). Whatman P5 medium porosity filter paper was used to separate the solid biomass from the filtrate. Whatman disposable filter devices (PVDF, 13 mm, 0.2 μm pore size) or Pall Life Sciences Acrodisc syringe filters (nylon, 13 mm, 0.2 μm pore size) were used to filter all samples before analysis via HPLC-RID. Autoclavable plastic vials (BioMed) were used during sulfuric acid induced hydrolysis and workup. Water (Sigma Aldrich, HPLC grade, >99%) was used as received for the mobile phase in the HPLC, and carbon dioxide gas (Air Gas, SFC grade, 99.99%). Distilled water was obtained from the Unit Operations laboratory at Georgia Tech. Corn stover biomass samples were obtained from Dr. Ragauskas from the School of Chemistry and Biochemistry at Georgia Tech. In order to reduce the biomass size for experimentation, the biomass samples were ground with a Wiley mill and then sifted through a #4 sieve.

Methods.

2.5 grams of biomass were placed in a 300 mL high-pressure Parr reactor from Parr Instrument Co. The temperature and agitation were kept constant by a heating jacket and tachometer controlled by a Parr Model 4842 controller. The reactor was sealed with a

PTFE o-ring and closed by tightening the bolts in a star configuration. The reactor was allowed to heat to the desired temperature, then the CO_2 was added with an Isco 500D syringe pump set at constant pressure. The reactor pressure was also displayed on the Parr controller via a pressure transducer connected to the reactor. Control experiments involving only H_2O were also conducted. After reaction, the liquid was filtered with a Whatman P5 medium porosity filter paper to separate the solid biomass from the filtrate. The experimental setup of the Parr reactor can be seen in Figure A-6.

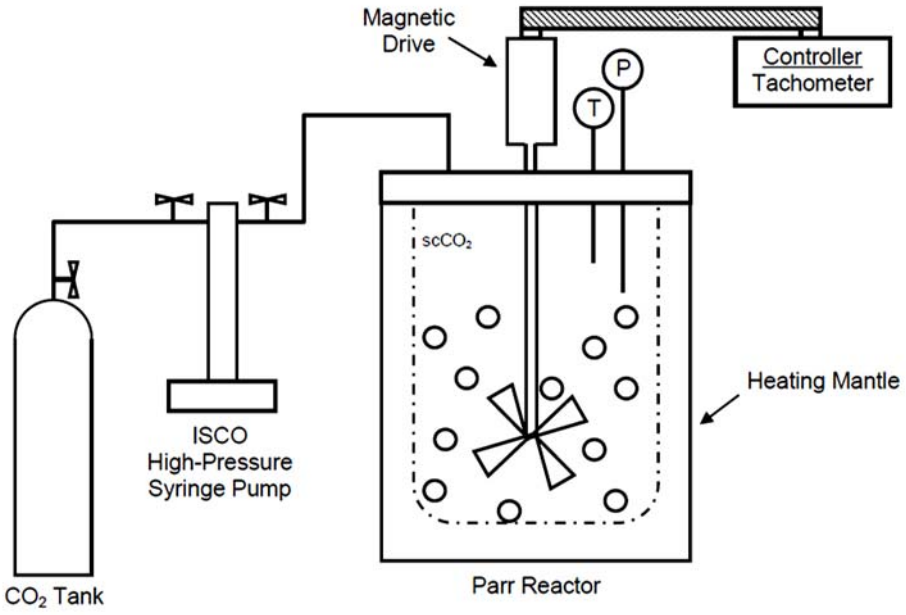

Figure A-6. Illustration of the Parr reactor used in the CO_2-enhanced sub-critical water experiments (modified from L. Draucker Ph.D. thesis [16]).

Equipment and Analysis.

After filtration, all samples were analyzed in a Hewlet-Packard (HP) Series 1100 High Performance Liquid Chromatograph (HPLC) equipped with an Agilent

Technologies 1200 Series Refractive Index Detector (RID). The HPLC method achieved separation in a BioRad Aminex HPX-87P column (lead resin, sulfonated divinyl benzene-styrene copolymer, 300 x 7.8 mm), preceded by a BioRad deasher cartridge. The autoclave used is a Cuisinart CPC-600 1000-Watt 6-Quart Electric Pressure Cooker.

Workup and Analysis Method.

Each experiment involved two different HPLC analyses. The exact analytical procedure was conducted as outlined for biomass liquid process samples by the National Renewable Energy Laboratory (NREL) [17]. Calibration curves for each sugar of interest were created to determine experimental results. One HPLC sample came directly from the liquid process fraction of the experiment. It underwent the basic procedure described in the sample workup section. The second sample underwent the workup procedure described below in "Sulfuric Acid Hydrolysis of Liquid Fraction Samples" before undergoing analysis via HPLC-RID. All analyses for this chapter focused on the liquid phase fraction of the biomass after pretreatment. There are many additional aspects that must be examined and studied to completely determine an optimal pretreatment. The analysis of the liquid phase fraction, however, does give significant indication as to whether or not the pretreatment is achieving the desired goals.

Initial Liquid Fraction Sample Workup.

A 5 mL aliquot of the liquid process fraction was placed in a plastic autoclave vial. The pH was measured using pH paper, and the sample was neutralized using calcium carbonate until the pH reached 5-6. The sample was centrifuged, and 1.5 mL of the supernatant was collected and filtered into a HPLC vial for analysis.

Sulfuric Acid Hydrolysis of Liquid Fraction Samples.

Liquid fraction aliquots of 5 mL were taken from each experiment and placed in a plastic autoclave vial. The pH of each sample was measured using pH paper, and the appropriate amount of 72 wt% sulfuric acid was added to each tube. For a pH of 2.43 and higher, which includes all samples tested during the course of these experiments, 174 μL must be added for 5 mL aliquots and 348 μL must be added for 10 mL aliquots. Individual sugar recovery standards were also made in the plastic autoclave vials. They consisted of 0.25 g of glucose and 0.25 g cellulose and xylose. The liquid process samples and sugar recovery standards were autoclaved for 1 hour at 121 ºC and 2 atm. The vials were allowed to cool to room temperature before they were neutralized with calcium carbonate. The pH of each sample was checked regularly with pH paper until all samples and sugar recovery standards reached a pH of 5-6. After neutralization, 1.5 mL of each sample and sugar recovery standards was filtered and put in HPLC vials for analysis.

HPLC-RID Calibration Curves.

Calibration curves were made for the following sugar samples: glucose, xylose, galactose, arabinose, and mannose. Each calibration curve was constructed twice to ensure accuracy. The RI absorbances of all sugar concentrations were linear with the $R^2 \geq 0.99$ for all samples.

HPLC-RID Method.

The HPLC-RID method used during analysis was obtained from the Department of Energy's laboratory procedure for the analysis of liquid biomass fractions. 10 μL of

sample was injected into the HPLC running an AMINEX 87-P column. The mobile phase was pure H_2O, degassed and 0.2 μm filtered. The flow rate was 0.6 mL/min and the column temperature was 80 ºC. The run time was approximately 20 minutes, and a sample of pure H_2O was run between samples to clean the column and extend time between samples.

A.3 Results

Based on previous research in our laboratory, CO_2-enhanced sub-critical water appeared to be the most promising pretreatment method investigated; however, the extent of success of our novel method in combination with the design of experiments was largely unknown. Previous research has demonstrated that the addition of CO_2 to sub-critical water significantly affected the concentration of carbohydrates recovered[10] and was indeed successful in altering the physical structure of the material as shown by SEM images. In a quantitative study, the extraction of carbohydrates was measured using pine wood chips as a feedstock. In this experiment, the change in carbohydrate concentration was measured between use of sub-critical water at 150 ºC and 20 min and compared with a sub-critical water experiment at the same temperature and time conditions but with the addition of CO_2. We found that two oligomer yields were increased by 10% and 20%, however, these oligomers were not identified due to limitations of our HPLC column; additionally, glucose yields increased 35%, galactose yields increased by 23%, and mannose yields actually decreased by less than 10%, as shown in Figure A-7, using sub-critical water vs sub-critical water plus CO_2 and pine wood chips as the feedstock (150 ºC, 1000 psi, 20 min) [10]. However, limitations were encountered with the use of the small volume titanium reactors including processing of small volumes, less than 2 mL

total, and the lack of stirring. In order to overcome limitations encountered, a Parr reactor (shown in Figure A-6) was used for further experiments. The Parr reactor allows for reaction of larger volumes (300 mL total reactor volume) and can stir the liquid phase during reaction thus reducing mass transfer limitations. We have installed a Biorad Aminex HPX 87-H column on the HPLC in order to analyze selected carbohydrates.

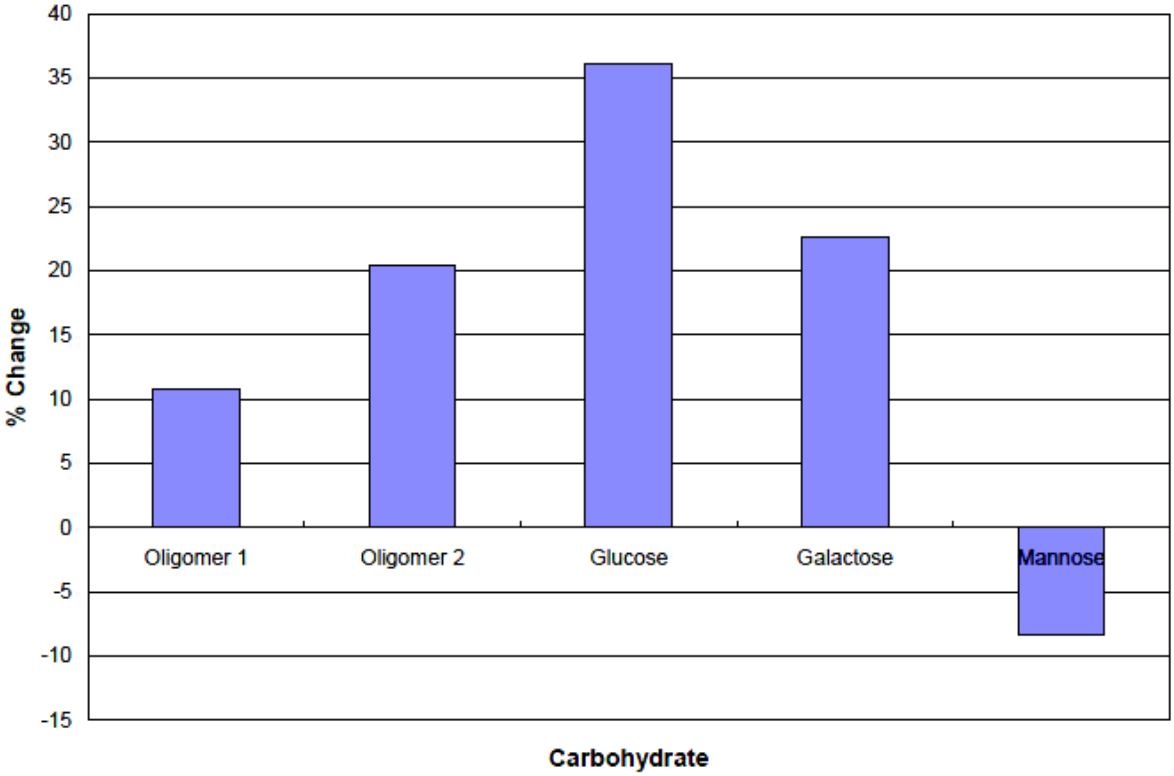

Figure A-7. Experiment comparing the change in carbohydrate concentration after adding CO_2 [10].

Individual carbohydrate extraction can be optimized as well as a selected group of carbohydrates, revealing optimal reaction conditions for a given type of biomass. Only

one type of lignocellulosic biomass, corn stover, was used in order to standardize experiments, unless otherwise noted. We have run reactions at all design points specified with the Box-Behnken design. In this design, we varied three variables – time, temperature, and pressure, each at two settings – high and low, and additionally, ran 3 experiments at the midpoint of the box for a total of 15 experiments.

Using the experimental midpoint as an example, a substantial increase in carbohydrate extraction is obtained with the addition of carbon dioxide to the reaction media; specifically, at the midpoint conditions – 45 minutes, 160 °C, we show the recovery when we keep the time and temperature constant and vary the pressure. 20% more glucose is obtained when 800 psi of carbon dioxide are added to the reaction system, and 27% more glucose is obtained when about 1700 psi of carbon dioxide are added (corresponding to an extracted glucose concentration of about 3.3 mg/mL). The impact of additional CO_2 pressure is even greater on xylose, with yields 54% higher at 800 psi of CO_2 and an 87% increase in extraction at about 1700 psi of CO_2 (corresponding to a concentration of 7.6 mg/mL). This is shown in Figure A-8 below. Other carbohydrates obtained include arabinose, galactose, and various oligosaccharides that are broken down to their monomer forms and detected in the above samples. The sample carbohydrates are separated by a Bio-Rad Aminex HPX 87-P carbohydrate column in an HPLC (high performance liquid chromatography) and detected with a Refractive Index detector. The National Renewable Energy Laboratory (NREL) and American Society for Testing and Materials (ASTM) have established standard procedures for analyzing biomass samples.

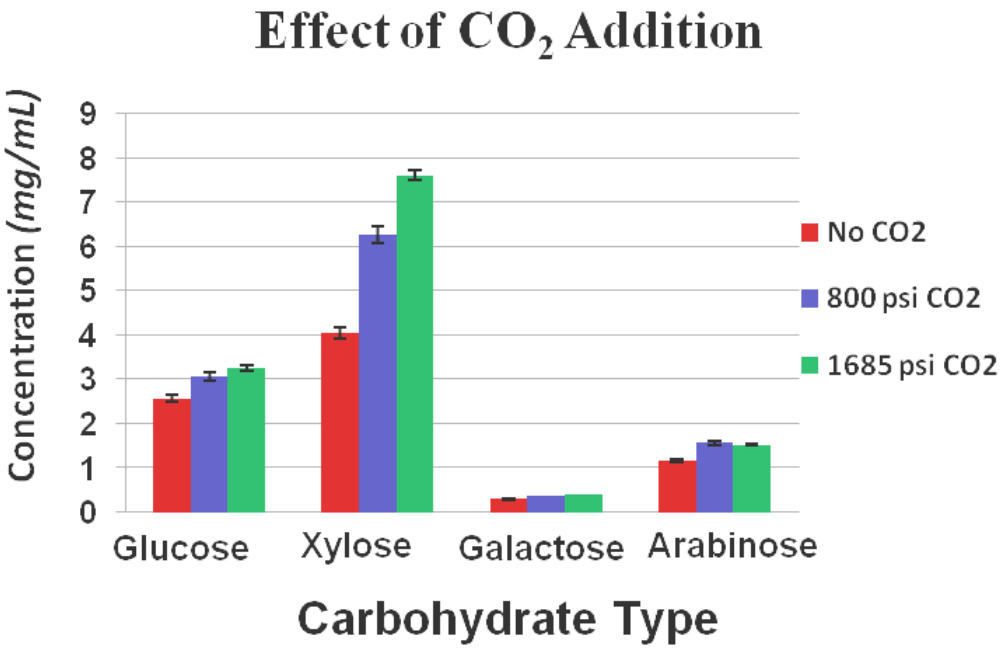

Figure A-8. Concentration of four primary carbohydrates extracted after pretreatment.

The design variables in the statistical design of experiments are time, temperature, and CO_2 pressure, and the response variable is carbohydrate concentration. The optimum glucose concentration is obtained within the design variables selected for the Box-Behnken design, as demonstrated in a glucose contour plot, Figure A-9 below. Temperature is set on the y-axis and time is set on the x-axis. The optimal glucose yield as predicted by Minitab is at a time of 65 minutes, temperature of 136 ^{O}C, and pressure of 1212 psi yielding a predicted concentration of 3.28 mg/mL (P=0.009). We confirmed this prediction by running an experiment at these conditions. The concentration obtained at these conditions is 3.11 mg/mL, which differs from the predicted concentration by about 5%.

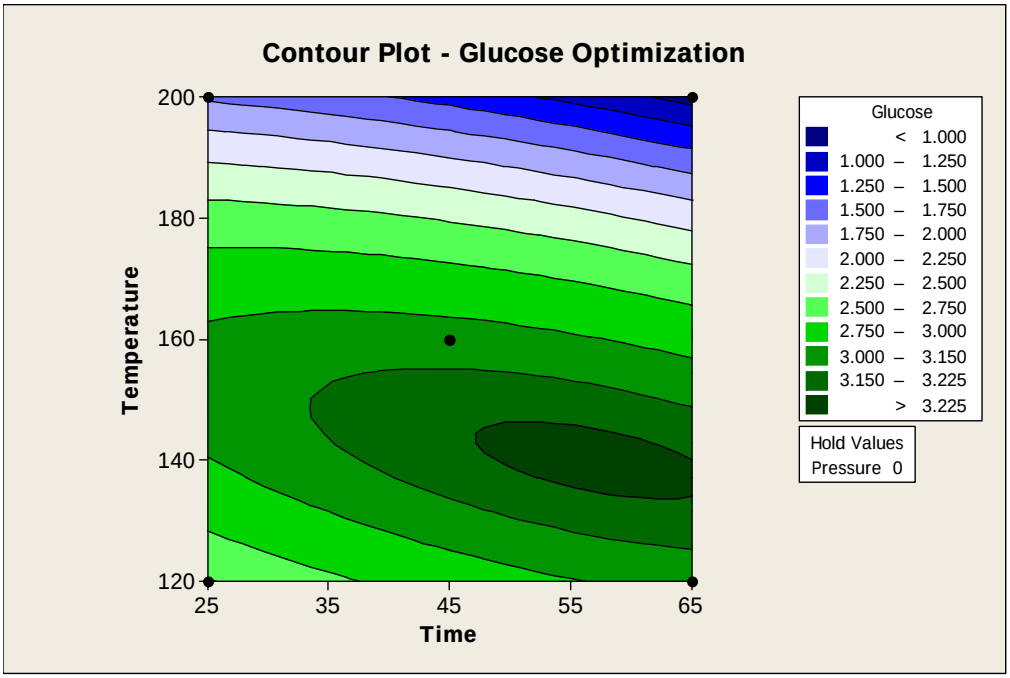

Figure A-9. Contour plot of glucose concentration as a function of temperature and time.

Xylose on the other hand, contains an optimum that is not within the Bechan-Box. Indeed, the contour plot indicates a drastically different concentration profile as compared to glucose, as shown in Figure A-10. Pressure is set on the y-axis and time is set on the x-axis in the contour plot. Additionally, we show the contour plot of pressure versus temperature in Figure A-11, where it is evident that optimal pressure exists at a higher pressure, outside of the originally selected range. The optimal xylose concentration as defined within the box occurs at a time of 25 minutes, temperature of 161 ^{O}C, and pressure of 1600 psi, yielding a predicted xylose concentration of 7.41 mg/mL. When experimentally run at these conditions in order to confirm the statistically predicted optimum, the concentration is 6.78 mg/mL, 8.5% less than predicted. However, it is likely that a higher concentration exists outside of the box, as evident by the

optimum positioned on the extreme of two of the design variables. The combined optimization of both glucose and xylose occurs at 35.5 minutes, 156.4 ^{O}C, and 1390 psi.

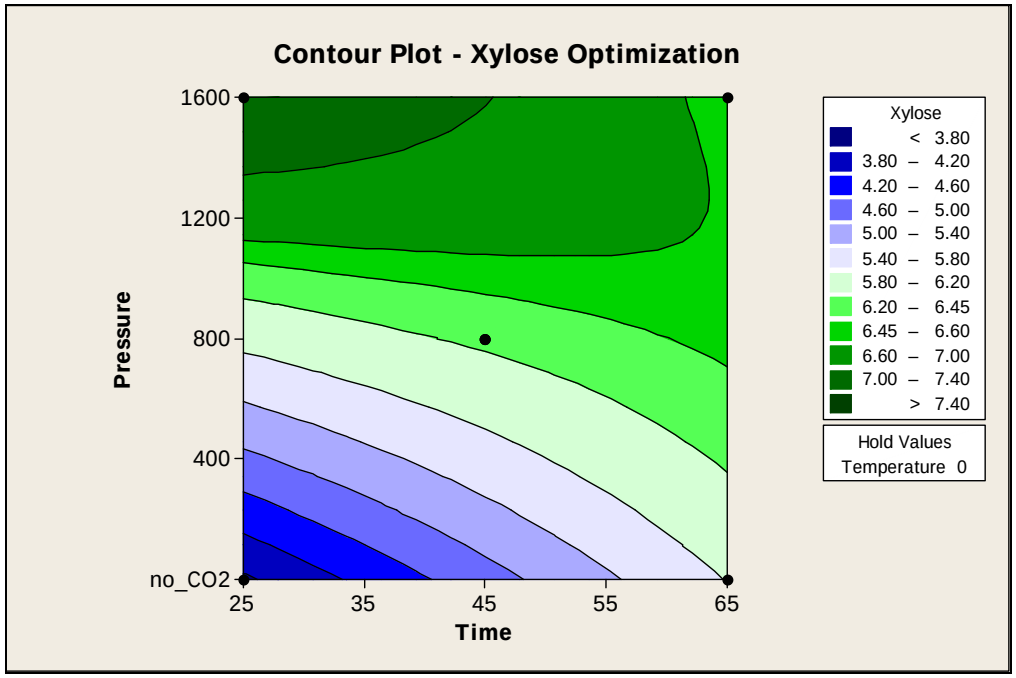

Figure A-10. Contour plot of xylose concentration as a function of pressure and time.

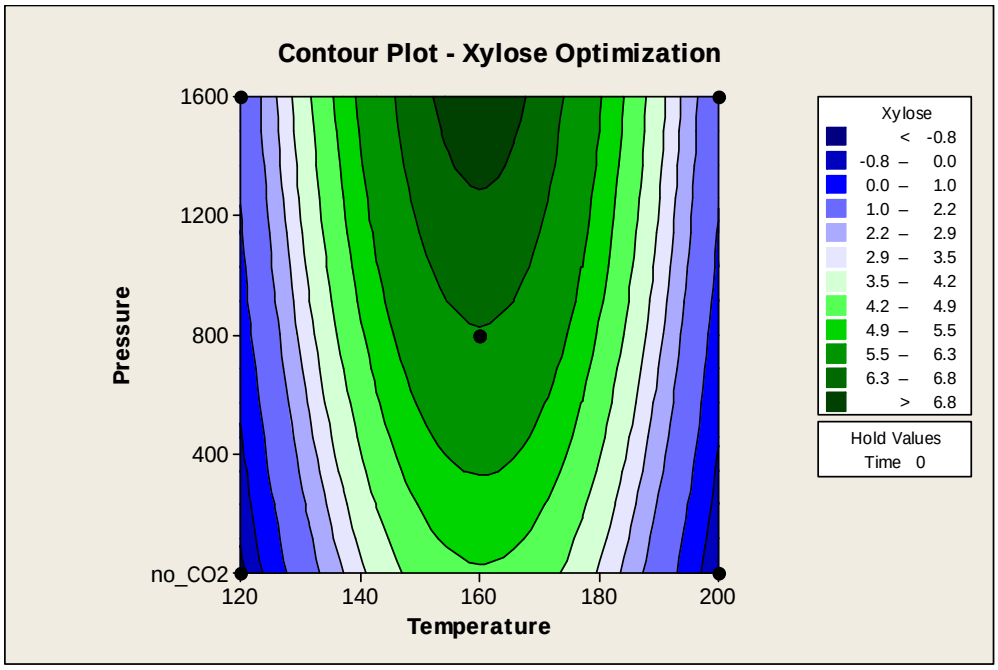

Figure A-11. Contour plot of xylose concentration as a function of pressure and temperature.

These optimizations indicate the influence of each design variable on carbohydrate extraction. Additionally, CO_2 enhanced sub-critical water is more efficient and has a more profound effect on extracting xylose in comparison to other carbohydrates, namely glucose; this result is further supported when considering the crystalline rigidity of glucose in comparison to the amorphous and more easily accessed structure of hemicelluloses, where xylose is extracted from. In comparing our solvent system to what is accepted by some to be the leading pretreatment method, dilute sulfuric acid, CO_2 enhanced sub-critical water can extract greater than 55% of available xylose and 14% available glucose, whereas dilute sulfuric acid extracts about 85% of available xylose and about 15% available glucose [11]. Higher extraction of xylose is likely with the design of a new Bechan-Box accounting for shorter residence times and higher

pressure. The advantages of our solvent system include a neutralization step that does not require acid or bases and subsequently does not involve formation of a salt producing additional separation steps. Although our process is environmentally benign and uses abundant compounds, high pressure and temperatures are needed in this process which require specialized pumping equipment and high pressure vessels that are compatible for solids handling and acids. Therefore, a valuable next step may be to perform an economic analysis to assess the process and equipment costs.

A.4 Conclusions

With an increasing demand for finite amount of petroleum-based fuel and resources, alternative fuel derived from renewable resources is becoming a more championed approach. Additionally, energy and transportation demands are rapidly increasing and regulation of liquid-based fuels is being implemented by government agencies throughout the United States and Europe.

Recent research has focused on use of abundant and non-edible resources as the starting material for bio-fuel production, including lignocellulosic biomass. Owing to the structural rigidity of the lignin component in lignocellulosic biomass, many approaches to develop a specialized pretreatment method have been investigated in order to increase the effectiveness of the subsequent steps of enzymatic saccharification and fermentation. The incorporation of CO_2 into sub-critical water adds substantial solvation power to the extraction of carbohydrates from lignocellulosic biomass, which can be later processed downstream to fuel ethanol. The advantage of using this combination of solvents is contained in the simple separation and benign nature. It would be difficult to find a method that uses more benign solvent components than water and carbon dioxide,

especially as both are inexpensive, abundant, and green. Furthermore, upon quenching and depressurization, the solvents are completely reversed, and downstream filtration and separation are made very effective.

A.5 References:

[1] Ragauskas, A. J.; Williams, C. K.; Davidson, B. H.; Britovsek, G.; Cairney, J.; Eckert, C. A.; Frederick Jr., W. J.; Hallett, J. P.; Leak, D. J.; Liotta, C. L.; Mielenz, J. R.; Murphy, R.; Templer, R.; Tschaplinski, T., *The Path Forward for Biofuels and Biomaterials*. Science, 2006. **311**: p. 484-489.

[2] *Biofuels in the U.S. Transportation Sector.* Annual Energy Outlook, February 2007. Available from http://www.eia.doe.gov/oiaf/analysispaper/biomass.html.

[3] Gardner, T., *Corn is not the future of U.S. ethanol: DOE.* Reuters, 2007. Available from http://www.reuters.com/article/environmentNews/idUSN2830990020070329. March 2007.

[4] Mosier, N.; Wyman, C.; Dale, B.; Elander, R.; Lee, Y. Y.; Holtzapple, M.; Ladisch, M., *Features of Promising Technologies for Pretreatment of Lignocellulosic Biomass*. Bioresource Tech., 2005. **96**: p. 673-86.

[5] Wooley R.; Ruth M.; Glassner D.; Sheehan J., *Process design and costing of bioethanol technology: A tool for determining the status and direction of research and development*. Biotechnology Progress, 1999. **15**(5): p. 794-803.

[6] Committee on Biobased Industrial Products, Biobased Industrial Products – Priorities for Research and Commercialization. National Research Council, 1999.

[7] Kuhlmann, B.; Arnett, E. M.; Siskin M., *Classical Organic Reactions in Pure Superheated Water*. J. Org. Chem., 1994. **59**: p. 3098-101.

[8] Sanchez, O. J.; Cardona, C. A., *Trends in Biotechnological Production of Fuel Ethanol from Different Feedstocks*. Bioresource Tech., 2008. p. 995270–5295.

[9] Minitab Computer Software Design of Experiments.

[10] Michelle K. Kassner Ph.D. Thesis, *Novel Sustainable Solvents for Bioprocessing Applications*. Georgia Institute of Technology, 2008.

[11] Wyman, C.; Dale, B.; Elander, R.; Holtzapple, M.; Ladisch, M.; Lee, Y., *Comparative sugar recovery data from laboratory scale application of leading pretreatment technologies to corn stover*. Bioresource Tech., 2005. **96**: p. 2026-32.

[12] Chheda, J.; Roma´n-Leshkov, Y.; Dumesic, J., *Production of 5-hydroxymethylfurfural and furfural by dehydration of biomass-derived mono- and poly-saccharides*. Green Chemistry, 2007. **9**: p. 342-50.

[13] Clark, J.H., *Green Chemistry: Challenges and Opportunities*. Green Chemistry, 1999. **1**: p. 1.

[14] Hunter, S.E.; and Savage, P.E., *Acid-catalyzed reactions in carbon dioxide-enriched high-temperature liquid water.* Industrial & Engineering Chemistry Research, 2003. **42**: p. 290-94.

[15] Hunter, S. E.; Ehrenberger, C. E.; Savage, P. E., *Kinetics and mechanism of tetrahydrofuran synthesis via 1,4-butanediol dehydration in high-temperature water.* Journal of Organic Chemistry, 2006. **71**: p. 6229-39.

[16] L. Draucker PhD Thesis in *School of Chemical and Biomolecular Engineering*, Georgia Institute of Technology, 2007.

[17] Sluiter, B.; Hames, R.; Ruiz, C.; Scarlata, J.; Templeton, D., D. o. Energy, 2005

APPENDIX B

HYSYS SIMULATION OF PIPERYLENE SULFONE

B.1 Introduction

In Chapter II, we studied the synthesis of the fully recyclable dipolar aprotic solvent, piperylene sulfone. Prior to our research, many of the reaction parameters had not been determined, and the common method of synthesizing PS was to combine the reactants into a bomb and stir the mixture for several days. The yields were relatively low at about 55%, and the purification was highly waste intensive, with well over 100 moles of waste generated for each mole of PS purified. We have overcome these barriers preventing efficient large scale synthesis and enabled the transition away from a laboratory synthesis. To this end, we have determined the kinetic parameters of PS formation, including the rate constant, activation energy, and reaction orders; we have suppressed undesirable polymerization and allowed for quantitative yields; and we have developed a novel separation method to substantially reduce the waste previously generated in purification. In this appendix, we use these developments to simulate the full scale industrial production of PS.

Process design and development engineers must consider a number of metrics in order to realize the successful implementation of a process. One critical metric to the successful large scale synthetic operation of PS is economic profitability. Additional metrics include reducing the environmental impact as discussed in Chapter II, and the low cost and abundant availability of raw starting materials. The production of piperylene

sulfone uses two consumable starting materials, piperylene and sulfur dioxide. Sulfur dioxide is a naturally occurring gas and commonly used in a wide range of industrial processes – it is important to note here that we are using sulfur dioxide in a recyclable process, and we are not generating it. Piperylene is a byproduct of ethylene production from crude oil. The uses of piperylene range from intermediate monomers in the manufacture of plastics, to the manufacture of adhesives and resins. As an example of the relative availability of piperylene for purchase on a large scale, we contacted Shell Chemicals who informed us that the "minimum entry point to do business [purchase of piperylene] is a single purchase order quantity of no less than 3,000 metric tons."

B.2 Results

In the HYSYS simulation of the full scale production of PS, we demonstrate the complete synthesis of PS using the reaction parameters obtained in Chapter II, separation and recycle of unconsumed SO_2 and CO_2, and the purification of the novel ionic inhibitor to significantly reduce waste in purification of the final product – PS. In Figure B-1, we show a simplified schematic of the actual HYSYS simulation, containing only the major unit operations without the pumps, heat exchangers, or mixers. We combine piperylene, inhibitor, and SO_2 into a reactor, where PS is formed. Then, we separate the excess SO_2 with a splitter where it is returned to the reactor. The PS and inhibitor are loaded into a high pressure vessel and liquid CO_2 is injected and mixed. The PS and CO_2 phase is then separated from the inhibitor, and upon flashing, the CO_2 is removed from the PS and recycled.

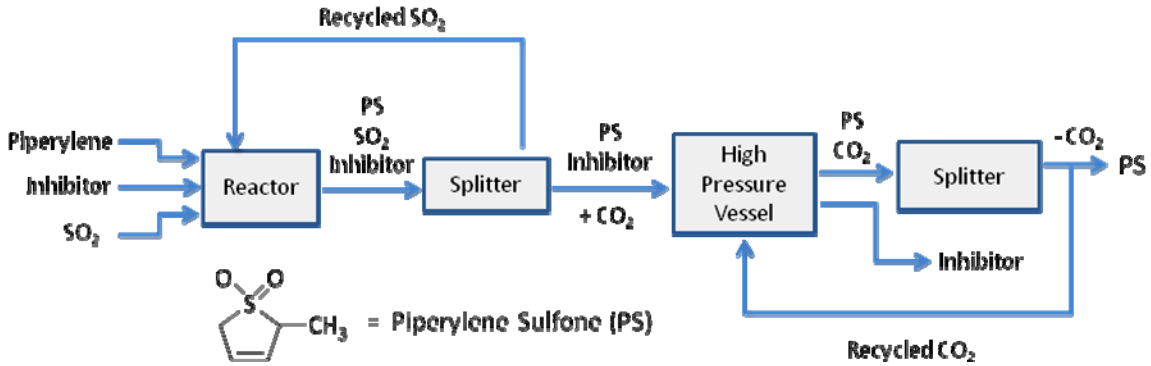

Figure B-1. Simplified schematic of the HYSYS simulation showing the major unit operations for piperylene sulfone production.

Next, the complete HYSYS simulation flowsheet is constructed, and is shown in Figure B-2. The major additions to the unit operations shown in Figure B-1 are all the supporting pumps, mixers, heat exchangers, separators and junctions. The compositions for all streams are shown in Table B-1. Additionally, the physical properties for each material stream are given in Table B-2. In this process, we first mix the piperylene feed (Piperylene Feed-2) and the ionic inhibitor, 8-anilino-1-naphthalenesulfonic acid magnesium salt, (Inhibitor Feed-2). This stream is combined with an SO_2 stream, which consists of purified and recycled liquid SO_2 (SO2 Recycle 2) at 343 kPa and a fresh liquid SO_2 stream (SO2 Liquid Excess) at 392 kPa, and entered into a reactor (CRV-100) operating at room temperature, 24 °C. A 99.1 mol% SO_2 rich phase (Outlet 1) leaves as the top product and is combined with a 94.5 mol% rich phase (Flash Vap) which is sent to a short column (T-100) for separation of waste from pure SO_2 which is recycled.

The second stream exiting the reactor (Outlet 2) is 89 mol% rich in SO_2 (and contains 5.2 mol% cis-piperylene (regarded as waste) and 5.3 mol% piperylene sulfone) which is easily separated using a flash tank (X-100). The bottoms product (Flash Liq) is mainly piperylene sulfone (94 mol%) and is pumped to the high pressure vessel (LLE)

for separation. It is combined with pressurized and liquefied CO_2 (Cooled CO2 1) which consists of a mixture of fresh CO_2 (Fresh CO2) and recycled CO_2 (CO2 Recycle 1). Exiting the LLE are two streams at 25 °C: the bottoms product (Bottom Outlet LLE) which is 96 mol% inhibitor rich and the top product (Top Outlet LLE) which is CO_2 rich and must be removed. The CO_2 is separated from the top product phase in a component splitter (X-102) with the removed CO_2 going through a tee (TEE-100), which was added in to account for a 1% loss in CO_2 during recycle. 99.98 mol% PS is recovered, and 0.02 mol% dissolved inhibitor remains. The heat flows are given in Table B-3, and the unit operation listings (including input and product streams) are given in Table B-4.

Lastly, in Table B-5, we perform an economic analysis using the mass and energy streams from the HYSYS simulation. The analysis is constructed on the annual production basis of 5095 kilograms PS. This analysis is separated into two parts: energy costs and raw materials costs. The energy requirements for each heat exchanger in the HYSYS simulation is converted to cost via the 2009 industrial standard $0.068/kWH and summed to provide a total energy cost per year of $1,123,600. The total capital costs are $2,900,000. Because our interests here are to determine the production cost of PS from a material and energy standpoint, we did not calculate the annual amortization costs. Additionally, the annual cost for all of the materials is calculated at $9,105,160. In fact, the raw materials account to about 90% of the total cost, and piperylene accounts for about 90% of those raw material costs. Thus, the total annual production cost is $10,228,760, yielding the price per kilogram of PS as $2.01. Note that we calculate a 24 hour per day operation for 330 days per year, and the piperylene cost is based on a bulk

quote from XTM Chemical, at 1562 USD per metric ton (FOB Tianjin, China, --- Tianjin Xintaimei Chemicals Co.,Ltd).

B.3 Conclusion

We have overcome previous barriers that have prevented the efficient large scale synthesis of PS. In Chapter II, we determined the parameters of PS reaction, demonstrated high yields, and developed a separation method to reduce the waste in purification. These developments were utilized here to simulate the full scale industrial production of PS via HYSYS. In this simulation, we show the complete synthesis and purification of PS, and we have used the material and energy streams to complete an economic analysis.

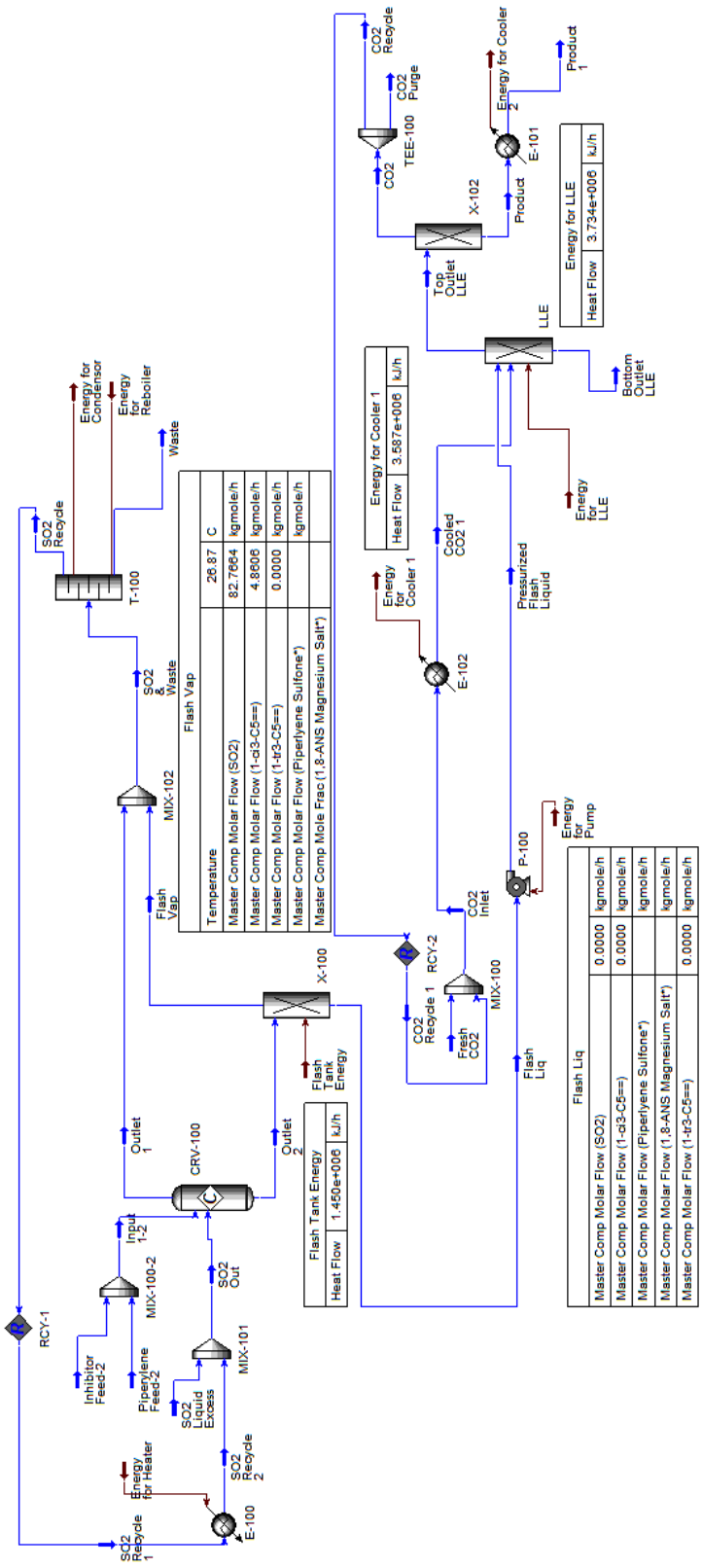

Figure B-2. HYSYS simulation flowsheet for the production of piperylene sulfone (PS)

Table B-1. Composition workbook for PS production in HYSYS.

Composition (in mole fraction)	*SO2 Liquid Excess*	*Flash Vap*	*Flash Liq*	*SO2 & Waste*
Sulfur Dioxide (SO2)	1.000	0.945	0.000	0.946
Trans-piperylene (1-tr3-C5==)	0.000	0.000	0.000	0.000
Cis-piperylene (1-ci3-C5==)	0.000	0.055	0.000	0.054
Carbon Dioxide (CO2)	0.000	0.000	0.000	0.000
Piperlyene Sulfone	0.000	0.000	0.952	0.000
Ionic Inhibitor (1,8-ANS Magnesium Salt)	0.000	0.000	0.048	0.000

Composition (in mole fraction)	*Inhibitor Feed-2*	*Piperylene Feed-2*	*Input 1-2*	*Outlet 1*
Sulfur Dioxide (SO2)	0.000	0.000	0.000	0.991
Trans-piperylene (1-tr3-C5==)	0.000	0.500	0.488	0.000
Cis-piperylene (1-ci3-C5==)	0.000	0.500	0.488	0.008
Carbon Dioxide (CO2)	0.000	0.000	0.000	0.000
Piperlyene Sulfone	0.000	0.000	0.000	0.002
Ionic Inhibitor (1,8-ANS Magnesium Salt)	1.000	0.000	0.024	0.000

Composition (in mole fraction)	*Outlet 2*	*SO2 Out*	*Top Outlet LLE*	*Bottom Outlet LLE*
Sulfur Dioxide (SO2)	0.892	1.000	0.000	0.000
Trans-piperylene (1-tr3-C5==)	0.000	0.000	0.000	0.000
Cis-piperylene (1-ci3-C5==)	0.052	0.000	0.000	0.000
Carbon Dioxide (CO2)	0.000	0.000	0.977	0.000
Piperlyene Sulfone	0.053	0.000	0.023	0.039
Ionic Inhibitor (1,8-ANS Magnesium Salt)	0.003	0.000	0.000	0.961

Composition (in mole fraction)	*Pressurized Flash Liquid*	*Cooled CO2 1*	*Fresh CO2*	*CO2 Inlet*
Sulfur Dioxide (SO2)	0.000	0.000	0.000	0.000
Trans-piperylene (1-tr3-C5==)	0.000	0.000	0.000	0.000
Cis-piperylene (1-ci3-C5==)	0.000	0.000	0.000	0.000

Carbon Dioxide (CO2)	0.000	1.000	1.000	1.000
Piperlyene Sulfone	0.952	0.000	0.000	0.000
Ionic Inhibitor (1,8-ANS Magnesium Salt)	0.048	0.000	0.000	0.000

Composition (in mole fraction)	*CO2*	*Product*	*CO2 Purge*	*CO2 Recycle*
Sulfur Dioxide (SO2)	0.000	0.000	0.000	0.000
Trans-piperylene (1-tr3-C5==)	0.000	0.000	0.000	0.000
Cis-piperylene (1-ci3-C5==)	0.000	0.000	0.000	0.000
Carbon Dioxide (CO2)	1.000	0.000	1.000	1.000
Piperlyene Sulfone	0.000	1.000	0.000	0.000
Ionic Inhibitor (1,8-ANS Magnesium Salt)	0.000	0.000	0.000	0.000

Composition (in mole fraction)	*CO2 Recycle 1*	*SO2 Recycle*	*Waste*	*SO2 Recycle 1*
Sulfur Dioxide (SO2)	0.000	1.000	0.000	1.000
Trans-piperylene (1-tr3-C5==)	0.000	0.000	0.000	0.000
Cis-piperylene (1-ci3-C5==)	0.000	0.000	0.999	0.000
Carbon Dioxide (CO2)	1.000	0.000	0.000	0.000
Piperlyene Sulfone	0.000	0.000	0.001	0.000
Ionic Inhibitor (1,8-ANS Magnesium Salt)	0.000	0.000	0.000	0.000

Composition (in mole fraction)	*SO2 Recycle 2*	*Product 1*
Sulfur Dioxide (SO2)	1.000	0.000
Trans-piperylene (1-tr3-C5==)	0.000	0.000
Cis-piperylene (1-ci3-C5==)	0.000	0.000
Carbon Dioxide (CO2)	0.000	0.000
Piperlyene Sulfone	0.000	1.000
Ionic Inhibitor (1,8-ANS Magnesium Salt)	0.000	0.000

Table B-2. Material streams workbook for PS production in HYSYS.

	Stream Name:	*SO2 Liquid Excess*	*Flash Vap*	*Flash Liq*
Vapor Fraction		0.00	0.86	0.00
Temperature	*C*	25	27	27
Pressure	*kPa*	392	343	343
Molar Flow	*kgmole/h*	4.9	87.6	5.1
Mass Flow	*kg/h*	313	5633	796
Liquid Volume Flow	*m^3/h*	0.224	4.276	0.951
Heat Flow	*kJ/h*	-1541345	-24452221	-1330622

	Stream Name:	*SO2 & Waste*	*Inhibitor Feed-2*	*Piperylene Feed-2*
Vapor Fraction		0.86	0.00	0.00
Temperature	*C*	27	25	25
Pressure	*kPa*	343	343	343
Molar Flow	*kgmole/h*	90.0	0.2	9.8
Mass Flow	*kg/h*	5786	151	665
Liquid Volume Flow	*m^3/h*	4.387	0.057	0.967
Heat Flow	*kJ/h*	-25152838	0	494261

	Stream Name:	*Input 1-2*	*Outlet 1*	*Outlet 2*
Vapor Fraction		0.00	1.00	0.00
Temperature	*C*	25	24	24
Pressure	*kPa*	343	343	343
Molar Flow	*kgmole/h*	10.0	2.4	92.8
Mass Flow	*kg/h*	816	153	6429
Liquid Volume Flow	*m^3/h*	1.024	0.111	5.227
Heat Flow	*kJ/h*	494261	-700616	-27232751

	Stream Name:	*SO2 Out*	*Top Outlet LLE*	*Bottom Outlet LLE*
Vapor Fraction		0.00	1.00	0.00
Temperature	*C*	25	25	25
Pressure	*kPa*	392	101	98
Molar Flow	*kgmole/h*	90.0	208.2	0.3
Mass Flow	*kg/h*	5766	9590	152
Liquid Volume Flow	*m^3/h*	4.132	11.733	0.059
Heat Flow	*kJ/h*	-28427633	-81230107	-2668

Stream Name:		Pressurized Flash Liq	Cooled CO2 1	Fresh CO2
Vapor Fraction		0.00	0.00	1.00
Temperature	C	30	-40	25
Pressure	kPa	5516	1013	101
Molar Flow	kgmole/h	5.1	203.3	2.0
Mass Flow	kg/h	796	8947	89
Liquid Volume Flow	m^3/h	0.951	10.840	0.108
Heat Flow	kJ/h	-1323975	-83642638	-800575

Stream Name:		CO2 Inlet	CO2	Product
Vapor Fraction		1.00	1.00	0.54
Temperature	C	25	25	85
Pressure	kPa	101	101	101
Molar Flow	kgmole/h	203.3	203.3	4.9
Mass Flow	kg/h	8947	8947	643
Liquid Volume Flow	m^3/h	10.840	10.840	0.892
Heat Flow	kJ/h	-80055982	-80055982	-1174125

Stream Name:		CO2 Purge	CO2 Recycle	CO2 Recycle 1
Vapor Fraction		1.00	1.00	1.00
Temperature	C	25	25	25
Pressure	kPa	101	101	101
Molar Flow	kgmole/h	2.0	201.3	201.3
Mass Flow	kg/h	89	8858	8858
Liquid Volume Flow	m^3/h	0.108	10.732	10.732
Heat Flow	kJ/h	-800560	-79255422	-79255407

Stream Name:		SO2 Recycle	Waste	SO2 Recycle 1
Vapor Fraction		0.00	0.00	0.00
Temperature	C	21	87	21
Pressure	kPa	343	343	343
Molar Flow	kgmole/h	85.1	4.9	85.1
Mass Flow	kg/h	5453	333	5453
Liquid Volume Flow	m^3/h	3.908	0.479	3.908
Heat Flow	kJ/h	-26909312	296156	-26908733

Stream Name:		*SO2 Recycle 2*	*Product 1*
Vapor Fraction		0.00	0.00
Temperature	*C*	25	25
Pressure	*kPa*	392	101
Molar Flow	*kgmole/h*	85.1	4.9
Mass Flow	*kg/h*	5453	643
Liquid Volume Flow	*m^3/h*	3.908	0.892
Heat Flow	*kJ/h*	-26886288	-1331465

Table B-3. Energy streams (heat flow) workbook for PS production in HYSYS.

Heat Exchanger		*Units*
Flash Tank Energy	1449909	kJ/h
Energy for LLE	3733838	kJ/h
Energy for Pump	6646	kJ/h
Energy for Cooler 1	3586656	kJ/h
Energy for Condensor	-2007353	kJ/h
Energy for Reboiler	547034	kJ/h
Energy for Heater	22445	kJ/h
Energy for Cooler 2	157340	kJ/h

Table B-4. Unit operations workbook for PS production in HYSYS.

Operation Name	T-100	TEE-100	E-101	E-102	P-100	X-102	LLE	X-100
Operation Type	Short Column	Tee	Cooler	Cooler	Pump	Component Splitter	Component Splitter	Component Splitter
Feeds	SO2 & waste, energy for reboiler	CO2	Product	CO2 inlet	Flash liq, energy for pump	Top outlet LLE	Pressurized flash liquid, cooled CO2 1, energy for LLE	Outlet 2, flash tank energy
Products	SO2 recycle, waste, energy for condenser	CO2 recycle, CO2 purge	Product 1, Energy for cooler 2	Cooled CO2 1, energy for cooler 1	Pressurized flash liq	CO2, product	Top outlet LLE, bottom outlet LLE	Flash vap, Flash liq
Operation Name	CRV-100	E-100	RCY-2	RCY-1	MIX-100	MIX-100-2	MIX-102	MIX-101
Operation Type	Conversion Reactor	Heater	Recycle	Recycle	Mixer	Mixer	Mixer	Mixer
Feeds	Input 1-2, SO2 out	SO2 recycle 1, energy for heater	CO2 recycle	SO2 recycle	Fresh CO2, CO2 recycle 1	Inhibitor feed-2, piperylene feed-2	Outlet 1, Flash Vap	SO2 liquid excess, SO2 recycle2
Products	Outlet 2, outlet 1	SO2 recycle 2	CO2 recycle 1	SO2 recycle 1	CO2 inlet	Input 1-2	SO2 & waste	SO2 out

Table B-5. Economic analysis for PS production costs based on HYSYS simulation.

Energy	**kJ/h**	**kW**		
Energy for Heater	22450	6.2361		
Flash Tank Energy	1450000	402.7778		
Energy for Condenser	-2007000	-557.5000		
Energy for Reboiler	547000	151.9444		
Pressurize Flash Liquid	13300	3.6944		
Energy for LLE	3734000	1037.2222		
Prime CO2	3750946	1041.9294	Cost/kWH	**Total Cost/hour**
Total Energy (kJ/h)	7510696	2086.3044	0.068	**$141.87**

Raw Materials	**Amount (kg/h)**	**Cost $/kg**	**Total Cost**
Liquid SO2*	312.6	$0.25	$79.09
Piperlyene***	664.6	$1.56	$1,038.11
Carbon Dioxide**	89.47	$0.25	$22.37

Energy:	**$1,123,600**
Raw Materials:	**$9,105,160**
Total Price per Year	**$10,228,760**
Price/ kg of PS Product	**$2.01**
Capitol Cost:	**$2,900,000**

Notes and Assumptions:

Cost ($/kWH) for Industry in 2009 in the United States: $0.068
24 hr/day operation for 330 days (standard)
Annual production of 5,095 tons per year.
Annual purchase of 151.5 kg inhibitor at $527/kg
* Price from ICIS
** Technical grade price from Sigma
*** XTM Chem Quote: USD 1562 / Metric Ton, FOB Tianjin, China
XTM Chem --- Tianjin Xintaimei Chemicals Co.,Ltd

VITA

Gregory Alan Marus

Gregory Alan Marus was born in Albuquerque, New Mexico. He graduated from La Cueva High School in 2003. Then, he attended the University of New Mexico and received a B.S. in Chemical Engineering in 2007 before coming to Georgia Tech to pursue a doctorate in Chemical and Biomolecular Engineering. He was advised by Dr. Charles Eckert and Dr. Charles Liotta and will receive his degree in the spring of 2012. When he is not working on his research, Gregory enjoys the company of close friends, car work and attending racing events, and the occasional swing dance on the weekends. After defending, he will move to Baton Rouge, LA where he has accepted a position at Albemarle. Selected publications and presentations follow.

Selected Publications

Marus, Gregory A.; Vyhmeister, Eduardo; Pollet, Pamela; Donaldson, Megan E.; Llopis-Mestre, Veronica; Faltermeier, Sean; Roesel, Renee; Tribo, Michael; Gelbaum, Leslie; Liotta, Charles L.; and Eckert, Charles A.; *Sustainable and Scalable Synthesis of Piperylene Sulfone: A "Volatile" and Recyclable DMSO Substitute*, Ind. Eng. Chem. Res., 2011, 50, 23.

Flack, Kyle; Marus, Gregory; Kitagawa, Kristen; Peterson, Olga; Medina-Ramos, Wilmarie; Pollet. Pamela; Liotta, Charles; Eckert, Charles; Richman, Kent; Stringer, Joy; Dubay, William; *Enabling a Meerwein-Ponndorf-Verley (MPV) Reduction: Batch and Continuous Processes*, Manuscript in progress for Org. Proc. Res. And Development.

Selected Presentations

Marus, G. (Speaker), et al., "The Sustainable and Scalable Synthesis of Piperylene Sulfone as a Recyclable Pharmaceutical Solvent" Green Chemistry and Engineering Conference, Poster Presentation, 2010

Peterson, O., et al., "Continuous Flow Reactors for Benign Production of Pharmaceuticals and Pharmaceutical Intermediates" AIChE National Meeting, Oral Presentation, 2010

Marus, G. (Speaker), et al., "The Sustainable and Scalable Synthesis of Piperylene Sulfone: A "Volatile" and Recyclable DMSO Substitute" AIChE National Meeting, Oral Presentation, 2010

Marus, G. (Speaker), et al., "Enabling the Sustainable Synthesis of A Recyclable DMSO Replacement" ACS National Meeting, Oral and Poster Presentation, 2011